

The role of cytomegalovirus infection in breast cancer

by

Zelei Yang

A thesis submitted in partial fulfillment of the requirements for the degree of

Doctor of Philosophy

Department of Biochemistry
University of Alberta

© Zelei Yang, 2020

Abstract

Human cytomegalovirus (HCMV) infects 40–70% of the adult population in developed countries, and this rate increases with age. HCMV infection is normally latent with no noticeable symptoms in individuals with a healthy immune system. However, the infection can cause problems in immune-compromised individuals and in the elderly people. Detection rates of >90% have been reported for HCMV DNA and/or proteins in breast tumors, suggesting an association between HCMV infection and breast cancer. However, controversies exist, and it is unclear what role HCMV infection plays in breast cancer. HCMV infection fulfills the criteria of the hallmarks of cancer, including tumor-promoting inflammation. We hypothesized that HCMV infection induces inflammation at the breast tumor site, which promotes breast tumor progression and metastasis.

This study reassessed the association between HCMV infection and breast cancer using a collection of 147 breast tumors and ten normal breast adipose tissues from women free of cancer that were obtained from a Canadian patient population. PCR detection methods for HCMV DNA were examined for sensitivity and specificity. Nested PCR targeting for HCMV glycoprotein B (gB) gene was found to be the optimum method of detection. HCMV gB DNA was detected in breast tumors and breast tissues at 40% and 30%, respectively. Although not statistically significant, there was a trend for a higher association of HCMV DNA detection with a negative expression of human epidermal growth factor receptor 2 (HER2) in breast tumors ($p=0.06$). We also investigated the effects of cytomegalovirus (CMV) infection both *in vitro* and *in vivo*.

The effects of HCMV challenge on human breast cancer cells and breast tissues were studied in culture, with a focus on viral transcription, replication and cellular

expression of inflammatory genes. HCMV did not fully replicate in breast cancer cells, but HCMV immediate early (IE) transcripts and proteins were produced, although in a limited number of cells. Breast cancer cells challenged with HCMV showed increased mRNA expression of inflammatory genes including interleukin (IL)-1 β , IL-6, and cyclooxygenase-2 (COX-2), which could be important in promoting cancer progression.

The effects of mouse CMV (mCMV) infection on breast tumor growth and metastasis was investigated in mouse models of breast cancer, including two syngeneic-orthotopic models and one transgenic model with spontaneous breast tumor growth. Prior to breast tumor development, mice were injected with mCMV or negative control medium for 4 days, 11 days or 10 weeks to establish active, intermediate or latent infections, respectively. Infection did not affect tumor growth regardless of these conditions, but latently infected mice showed enhanced development of lung metastases. The breast tumors in latently infected mice also showed worse tumor phenotypes including enhanced vasculature and decreased collagen content, which are features promoting metastasis. Latently infected mice also had increased plasma levels of IL-6 and IL-13, suggesting enhanced inflammation.

This work provides insights into the association between CMV infection and breast cancer, with inflammation as an important aspect. These novel results directly linking CMV infection to breast cancer metastasis have important clinical implications since an increased metastasis is prognostic of decreased survival. This work provides evidence that treating or preventing HCMV infections may increase the life expectancy of breast cancer patients by decreasing metastasis.

Preface

This thesis is an original work by Zelei Yang. The patient samples and de-identified patient data were obtained with the approval of the University of Alberta Health Research Ethics Board (Pro00018758) with written informed consent. Animal studies were conducted in compliance with the Canadian Council of Animal Care as approved by the University of Alberta Animal Welfare Committee (Animal User Protocol 00000226).

Components of Chapter 5 have been published as:

Yang, Z., Tang, X., Meng, G., Benesch, M.G.K., Mackova, M., Belon, A.P., Serrano-Lomelin, J., Goping, I.S., Brindley, D.N., and Hemmings, D.G., *Latent cytomegalovirus infection in female mice increases breast cancer metastasis*. *Cancers (Basel)*, 2019. **11**(4):447

Acknowledgements

I would like to thank my co-supervisors Dr. David Brindley and Dr. Denise Hemmings for all of their support and guidance through this project. I am very grateful for having two excellent role models who cared for me. They have taught me a lot through these years and encouraged me along the way. I really appreciated all the lab meetings we had, where I learned to present, discuss, and think in depth about the project and research in general. Also thank you to Dr. Deborah Burshtyn and Dr. Ing Swie Goping for being on my supervisory committee and providing advice on the project. I would also like to thank the Goping Lab for helping to establish the transgenic mouse model used in this study. Also thank you to Dr. Todd McMullen, who we have joint lab meetings with, for advice through the project and providing human specimens used in this study. Thank you to Dr. Mary Hitt for examining my PhD Candidacy. Also thank you to Dr. Larry Fliegel for examining and Dr. David Stuart for chairing both of my PhD Candidacy and thesis defense. I would also like to thank Dr. Olivier Peyruchaud for agreeing to participate in my thesis defense as the external examiner.

I would like to thank the former and present members of the Brindley and Hemmings Labs for their assistance through these years: Xiaoyun Tang, Guanmin Meng, Matthew Benesch, Ganesh Venkatraman, Raie Bekele, Yuliya Fakhr, and Martina Mackova. I am grateful for being able to work in a very supportive environment where everyone in the both labs are willing to provide help to others. I really enjoyed the time we spent together drinking, eating and celebrating.

I want to thank my family and friends for their love and support throughout the study. My dad, Jiliang Yang, who is also a Ph.D., taught me a lot of his experiences of

being a scientist. My mom, Ailing Cui, always cared for me and encouraged me when I have encountered moments of depression. My brother Zehua and my sister Zefeng are the sweetest siblings and the time spent with them during holidays always made me feel relieved. I also want to thank my boyfriend, Mengqi Hao, who provided joy, support and encouragement to me all these years. I also want to thank Kim Jaejoong and Cai Xukun, their songs accompanied me during stressful moments from work and study.

I would also like to thank all the funding agencies for making this study possible: University of Alberta Faculty of Graduate Studies and Research (Dean's Doctoral Student Award, 75th Anniversary Graduate Studentship, Queen Elizabeth II Graduate Studentship), Cancer Research Institute of Northern Alberta (La Vie en Rose Scholarship for Breast Cancer Research), Women & Children's Health Research Institute, Breast Cancer Society of Canada, Canadian Cancer Society, and Canadian Breast Cancer Foundation.

Table of Content

Chapter 1: Introduction	1
1.1 Overview	2
1.2 Breast cancer	2
1.2.1 Overview of breast cancer	2
1.2.2 Breast tumor development.....	4
1.2.2.1 Angiogenesis.....	5
1.2.2.2 Cells within the tumor microenvironment	6
1.2.2.3 Tumor-promoting inflammation	6
1.2.3 Breast cancer metastasis	8
1.2.4 Breast tumor receptor positivity	11
1.3 HCMV infection as a risk factor for cancer	13
1.3.1 Oncogenic role of HCMV	13
1.3.2 Oncomodulatory role of HCMV.....	15
1.4 Cytomegalovirus (CMV).....	16
1.4.1 Overview of CMV	16
1.4.2 Cell tropism	18
1.4.3 Life cycle of CMV.....	20
1.4.3.1 CMV transcripts and proteins	22
1.4.4 Host immune responses against CMV infection	23
1.4.5 CMV infection regulates cellular responses.....	24
1.5 HCMV and breast cancer	25
1.5.1 Epidemiological studies of HCMV and breast cancer.....	25
1.5.2 Detection of HCMV in breast tumors.....	26
1.5.3 Association between HCMV and breast cancer patient characteristics	35
1.5.4 <i>In vitro</i> studies for the interaction between HCMV and breast cancer	36
1.6 Summary and thesis objectives	37
Chapter 2: Methods.....	39
2.1 Reagents	40
2.2 Human breast tumors and breast adipose tissues	40
2.3 Cell lines.....	41
2.4 CMV preparation.....	41

2.4.1	Virus propagation	41
2.4.1.1	HCMV.....	41
2.4.1.2	mCMV	42
2.4.2	Determination of the viral titre	43
2.4.2.1	Staining for HCMV IE antigen.....	43
2.4.2.2	LacZ staining for mCMV RM427+	44
2.4.3	Generation of CMV negative control solutions.....	44
2.5	Cell and tissue cultures.....	46
2.5.1	Human breast cancer cells	46
2.5.2	Mammary adipose tissue culture	46
2.5.3	Infecting cell and adipose tissue cultures with CMV	47
2.5.4	Determination of HCMV IE expression in human breast cancer cells.....	49
2.5.5	Examination for productive infection of HCMV in cells.....	49
2.6	Mouse Models.....	50
2.6.1	Animal housing.....	50
2.6.2	Syngeneic orthotopic breast cancer model	51
2.6.3	Spontaneous breast cancer model.....	52
2.6.3.1	Genotyping of transgenic mice	52
2.6.4	Mouse infection with mCMV	54
2.6.4.1	Verification of active mCMV infection in mice.....	54
2.6.4.2	Establishment of active, intermediate and latent mCMV infection statuses in mice.....	54
2.6.5	Tumor growth and tissue collection	55
2.6.6	Metastasis quantification	56
2.7	Detection of CMV viral DNA.....	57
2.7.1	LightCycler (LC) PCR.....	57
2.7.2	Nested PCR amplification and visualization	58
2.7.3	Sequencing of PCR product	59
2.7.3.1	Re-extraction of DNA from agarose gel.....	59
2.7.3.2	Cloning of PCR product into T-vector.....	61
2.8	Measurement of mRNA expression	62
2.8.1	mRNA isolation and reverse transcription	62
2.8.2	Quantitative Real-Time PCR.....	64

2.9 Immunohistochemistry.....	66
2.10 Picro-Sirius red staining for collagen.....	68
2.11 Multiplex ELISA for cytokine/chemokine and matrix metalloproteinase (MMP) levels.....	68
2.12 Measurement of ATX activity.....	69
2.13 Statistical analysis.....	71
Chapter 3: Detection of HCMV genome and viral transcripts in human breast tumors and normal breast adipose tissues.....	72
3.1 Introduction.....	73
3.2 Detection of HCMV gB DNA using LightCycler Real-time PCR (LC-PCR) and nested PCR.....	75
3.3 Determination of nested PCR specificity using different viral genes for detecting HCMV DNA in human specimens.....	75
3.4 Incidence of HCMV gB detection in human breast tumors and normal breast tissues at the DNA level.....	80
3.5 mRNA expression of HCMV IE was not detected in human breast tumors and breast tissues.....	83
3.6 Discussion.....	85
Chapter 4: CMV infection in breast cancer cells and breast adipose tissues.....	91
4.1 Introduction.....	92
4.2 Human breast cancer cells challenged with HCMV expressed low levels of IE protein.....	94
4.3 Human breast cancer cells were not productively infected by HCMV.....	94
4.4 HCMV challenge stimulated expression of viral genes at the mRNA level in human breast cancer cells.....	97
4.5 HCMV challenge stimulated expression of cytokines and inflammatory mediators at the mRNA level in human breast cancer cells.....	98
4.6 UV-inactivated HCMV did not stimulate mRNA responses in breast cancer cells.....	100
4.7 mRNA expression of cytokines and inflammatory mediators in cultured breast tissues challenged with HCMV.....	101
4.8 Discussion.....	104
Chapter 5: The effect of mCMV infection on breast tumor growth and metastasis in mice.....	111
5.1 Introduction.....	112

5.2 Active infection of mCMV was detected in mice 4 days post-infection	113
5.3 mCMV infection had no significant effect on breast tumor growth	114
5.4 Latent mCMV infection of MMTV-PyVT mice changed the breast tumor phenotypes.....	120
5.5 Lung metastasis was increased in latently infected BALB/c and MMTV-PyVT mice	125
5.6 Mice latently infected with mCMV showed enhanced cell proliferation in lung metastatic nodules but not in primary breast tumors.....	127
5.7 mCMV DNA but not mRNA was detectable in tissues, metastatic nodules and tumors from mice latently infected with mCMV	129
5.8 Cytokine expression was altered in breast tumors and plasma from mice with latent mCMV infections.....	133
5.9 Discussion	136
Chapter 6: General discussion and future directions	145
6.1 Introduction	146
6.2 Evaluation of HCMV detection in human specimens.....	146
6.3 CMV viral transcripts as stimuli for inflammation	152
6.4 Latent CMV infection as a factor promoting worse breast tumor phenotypes and metastasis	156
6.5 Future directions.....	158
Bibliography.....	162

List of Tables

Table 1.1. Percent of positive detection for HCMV protein, DNA and mRNA in human breast tumors.....	27
Table 1.2. Detection of HCMV DNA and/or protein in human breast tumors and non-cancerous breast tissues.	28
Table 2.1. Primer sequences for nested PCR.....	60
Table 2.2. Primer sequences of genes assayed by qPCR.....	65
Table 2.3. Analytes quantified by the Mouse Cytokine/Chemokine Discovery array 31-plex.....	70
Table 3.1. Detection of HCMV glycoprotein B DNA in human breast tumors and breast tissues.....	80
Table 3.2. Patient characteristics for breast tumors analyzed.	81
Table 3.3. Cellular receptor positivity for breast tumors analyzed.	82
Table 5.1. Average tumor volume, mass and density in MMTV-PyVT mice with and without latent mCMV infection.	119
Table 5.2. Severity of tumors in MMTV-PyVT mice with and without latent mCMV infection.	121
Table 5.3. Detection of mCMV glycoprotein B DNA in specific tissues, nodules or tumors from each mouse in all animal groups.	131

List of Figures

Figure 1.1. Breast cancer stages and 5-year overall survival rate.....	3
Figure 1.2. Anatomy of normal breast.....	4
Figure 1.3. The cascade of metastasis.....	9
Figure 1.4. HCMV seroprevalence rates in adults worldwide.....	17
Figure 1.5. HCMV virion envelope glycoproteins for viral entry.	19
Figure 1.6. Replication of CMV following entry of host cell.....	20
Figure 2.1. UV irradiation inactivates mCMV.	45
Figure 2.2. Mouse breast adipose tissues cultured with different amount of mouse CMV (mCMV).....	48
Figure 2.3. Positive standard curve for HCMV DNA detection using LC-PCR.	58
Figure 3.1. The detection limit of LightCycler PCR (LC-PCR) and nested PCR for HCMV glycoprotein B (gB) DNA.....	76
Figure 3.2. Specificity of HCMV glycoprotein (gB) DNA detection using nested PCR.	78
Figure 3.3. Specificity of HCMV immediate early (IE) DNA detection using nested PCR.	79
Figure 3.4. mRNA expression of HCMV immediate early (IE) gene in human breast tumor samples.	83
Figure 4.1. HCMV challenge of human breast cancer cells leads to a low number of cells expressing HCMV IE antigen.....	95
Figure 4.2. HCMV does not productively infect human breast cancer cell line MDA-MB-231.....	96
Figure 4.3. HCMV-challenged breast cancer cells showed increased expression of viral genes at the mRNA level during initial infection.	97
Figure 4.4. MDA-MB-231 breast cancer cells challenged with HCMV showed increased expression of cytokines and inflammatory mediators at the mRNA level.	99
Figure 4.5. MCF-7 breast cancer cells challenged with HCMV showed increased expression of IL-6 but not other inflammatory mediators at the mRNA level.....	100
Figure 4.6. UV-inactivated virus did not stimulate mRNA expressions of viral genes and cytokines in breast cancer cells.....	102
Figure 4.7. mRNA expressions of cytokine and inflammatory mediators in human breast adipose tissues challenged with HCMV.	103
Figure 4.8. mRNA expressions of cytokines and inflammatory mediators in mouse breast adipose tissues challenged with mCMV.....	104

Figure 5.1. Verification of active infection 4 days post mCMV injection in mice.....	115
Figure 5.2. Estimated volume of breast tumors developed over time in BALB/c and C57BL/6 mice with and without active, intermediate or latent mCMV infections.	116
Figure 5.3. Breast tumor mass was not significantly affected in mice with active or intermediate mCMV infections.....	117
Figure 5.4. Latent mCMV infection has minimal effects on breast tumor mass.	118
Figure 5.5. MMTV-PyVT mice latently infected with mCMV developed more breast tumors with severe phenotypes associated with metastasis.	120
Figure 5.6. Tumors from MMTV-PyVT mice latently infected with mCMV had increased microvasculature and decreased collagen content.	123
Figure 5.7. Expressions of matrix metalloproteinase (MMP) in breast tumors were not affected by mCMV infection in the MMTV-PyVT mice.	124
Figure 5.8. Tumors from BALB/c mice actively infected with mCMV or UV-inactivated control showed no differences in the expressions of CD31 and collagen content.....	125
Figure 5.9. Lung metastasis was increased in mice latently infected with mCMV, but not in active or intermediate infection models.....	126
Figure 5.10. Negative detection of micro-metastasis.....	127
Figure 5.11. Enhanced cancer cell proliferation in lung metastatic nodules but not in the breast tumors in mice latently or actively infected with mCMV.....	128
Figure 5.12. DNA for mCMV glycoprotein B (gB) was detected in MMTV-PyVT mice latently infected with mCMV.	130
Figure 5.13. Negative detection for actively transcribing or replicating mCMV in the latently infected mouse models.....	134
Figure 5.14. Autotaxin (ATX) activity in the plasma from MMTV-PyVT mice was not altered by mCMV latent infection.	135
Figure 5.15. Differences in cytokine concentrations in breast tumors and plasma from MMTV-PyVT mice latently infected with mCMV.	136
Figure 6.1. CMV infection in the tumor microenvironment and effects on breast cancer cells.	155
Figure 6.2. Latent CMV infection promotes breast cancer metastasis.	156

List of Abbreviations

ANOVA	analysis of variance
ATX	autotaxin
BCA	bicinchoninic acid
BLAST	Basic Local Alignment Search Tool
BM	basement membrane
cDNA	complementary DNA
CMV	cytomegalovirus
COX-2	cyclooxygenase 2
DAB	3,3'-Diaminobenzidine
E	early
EBV	Epstein-Barr virus
ECM	extracellular matrix
EDTA	ethylenediaminetetraacetic acid
EGFR	epidermal growth factor receptor
EMT	epithelial-to-mesenchymal transition
ER	estrogen receptor
FCMV	filtered CMV
GAPDH	glyceraldehyde 3-phosphate dehydrogenase
gB	glycoprotein B
HBS	HEPES-buffered saline
HCMV	human cytomegalovirus
HEL	human embryonic lung
HER2	human epidermal growth factor receptor 2
HPRT	hypoxanthine-guanine phosphoribosyltransferase
HPV	human papillomavirus
HRP	horseradish peroxidase
IBC	inflammatory breast cancer

IE	immediate early
IF	infection focus
IgG	immunoglobulin G
IgM	immunoglobulin M
IHC	immunohistochemistry
IL	interleukin
L	late
LB	Luria broth
LC	LightCycler
LPA	lysophosphatidic acid
LPAR	lysophosphatidic acid receptor
LPC	lysophosphatidylcholine
mCMV	mouse CMV
MET	mesenchymal-to-epithelial transition
MMP	matrix metalloproteinase
MMTV	mouse mammary tumor virus
MMTV-PyVT	B6.FVB-Tg (MMTV-PyVT)634Mul/LelJ
MOI	multiplicity of infection
mRNA	messenger RNA
NK	natural killer
OCT	optimal cutting temperature
PBS	phosphate buffered saline
PDGFR- α	platelet derived growth factor receptor alpha
PI3K/AKT	phosphatidylinositol 3-kinase/protein kinase B
PPIA	peptidylprolyl isomerase A
PR	progesterone receptor
PTGS	prostaglandin-endoperoxide synthase
PyVT	polyomavirus middle T

qPCR	quantitative Real-Time PCR
RIPA	radioimmunoprecipitation
SEM	standard error of the mean
TGF β	transforming growth factor beta
TLR2	toll-like receptor 2
TNF- α	tumor necrosis factor alpha
UV	ultraviolet
VEGF	vascular endothelial growth factor

Chapter 1: Introduction

1.1 Overview

Breast cancer is the most common malignancy and the leading cause of cancer death among women worldwide [1]. The net five-year survival rates are 87% for all patients diagnosed with breast cancer, but once the tumors metastasize, the survival rate decreases dramatically to 22% [2]. Therefore, it is vital to develop new strategies to prevent metastasis and overcome breast cancer. Infectious agents are an important risk factor that attributes to over 15% of all cancers, with 64% of these due to viruses [3]. In the recent decade, increasing evidence shows that human cytomegalovirus (HCMV) plays a role in breast cancer [4-6]. However, it is still unclear about how HCMV infection contributes to breast cancer progression. In this work, I have investigated further the association between CMV infection and breast cancer. The aspects studied include the incidence of HCMV genome detection in human specimens, the direct effect of HCMV challenge on human breast cancer cells, and the effects of mouse CMV (mCMV) infection on breast cancer progression in mouse models.

This chapter will provide a background review of breast cancer and metastasis (Section 1.2). This is then followed by the introduction of HCMV as a potential risk factor for breast cancer and an overview of CMV (Section 1.3 and 1.4). Our current knowledge about the association between HCMV and breast cancer will be discussed (Section 1.5). The chapter is concluded with the thesis objectives, goal of this research, and the hypotheses (Section 1.6).

1.2 Breast cancer

1.2.1 Overview of breast cancer

Breast cancer is the most common malignancy among women worldwide and it is estimated that 1 in 8 Canadian women will develop breast cancer during their lifetime [1,

7]. Examples of risk factors that can increase the possibility of breast cancer development include aging, family history, mutation, reproductive factors, endogenous and exogenous use of estrogen, unhealthy life style, high body-mass index, and dense breast tissue [8-12].

Most breast cancers are carcinomas, where breast cancer arises from the epithelial component of the breast [13]. The epithelial cells line the lobules and milk ducts in the breast [14, 15]. Uncontrolled growth of ductal cells leads to ductal carcinoma, including non-invasive (*in situ*), invasive, and metastatic breast cancers [16].

The stages of breast cancer are reported based on the size and type of tumor, and the penetration of cancer cells in the breast tissue [17]. The breast cancer stages are categorized from 0 to IV with increasing severity, with stage 0 as localized and non-invasive nodules to stage IV with metastasis to distant organs [8]. The five-year overall survival rates for patients at stages 0-III are promising (>70%), but for patients with metastasis, the survival decreases dramatically to 22% (Figure 1.1) [2].

5 year Overall Survival by Stage		
Stage	5- year overall survival	Classification
0	100%	In situ
I	100%	Cancer formed
II	93%	Lymph nodes
III	72%	Locally advanced
IV	22%	Metastatic

Figure 1.1. Breast cancer stages and 5-year overall survival rate. Adapted from [2].

Effective prevention of breast cancer mortality requires early detection of the primary breast tumor, where the tumor can be removed by surgery and effectively treated by chemotherapy [18, 19]. Diagnostic methods for breast tumors include family history check, physical examination, ultrasound breast imaging, biopsy examination, mammography, and magnetic resonance imaging [20-23].

1.2.2 Breast tumor development

The breast is composed of fatty tissues called adipose tissue, with networks of lobules and ducts that are lined with epithelial cells (Figure 1.2) [16]. The adipose tissues comprise primarily adipocytes, as well as cells including fibroblasts, macrophages, lymphocytes, and endothelial cells [24]. The breast can undergo dramatic morphologic changes during puberty, pregnancy and lactation in response to hormones and growth factors, with the signaling mechanisms tightly regulated for the growth of epithelial cells [25]. In the case of cancer, the signaling pathways are altered, leading to dysregulation of

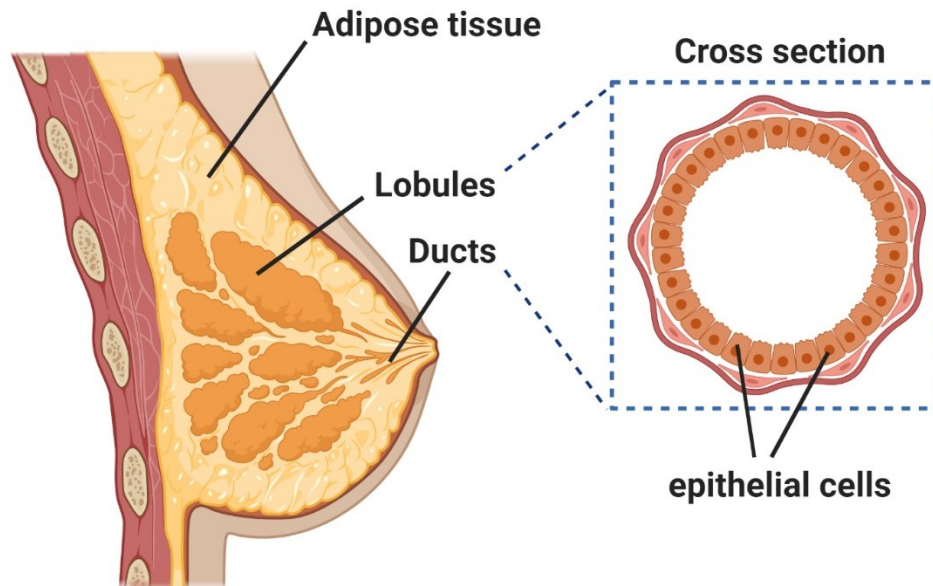


Figure 1.2. Anatomy of normal breast. Most breast cancers arise from the epithelial component of the breast that lines the lobules and ducts, leading to carcinoma. Created with BioRender.com.

cell proliferation, survival and migration [26]. This tumorigenesis process can result from hyperactivation of proto-oncogenes such as human epidermal growth receptor 2 (HER2) [27] and/or loss of tumor suppressor genes such as breast cancer associated gene 1 and 2 [28, 29].

Further tumor development can be influenced by the tumor microenvironment, as described later in the section. Blood vessels are crucial for survival and growth of the tumors, with angiogenesis as a hallmark of cancer [30]. Macrophages infiltrated into the tumor site generate an inflammatory microenvironment, where production of cytokines and inflammatory mediators in the breast tumors and the tumor-associated breast adipose tissues promote tumor progression and metastasis [31, 32].

1.2.2.1 Angiogenesis

Tumor growth requires the process of angiogenesis, which is the formation of new blood vessels from the existing vessels. Under normal physiological situations, angiogenesis occurs during normal growth, wound healing, human female menstrual cycle and pregnancy [33]. In the case of cancer, the growth and survival of malignant tumors are dependent on angiogenesis for supplying blood, where oxygen and nutrients are obtained [34, 35]. Angiogenesis is stimulated by the production of pro-inflammatory and pro-angiogenic cytokines such as tumor necrosis factor alpha (TNF- α), vascular endothelial growth factor (VEGF) and interleukin (IL)-8, from the cancer cells and the surrounding stromal cells [34]. Other molecules such as sphingosine-1-phosphate, a bioactive lipid mediator, also contributes to angiogenesis by signaling processes involved in vascular maturation and permeability [36, 37].

1.2.2.2 Cells within the tumor microenvironment

One of the major cell types present in the tumor microenvironment is cancer-associated fibroblasts. The majority of these cells are derived from resident fibroblasts that are activated in response to growth factors and cytokines including transforming growth factor beta (TGF β) and platelet derived growth factor that are abundantly expressed at the tumor site [38]. In turn, cancer-associated fibroblasts produce growth factors and cytokines that are important in promoting tumor growth and angiogenesis [39]. The activated cancer-associated fibroblasts release proteolytic enzymes such as the matrix metalloproteinases (MMPs) and heparinase for extracellular matrix (ECM) remodeling [40].

Massive numbers of immune cells are present in the tumor microenvironment, including innate immune cells such as macrophages, mast cells, neutrophils, dendritic cells, myeloid derived suppressor cells and natural killer (NK) cells, as well as adaptive immune cells such as T and B lymphocytes [41]. The tumor-associated macrophages are differentiated from monocytes and can be polarized into M1 or M2 subtypes, which are reversible [42]. The M1 macrophages are activated by interferon gamma and considered to have tumoricidal effects, whereas the M2 macrophages are activated in response to IL-4 and IL-13 to have tumorigenesis effects [43, 44]. Cells in the tumor microenvironment regulate the polarization of macrophages, such as the production of IL-4 by cancer cells and CD4⁺ T cells [45].

1.2.2.3 Tumor-promoting inflammation

Inflammation is a critical response for wound repair and elimination of infections [46]. A controlled inflammatory response is beneficial, whereas a dysregulated

inflammatory response can lead to common chronic diseases such as atherosclerosis, fibrosis, obesity and cancer [47].

Inflammation can be mediated by cytokines, chemokines and other inflammatory mediators. Cytokines and chemokines are small signaling protein molecules that regulate immune responses. Chemokines mediate chemo-attraction between cells [48]. Pro-inflammatory cytokines such as TNF- α , IL-1, IL-8 and IL-6 are secreted in response to the initial inflammatory stimuli, which is followed by secretion of chemokines to recruit immune cells like macrophages and lymphocytes to the site of infection or damage [49]. This results in acute inflammation that can be rapidly resolved within hours or days [47]. When the initial stimulus is resolved, there is a shift from pro-inflammatory to anti-inflammatory cytokine production, such as IL-4, IL-10 and IL-13 [50]. These would limit the progression of inflammation and allow the affected site to restore its normal conditions. However, if the acute inflammation is unable to be resolved, it will transit into chronic inflammation [51]. One of the factors that can drive chronic inflammation would be lysophosphatidic acid (LPA).

LPA is a bioactive lipid produced from lysophosphatidylcholine (LPC) by the secreted enzyme autotaxin (ATX) [52]. LPA binds to at least six different LPA receptors (LPAR1-6) that are coupled to G proteins, leading to activation of signaling pathways involved in wound healing, inflammatory diseases and cancer [53-55]. ATX/LPA signaling stimulates angiogenesis, inflammation, tissue remodeling, cell proliferation, differentiation, motility and survival, leading to cancer progression and metastasis [56-58]. In tumors such as neuroblastoma, melanoma and thyroid tumor, ATX is produced directly from the cancer cells [59, 60]. However, in breast cancer, ATX is abundantly produced in tumor-associated

breast adipose tissue instead of the tumor itself [31]. Breast cancer cells secrete inflammatory mediators that increase the production of ATX in the tumor-associated breast adipose tissue, leading to production of LPA, which signals further inflammation and results in a vicious cycle that drives tumor progression and metastasis [31].

Extensive infiltration of immune cells is observed in solid tumors, which is similar to the inflammatory conditions observed in the wound healing process of non-cancerous tissues [61]. This leads to the description of tumors as “wounds that do not heal” [61]. The inflammation at the tumor site can contribute to tumor progression through the production of molecules that induce processes including cell proliferation, limited cell death, promotion of angiogenesis, and modification of the extracellular matrix [30, 62, 63].

1.2.3 Breast cancer metastasis

Metastases occur when cancer cells spread from the primary tumor to distant sites of the body, where they seed and proliferate into secondary tumors [64]. Tumor metastases are responsible for approximately 90% of deaths in cancer patients [65]. About 25-50% of breast cancer patients will develop metastases, which can develop even after the removal of the primary tumors due to previous seeding of the cancer cells at the metastatic site [65]. Our current therapeutic methods against breast cancer are not effective in preventing and treating breast cancer metastases.

Metastasis involves a complex cascade of events that are further described below:

- 1) angiogenesis at the primary tumor site leading to extensive blood supply allowing for tumor growth and metastasis to occur,
- 2) de-adhesion of the cancer cells to escape from the primary tumor site,
- 3) invasion of and migration through the basement membrane and extracellular matrix of the tumor site and blood or lymphatic vessels,
- 4) invasion of the

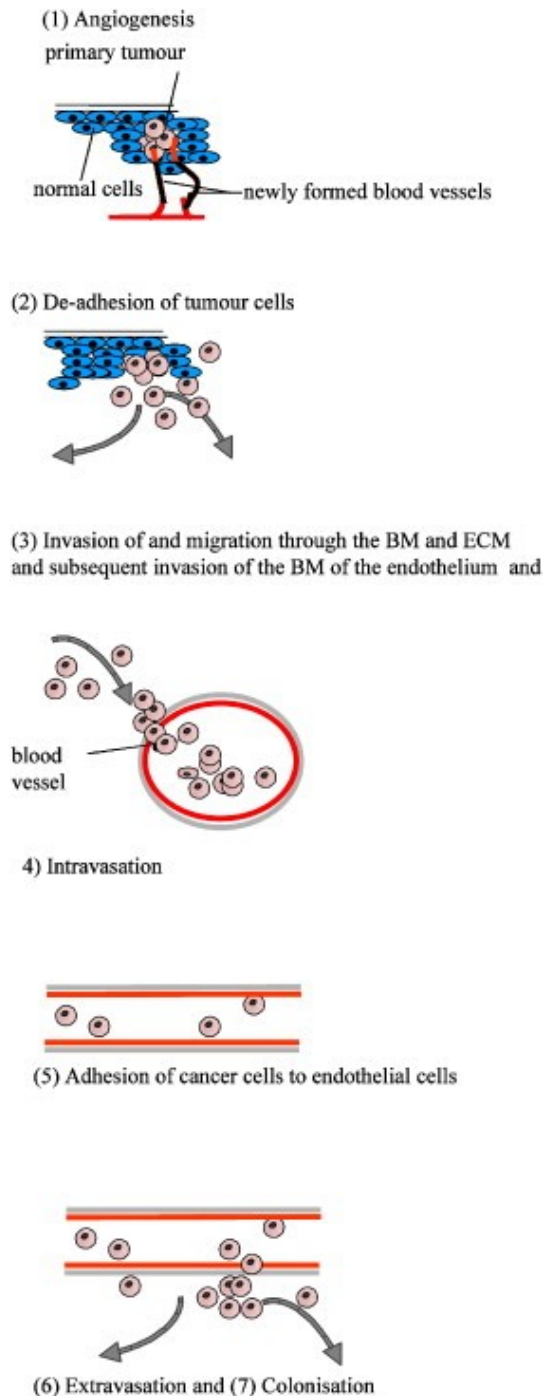


Figure 1.3. The cascade of metastasis. (1) angiogenesis at the primary tumor site leading to extensive blood supply allowing for tumor growth and metastasis to occur (2) de-adhesion of the cancer cells to escape from the primary tumor site (3) invasion of and migration through the basement membrane (BM) and extracellular matrix (ECM) of the tumor site and blood or lymphatic vessels (4) invasion of the cancer cells into blood or lymphatic vessels for transport (5) adhesion of the circulating cancer cells to the endothelial cells at the target organ site (6) Extravasation of the cancer cells through the endothelial cell and BM at the target organ site (7) Colonization and growth of tumor at the secondary site. Adapted from [66].

cancer cells into blood or lymphatic vessels for transport, 5) adhesion of the circulating cancer cells to the endothelial cells at the target organ site, 6) extravasation of the cancer cells through the endothelial cells and basement membrane at the target organ site, 7) colonization and growth of tumor at the secondary site (Figure 1.3) [66].

Metastatic disease could not progress without angiogenesis, which provides the blood supply required for tumor growth [34]. The incompletely formed new intratumoral vessels often have more permeable vessel walls that allows cancer cells to enter the systemic circulation [67]. The disaggregation of cancer cells from the primary tumor is due to loss of cell-cell adhesion, where the expression of adhesion molecules like cadherins are altered [68].

Cancer cells gain motility by adopting an elongated mesenchymal morphology in order to be metastatic [69]. An epithelial-to-mesenchymal transition (EMT) is normally observed in cells that are metastatic. Networks of signaling pathways mediate EMT, involving molecules such as TGF β , extracellular signal-regulated kinases/mitogen-activated protein kinases, phosphatidylinositol 3-kinase/protein kinase B (PI3K/AKT) and transcription regulators Twist and Snail [70]. Markers for identifying cells that undergo EMT include down-regulation of E-cadherin expression, which is a transmembrane protein forming adherence junctions between the epithelial cells [70].

The dissemination of cancer cells from the tumor site involves the dissolution of the extracellular matrix components like collagen [71]. This is facilitated by cancer or stromal cell production of hydrolytic enzymes, such as cathepsins and MMPs [72]. The action of these enzymes is also important for cancer cell extravasation at the secondary site.

The selection of secondary tumor site for metastatic dissemination varies for cancer cells arising from different primary sites. The “seed and soil hypothesis” proposes that particular cancer cells (“seed”) will find a suitable environment (“soil”) in which to develop and grow [73]. An alternative hypothesis is that circulating cancer cell aggregates simply become trapped in the first vascular bed that they encounter [74]. However, some metastatic sites such as long bones, brain, and adrenal gland that arise from breast cancer are difficult to explain [75].

1.2.4 Breast tumor receptor positivity

Cellular markers like receptor positivity of the breast tumor is often examined for determination of prognosis and therapeutic management strategies [76]. These receptors are estrogen receptor (ER), progesterone receptor (PR), and HER2, with determination using immunohistochemistry (IHC) or fluorescent *in situ* hybridization [77]. The threshold for positivity of ER and PR is determined when at least 1% of the cancer cells are positively stained in the breast tumor sample [78], whereas the threshold for HER2 positivity is 30% strong immunostaining [79].

About 70-80% of breast cancers express ER and/or PR, and their presence in breast tumors are recognized as a favorable prognostic biomarker with target therapies available [80, 81]. Common therapies include tamoxifen, a synthetic antiestrogen that acts as a competitive inhibitor of estrogen, although aromatase inhibitors are used in postmenopausal women [82]. The expression of ER and PR in the normal pre-menopausal adult breast is at low basal levels and with sparse distribution [83]. Both ER and PR are members of the nuclear receptor family that regulate cellular gene expression when activated, with estrogen and progesterone as the ligands, respectively [84]. Estrogen and

progesterone are hormones important in female normal breast development, including the formation of the ductal structures and elaboration of lobules of the normal epithelium, which are processes that become subverted in breast cancer development [85-87]. The ER signaling pathway contributes to pro-survival and proliferation signals that overwhelm pro-death and quiescence signals in many malignant breast cells [88]. The overexpression of PR in breast cancer cells induces the carcinogenic phenotype of invasion into stromal layers [89].

The HER2 overexpressing or positive breast cancer makes up 15-20% of all invasive breast cancer cases, most often lacking expression of ER and PR [90, 91]. HER2 is a membrane receptor tyrosine kinase, and when activated, it stimulates intracellular signaling pathways like PI3K/AKT, important for epithelial cell growth and differentiation [92]. Amplification of HER2 gene in breast cancer is associated with increased cell proliferation, cell motility, angiogenesis, tumor invasiveness, metastasis, and reduced cell apoptosis [93]. Overexpression of HER2 is associated with high tumor grade, worse prognosis, and higher rates of recurrence [94]. The HER2 positive breast cancer is more likely to have early metastases if untreated, especially development of central nervous system metastases [95]. However, targeted therapies against HER2 exist, including a monoclonal antibody trastuzumab and the small molecule tyrosine kinase inhibitor lapatinib [96, 97].

Triple-negative breast cancer is where ER and PR are not expressed and HER2 is not amplified or overexpressed [98]. It accounts for 10-20% of breast cancer cases and there are no standard target treatments available [99, 100]. The most frequently used treatment is doxorubicin-based chemotherapy, although the response rate is only 40-70%

[101]. Triple-negative breast cancer is more aggressive with a higher chance of brain metastasis and with poor prognosis including a higher chance of recurrence and shorter survival following the first metastatic event [76].

1.3 HCMV infection as a risk factor for cancer

1.3.1 Oncogenic role of HCMV

Infectious agents contribute to over 15% of all cancers and 64% of these agents are estimated to be viruses [3]. The determination of whether a virus has a causal relationship to cancer can be difficult and often undergoes many years of debate before it is well accepted as an oncovirus [102]. The criteria of determining an oncovirus is described as the following: 1) association between viral infection and malignancy based on epidemiologic evidence; 2) finding of integrated or episomal viral genomes and gene products in the cancer cells; 3) clonal amplification of viral sequences in tumors; 4) virus having direct oncogenic properties, which can transform cells [103].

Epstein-Barr virus (EBV) that was discovered in cultured cancer cells of Burkitt's lymphomas provided the first evidence that viral infections cause cancer in human beings [104]. EBV genome and antigens are detected in a wide range of cancer types [105]. Epidemiological evidence showed EBV-infected individuals had increased risk of developing Burkitt's lymphoma [106], and EBV has the capacity of transforming normal lymphocytes [107]. Human papillomavirus (HPV) is another well-accepted oncovirus that has a causal role in cervical cancer, with the HPV DNA detected in cervical cancer biopsies [108, 109]. Oncogenes are present in high-risk HPV strains, which facilitate the cell transforming capacity of the virus [110]. The current clinical use of the HPV vaccine that

is preventing infection and reducing the incidence of cervical cancer in the long run is very compelling [111, 112].

Apart from the current well-recognized oncoviruses, there are other viruses that show association with cancers and have been investigated for their oncogenic role, like HCMV. The study of glioma in a mCMV-infected mouse model shows increased tumor progression and reduction in animal survival [113]. Research studies have shown the detection of HCMV viral proteins and DNA in various cancer tissues, including glioblastoma [114], colorectal cancer [115], prostate cancer [116], ovarian cancer [117], and breast cancer [118]. However, controversies do exist, where several studies failed to detect HCMV genome and/or proteins in any of the specimens tested [119-121]. Suggestions have been made to explain this inconsistency, including sample preparation (degradation of DNA in formalin-fixed and paraffin-embedded tissues), differences in primers and antibodies used, and features of the virus [122, 123]. Currently, there is not a clear conclusion.

It has been proposed that HCMV viral products could have the potential to transform cells and cause malignancy. There is evidence that the HCMV immediate early (IE) proteins pUL122 and pUL123 stimulate cell entry into the S phase [124]. Fibroblasts and human mammary epithelial cells infected with HCMV show pUL122 binding to the tumor suppressor p53, which inhibits p53 activity and increases cell cycle progression [6, 125]. The pUL123-expressing glioblastoma cells shows enhanced proliferation due to the activation of the PI3K/AKT pathway [126]. It has also been reported that a clinical isolate of HCMV, strain DB, transforms human mammary epithelial cells, and these cells develop tumors when injected into mice [6]. Furthermore, these HCMV-infected human mammary

epithelial cells show upregulated expression of several oncogenes, enhanced activation of pro-survival genes, and upregulated markers of cell proliferation and EMT [127].

1.3.2 Oncomodulatory role of HCMV

Apart from being oncogenic, HCMV has also been proposed to have an oncomodulatory role in enhancing malignancy, where the infected cells show increased oncogenesis and/or the infection alters various intracellular signaling pathways that would promote oncogenesis [128, 129]. HCMV-infected neuroblastoma cells are more invasive due to the downregulation of the Neural Cell Adhesion Molecule on the cancer cells [130]. HCMV-infected colorectal cancer-derived stem cell-like cells show enhanced cell proliferation and migration due to activation of the EMT pathway [131]. HCMV infection also activates EMT features in human mammary epithelial cells [6]. On the other hand, there are reports showing HCMV infection as having an inhibitory role in malignancy. It has been reported that HCMV challenge induces a mesenchymal-to-epithelial transition (MET) in the MDA-MB-231 and SUM1315 cancer cell lines, causing a reduced migratory capacity [132]. Mice with xenografted HCMV infected HepG2 cells show limited tumor growth, increased apoptosis and even the absence of tumors in the liver compared to the mock-treated mice [133]. A HCMV homolog of the human cellular IL-10, cmvIL-10, is secreted from the HCMV-infected cells and binds to the cellular IL-10 receptor [134]. The MDA-MB-231 and MCF-7 breast cancer cells that are exposed to cmvIL-10 show enhanced proliferation and migration [5, 135, 136].

Further evidence shows that HCMV infection fulfills many criteria of the hallmarks of cancer, including sustaining proliferative signaling, evading growth suppressors, avoiding immune destruction, enabling replicative immortality, tumor-promoting

inflammation, activating invasion and metastasis, inducing angiogenesis, genome instability and mutation, resisting cell death, and deregulating cellular energetics [30]. HCMV proteins, such as the previously described IE and cmvIL-10 are primarily involved in these processes [137].

HCMV infection can also affect tumor progression by modulating the tumor microenvironment. The tumor-associated macrophages that display an M2 phenotype are tumor-promoting and mostly produce anti-inflammatory cytokines such as IL-10 and TGF β [138]. HCMV-infected glioma cancer stem cells produce cmvIL-10, a homolog of IL-10, which induces monocytes to produce an M2 phenotype to repress host immune responses [139, 140]. On the contrary, a study shows HCMV-infected monocytes display a skewed polarization towards the pro-inflammatory M1 phenotype [141].

1.4 Cytomegalovirus (CMV)

1.4.1 Overview of CMV

CMV is a β -herpesvirus that belongs to the *Herpesviridae* family. It is a double-stranded DNA virus with a large and complex genome [142]. CMV is a highly host-specific virus and species-specific strains have been identified in many species including mice, chimpanzee and human beings [143]. Transmission of CMV is commonly through direct contact with body fluids such as blood, saliva, urine, tears and breast milk, where the infectious viral particles can be shed [144-146]. The virus can also be transmitted through organ transplantation when the donor is seropositive, from infected mother to the child through placenta, and during birth when the child contacts with the virus in the genital tract of a seropositive mother [147]. HCMV produces lifelong infections with 40-70% of the adult population in developed countries being infected [148, 149]. This rate increases to

~85-90% when people reach 75-80 years of age [150]. The highest HCMV seroprevalence is observed in South America, Africa, and Asia (Figure 1.4) [151]. Factors such as geography, ethnicity, race, socioeconomic status and exposure to HCMV transmission routes contribute to the difference in seroprevalence [152].

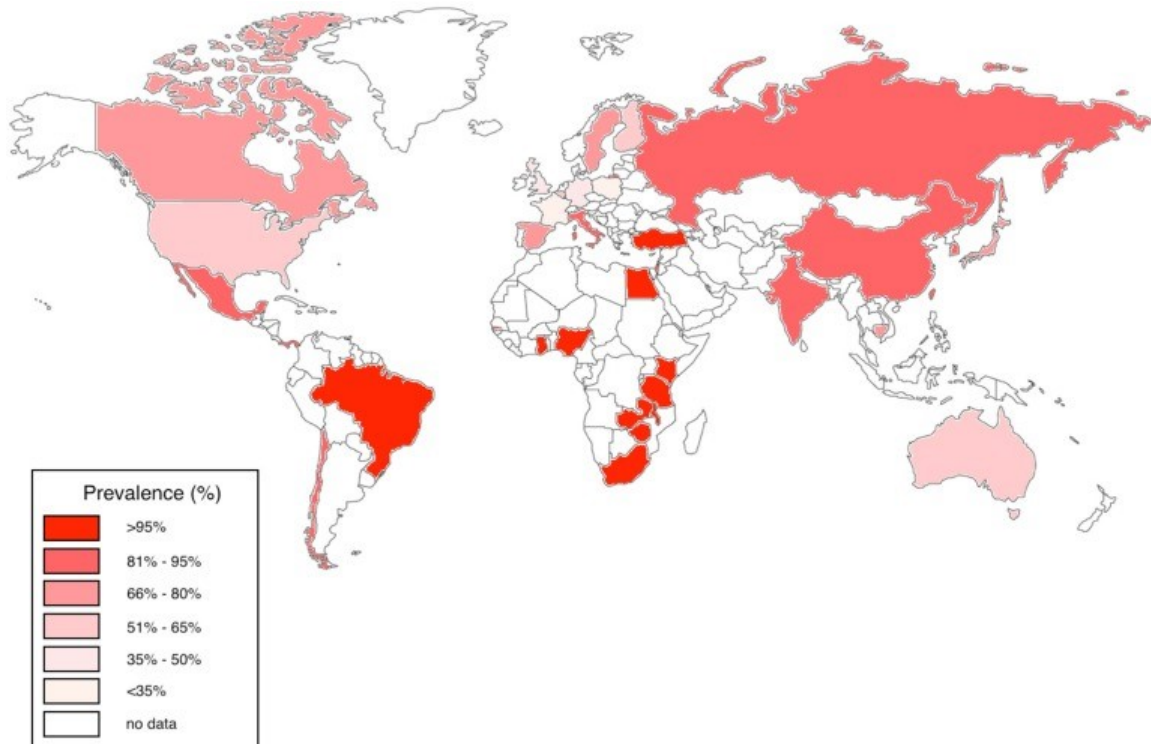


Figure 1.4. HCMV seroprevalence rates in adults worldwide. Representing studies published between 2005-2015 for adults 16-50 years of age. Adapted from [151].

HCMV infection normally causes no noticeable symptoms in immunocompetent individuals [153]. For adults, HCMV infection can be associated with fever, malaise, abnormal liver function test results, and infectious mononucleosis [154, 155]. Congenital HCMV infection can lead to consequences such as chorioretinitis and sensorineural hearing loss [156]. In immunocompromised hosts, HCMV infection can lead to morbidity and mortality, such as retinitis and hepatitis in organ transplant recipients and increased cardiovascular disease in the aging population [157, 158].

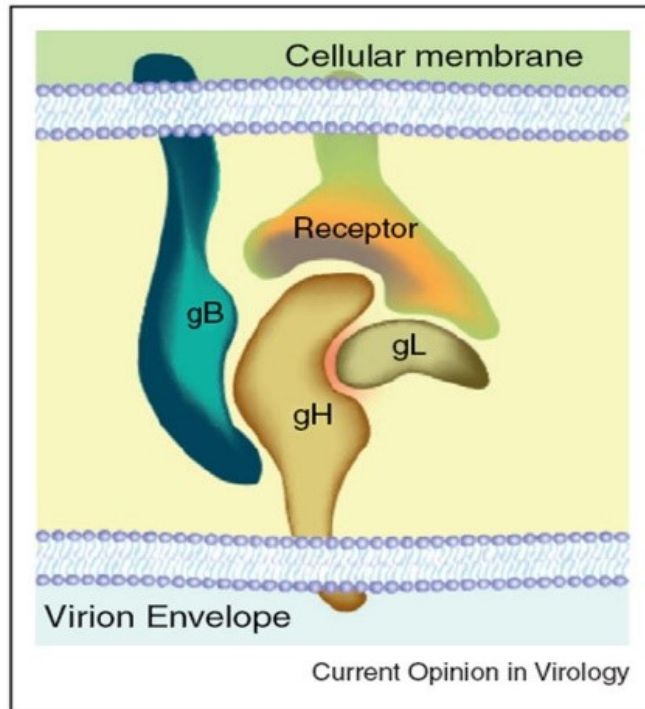
1.4.2 Cell tropism

CMV has a broad cell tropism, where it enters and replicates in a wide range of cell types, including fibroblasts, epithelial cells, endothelial cells, smooth muscle cells, neural stem/progenitor cells and macrophages [159-162]. However, the laboratory strains of HCMV that have been extensively passaged in fibroblasts possess mutations leading to the loss of this broad cell tropism [163].

The HCMV virion envelope contains multiple membrane glycoproteins that are important for viral entry (Figure 1.5) [164]. The glycoprotein B (gB) is essential for initial attachment to the cell surface through interactions with heparan sulphate glycosaminoglycans [165], viral entry through processes including fusion [164], and interaction with various cellular receptors like epidermal growth factor receptor (EGFR) and platelet derived growth factor receptor alpha (PDGFR- α) [166, 167]. The gH-gL complex is essential for HCMV entry into all cell types [164]. It can form a pentameric complex with UL128, UL130, and UL131, which is required for entry into epithelial cells, endothelial cells and monocytes [160, 168]. The laboratory strains of HCMV contain mutations in genes such as UL128, and therefore are unable to infect cell types such as epithelial cells and macrophages, that are susceptible to the wild-type or clinically isolated strains [163].

Oncogenic alleles such as simian virus 40 T antigen inhibit HCMV infection at several stages, including viral entry, viral gene transcription, and production of infectious

a)



b)

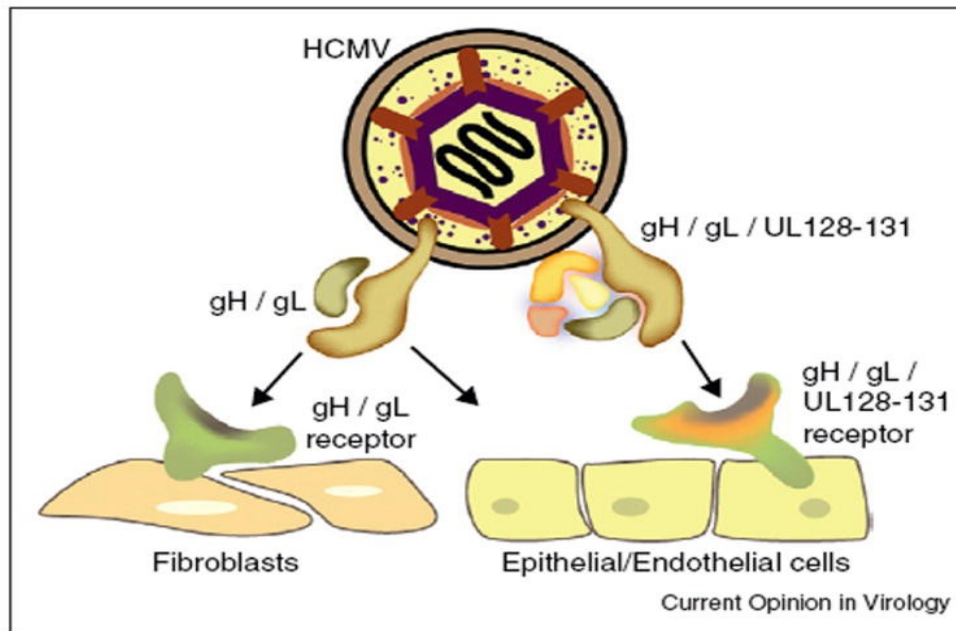


Figure 1.5. HCMV virion envelope glycoproteins for viral entry. Glycoprotein B (gB) facilitates HCMV fusion and attachment to susceptible cells (a). The role of gH/gL complex and UL128/UL130/UL131 (UL128-131) complex for HCMV entry into different cell types (b). Adapted from [164].

viral particles [169]. Viral entry into cells expressing SV40 Tag can be rescued by overexpression of PDGFR- α , but the full production of viral antigens and infectious viral particles is not rescued [169].

Some cell types do not support full CMV replication, such as lymphocytes and neutrophils, where only IE antigen is expressed but not late antigen. However, these cells may traffic CMV through the circulation [170]. In combination with the broad cell tropism, CMV can be detected in various organs throughout the body of an infected host, such as salivary glands, kidneys, spleen, and lungs [171, 172].

1.4.3 Life cycle of CMV

After entry into susceptible cells, CMV produces viral proteins in three stages: immediate early (IE), early (E) and late (L) (Figure 1.6) [173]. At each stage, these viral

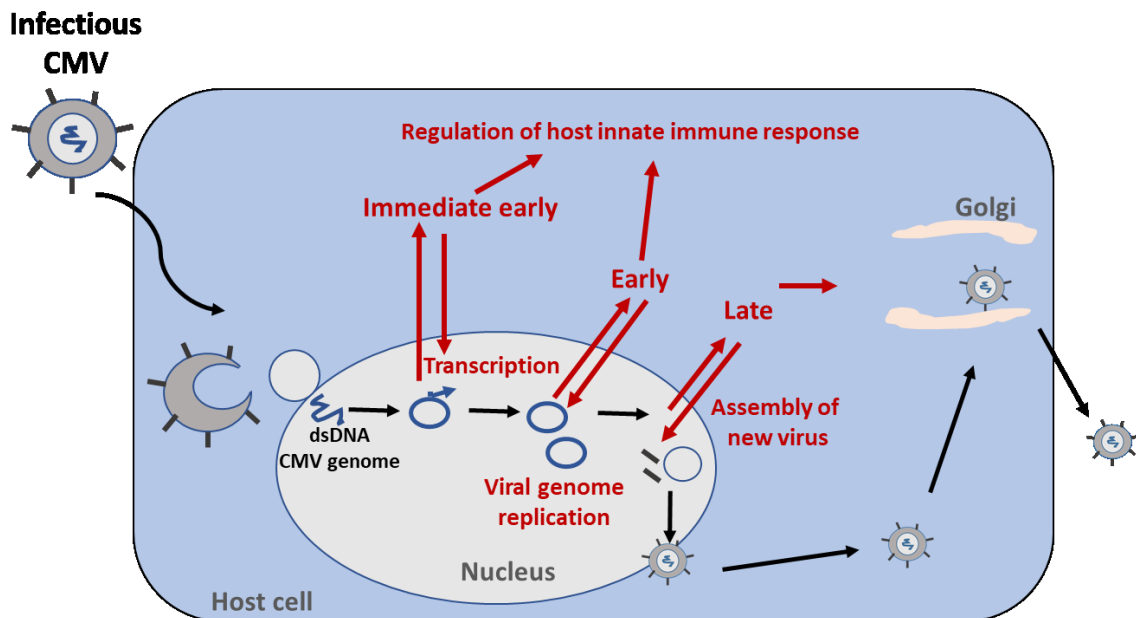


Figure 1.6. Replication of CMV following entry of host cell. Three stages occur following CMV entry into the susceptible cell, including immediate early, early and late stages, each producing corresponding viral proteins that are responsible for various aspects of virus replication.

proteins have essential roles in establishing a productive CMV infection. The IE proteins are important for transcription regulation, the E proteins support viral replication, and the L proteins are needed for the assembly of new viral particles [174].

Apart from undergoing lytic replication, CMV infection can also enter a latent state where the viral genome is retained in the host with restricted expression of viral genes [175]. In contrast to the initial active infection where virus replication is high, replication in chronic and presumed latent infections is at low subclinical levels, if present at all [176]. The establishment of latency is a strategy for HCMV to evade or delay the host immune responses against the virus, while allowing the viral genome to be maintained in the host [177]. This latent state has been described as symbiotic since it can confer immune benefits to the host against other infections [178, 179].

Reactivation to full virus replication and production of infectious virus can occur during inflammation and stress, in the aging population, and in immunocompromised hosts including organ transplant recipients undergoing immunosuppressive therapies [157, 180-182]. Reactivation of HCMV infection can be life-threatening, especially in immunocompromised or critically ill patients [183]. Also, HCMV reactivation in patients with solid tumors can lead to clinically relevant HCMV disease where the HCMV genome is detected by PCR in the serum at >1000 copies/mL and fever of unknown origin persists despite broad antibiotic treatment [184].

CMV latency is established in hematopoietic progenitor cells and in cells of the myeloid/monocyte lineage that serve as a reservoir for the viral genome [185, 186]. The reactivation of CMV occurs in differentiated myeloid macrophages and dendritic cells [187-189]. For human beings, salivary glands are major sites for retaining the HCMV

genome and with frequent reactivation [171]. As for the mouse, the lungs serve as a major site for retaining mCMV viral genomes during latency [172].

1.4.3.1 CMV transcripts and proteins

CMV contains double-stranded DNA that is large and complex, with the HCMV genome approximately ~240 kbp in length and encoding more than 700 open reading frames [190]. There are two major regions in the genome, the unique long and unique short segments [191]. The unique long segment encodes some of the well-known HCMV gene products including IE1 (UL123), IE2 (UL122), gB (UL55), pp65 (UL83), and cmvIL-10 (UL111A) [191]. IE genes are immediately transcribed within one hour post-infection, with the proteins produced for regulation of viral replication [192]. Viral proteins gB and pp65 are produced at the late stage of HCMV infection for assembly of the new viral particles [174]. cmvIL-10 is important to repress the host immune responses [140].

There are also latency-associated transcripts and proteins that exert functions including anti-apoptotic effects, heterochromatic modification of histones, and generation of virally encoded microRNA that regulates cellular gene expression [193-195]. One example is HCMV latency-associated-cmvIL10 (UL111.5A), which has homology to IL-10 and cmv-IL10, but is expressed during the latent phase of infection for avoiding immune recognition and clearance [196]. There are also non-coding transcripts detected during HCMV latency, including beta 2.7 and Inc4.9, where Inc4.9 is hypothesized to contribute to epigenetic silencing of IE gene expression during the establishment of latency [197]. HCMV microRNA like miR-UL112-3p can target and downregulate toll-like receptor 2 (TLR2) expression, leading to decreased expression of proinflammatory cytokines in order for HCMV to maintain a latent infection [198].

1.4.4 Host immune responses against CMV infection

A strong innate immune response is produced during the initial CMV infection in the host. Initial recognition of CMV in the infected host is through pattern recognition receptors such as TLR2 and TLR9 that are located on the plasma and endosomal membranes [199-201]. This stimulates production of proinflammatory cytokines such as type I interferons that are important for antagonizing HCMV infection [202]. Another key player in the host innate immune response is the NK cell, where it recognizes the stress-induced ligands expressed on the surface of infected cells, leading to cell destruction [203]. For both human and mouse, genetic defects in their NK cell responses show extreme susceptibility to CMV infection [204-206]. To avoid clearance, CMV encodes proteins that target and destroy a major stress protein expressed on the surface of infected cells [207]. In addition, a rhesus macaque model of CMV shows *cmvIL-10* attenuates innate immune responses against CMV infection, leading to a long-term deficit of adaptive antiviral immunity [208].

About seven days after maximum replication of CMV in the infected host, the adaptive immune responses against the infection start to mature, with CD4⁺ and CD8⁺ T cells specific for CMV observed in the peripheral blood [209, 210]. These CMV-specific T cells dominate the memory compartments of the infected individual [211]. The establishment and maintenance of the adaptive immunity against CMV is important for keeping the virus at latency, where viral replication is restrained [211]. In immunocompromised hosts or individuals under situations such as stress, CMV can be reactivated to produce infectious viral particles again [212].

The immunoglobulin M (IgM) antibody against CMV is produced following primary infection, as well as due to reinfection with a different strain of CMV [213]. The immunoglobulin G (IgG) antibody against CMV also establishes in the infected host following primary infection. The IgG titre is higher during initial infection, which then gradually declines although it is still detectable [214]. Therefore, the presence of IgG antibody against CMV indicates whether the host was ever infected with CMV.

1.4.5 CMV infection regulates cellular responses

CMV infection can lead to the production of immunosuppressive factors, such as TGF β and IL-10 [215]. This immunosuppressive effect is further enhanced by HCMV infection through the production of cmvIL-10, which binds to the IL-10 receptor like the natural ligand [134]. cmvIL-10 is only found to be encoded by HCMV and not CMV targeting other species such as mouse.

HCMV infection also induces inflammation and could lead to a variety of inflammatory diseases such as atherosclerosis, retinitis, and hepatitis [171, 216]. CMV is recognized by TLR2 and CD14, triggering inflammatory cytokine production through TLR2 dependent activation of NF- κ B [217]. Inflammatory genes such as IL-6, IL-7, IL-11, and cyclooxygenase 2 (COX-2) are upregulated by CMV infection [218, 219]. The expression of IL-1 β is regulated by the HCMV IE gene [220], and in turn IL-1 β can inhibit HCMV replication [221]. These inflammatory responses are suggested to play a role in cancer. HCMV infection increases IL-6 production and mediates an inflammatory response in patients with salivary gland cancer, which associates with tumor development [222]. A correlation is also found between HCMV IE protein and overexpression of COX-2 in breast tumors of breast cancer patients [223].

1.5 HCMV and breast cancer

1.5.1 Epidemiological studies of HCMV and breast cancer

Although HCMV can be detected in and transmitted through breast milk, there is no evidence showing that transmission of a virus in breast milk increases the risk of breast cancer in women who were breast-fed [224, 225]. In fact, it has been hypothesized that a late exposure to HCMV in life leads to an increased risk of breast cancer [226]. A study in Australia was conducted on cases of invasive breast cancer and control patients that were all at age less than 40 years old, resulting in no difference in seropositivity, which is at 59% and 57%, respectively [227]. However, in seropositive women, the mean IgG values are higher in women with breast cancer compared to the control group (1.20 vs 0.98 OD unit, $p=0.005$) [227]. It has also been reported that elevation in serum HCMV IgG antibody levels precedes the development of breast cancer in some women [228]. A correlation between HCMV IgG level and breast cancer has been supported by several groups [226-228]. This correlation was not found with EBV seropositivity, which is another virus from the *Herpesviridae* family [227, 228]. On the other hand, a study in India shows all tested women to be positive for IgG against HCMV, but the antibody titres are not significantly different between patients with invasive breast cancer and patients with benign breast disease (163.52 U/mL vs 159.53 U/mL, $p=0.76$) [229].

It is unclear whether breast cancer patients are more susceptible to HCMV infection. With the high seroprevalence of HCMV infection in the adult population, it is likely that the HCMV seropositive breast cancer patients were already infected prior to breast tumor development. The study in India where they observed that all women with breast cancer or benign breast disease were positive for IgG against HCMV, none of these women were IgM positive against HCMV [229]. The lack of IgM against HCMV indicates that there is

no reinfection with another strain of HCMV in these breast cancer patients, therefore there is no indication that they were more susceptible to the virus.

1.5.2 Detection of HCMV in breast tumors

The presence of HCMV protein, DNA and RNA in patient breast tumors has been examined by several laboratories across the world, but the results are controversial (Table 1.1). High detection of >90% for HCMV viral presence in the breast tumors is supported by several groups, with the patient populations from Sweden, USA, Norway, China and Iraq (Table 1.1) [4, 118, 230-232]. This is particularly evident when the detection targeted HCMV proteins using immunohistochemistry (IHC), but the high positivity rate is also observed when verified using other detection methods such as *in situ* hybridization (ISH) that targets viral DNA and RNA (Table 1.1). Some studies used IHC and PCR detection methods, resulting with 40-80% positive detection for HCMV viral presence in breast tumors from patient populations examined in Egypt, China, and Iran (Table 1.1) [233-237]. However, there are studies from Australia, New Zealand, Mexico, Egypt, and Iran showing very little or no detection of HCMV DNA and/or proteins in the examined breast tumors, with most of the detections performed using quantitative real-time PCR (qPCR) (Table 1.1) [121, 238-241]. A “hit-and-run” hypothesis was suggested for this low detection observed, which is a mechanism where the virus can mediate cellular transformation through an initial “hit”, but the viral molecule is lost (“run”) when cells are maintaining the transformed state [241]. The association between HCMV and breast cancer remains unclear when looking at the presence of viral proteins and/or DNA in breast tumors due to the highly variable results obtained from different groups.

Table 1.1. Percent of positive detection for HCMV protein, DNA and mRNA in human breast tumors.

Methods	Percent of positive detection (Number of papers)	Country (References)
Protein		
IHC	90-100% (5)	USA (Harkins, L.E., et al, <i>Herpesviridae</i> , 2010) [118] Sweden (Taher, C., et al, <i>PLoS One</i> , 2013) [4] Norway (Rahbar, A., et al, <i>Clin Breast Cancer</i> , 2017) [230] China (Cui, J., et al, <i>Cancer Biomark</i> , 2018) [231] Iraq (Al-Nuaimi, B. N., et al, <i>Biochemical and Cellular Archives</i> , 2019) [232]
	40-80% (2)	Egypt (El Shazly, D. F., et al, <i>Clin Breast Cancer</i> , 2018; Ahmed, R. A., et al, <i>Journal of Solid Tumors</i> , 2016) [233, 242]
	0% (1)	Iran (Mohammadzadeh, F., et al, <i>Infect Agent Cancer</i> , 2017) [238]
DNA		
ISH	90-100% (2)	USA (Harkins, L.E., et al, <i>Herpesviridae</i> , 2010) [118] Norway (Rahbar, A., et al, <i>Clin Breast Cancer</i> , 2017) [230]
qPCR	100% (2)	Sweden (Taher, C., et al, <i>PLoS One</i> , 2013) [4] China (Cui, J., et al, <i>Cancer Biomark</i> , 2018) [231]
	0-20% (5)	Australia (Antonsson, A. et al, <i>PLoS One</i> , 2012) [239] New Zealand (Richardson, A.K., et al, <i>PLoS One</i> , 2015) [240] Iran (Mohammadzadeh, F., et al, <i>Infect Agent Cancer</i> , 2017) [238] Mexico (Utrera-Barillas, D., et al, <i>Infect Agent Cancer</i> , 2013) [241] Egypt (El Shazly, D. F., et al, <i>Clin Breast Cancer</i> , 2018) [233]
Standard PCR	40-80% (2)	China (Tsai, J.H., et al, <i>J Med Virol</i> , 2005) [243] Iran (Sepahvand, P., et al, <i>Asian Pac J Cancer Prev</i> , 2019) [236]
	0% (1)	Iran (Bakhtiyarizadeh, S., et al, <i>Asian Pac J Cancer Prev</i> , 2017) [121]
Nested PCR	40-80% (2)	Egypt (El-Shinawi, M., et al, <i>Ann Surg Oncol</i> , 2016) [237] USA (Harkins, L.E., et al, <i>Herpesviridae</i> , 2010) [118]
RNA		
ISH	100 (1)	Norway (Rahbar, A., et al, <i>Clin Breast Cancer</i> , 2017) [230]

Abbreviations used: IHC: immunohistochemistry; ISH: in situ hybridization; qPCR: quantitative real-time PCR

Table 1.2. Detection of HCMV DNA and/or protein in human breast tumors and non-cancerous breast tissues.

Country Sample storage Mean patient age Reference	Type of PCR Target gene Verification	Sample type (number positive/total number, % HCMV positive)	Other analysis	Percent of DNA positivity in tumor Comment
China Frozen 51 for breast cancer; 50 for non- cancerous Tsai, J.H., et al, <i>J Med Virol</i> , 2005 [235]	Standard PCR (DNA) IE2 Each sample tested three times. DNA confirmed by Southern hybridization	Breast tumor (47/62, 76%) Normal breast from non- cancerous (8/12, 67%) Fibroadenoma (20/32, 63%)	NA	76% Not significant between sample types
USA FFPE 48 for breast cancer; 36 for non- cancerous Harkins, L.E., et al, <i>Herpesviridae</i> , 2010 [118]	Nested PCR (DNA) gB Sequencing and Blast search	Breast tumors (6/8, 75%) Normal breast from non- cancerous (1/4, 25%)	IHC (Protein): Breast tumors (IE: 31/32, 97%; E/L: 21/25, 84%, L: 15/27, 56%) Normal breast from non- cancerous (IE: 17/27, 63%; E/L: 6/28, 21%, L: 11/28, 39%) Paired breast from breast cancer patient (IE: 12/13, 92%; E/L: 11/15, 73%, L: 10/13, 77%)	75% Greater detection when using IHC, especially for IE, with significantly higher detection in breast tumors PCR as a verification and performed in a small number of samples

			ISH for IE1 (DNA): Breast tumors (16/18, 89%) Normal breast from non-cancerous (11/18, 61%)	
Australia Frozen 57 for breast cancer Antonsson, A., et al, <i>PLoS One</i> , 2012 [239]	qPCR (DNA) IE NA	Breast tumor (0/54, 0%) Paired breast from breast cancer patient (0/10, 0%)	NA	0% No detection in any sample when using Real-time PCR
Sweden FFPE 57 for breast cancer Taher, C., et al, <i>PLoS One</i> , 2013 [4]	qPCR (DNA) IE NA	Brest tumor (12/12, 100%) Metastatic sentinel lymph node (10/11, 91%) Non-metastatic sentinel lymph node (0/5, 0%)	IHC (Protein): Breast tumor (IE and L: 73/73, 100%) Metastatic sentinel lymph node (IE and L: 32/34, 94%) Non-metastatic sentinel lymph node (IE and L: 20/35, 57%)	100% High detection in breast tumor and metastatic sentinel lymph node, suggesting association with metastasis PCR as a verification and performed in a small number of samples In contrast to most studies, high detection even with real-time PCR
Egypt Fresh	Nested PCR (DNA) IE	Non-IBC breast tumor (26/49, 53%)	HCMV IgG antibody: non-IBC (32/49, 65%)	53% We did not get specific PCR product when

53.3 for non-IBC; 48.9 for IBC El-Shinawi, M., et al, <i>PLoS One</i> , 2013 [244]	Sequencing and Blast search	Non-IBC non-cancerous breast (2/49, 4%) IBC breast tumor (22/28, 79%) IBC non-cancerous breast (0/28, 0%) Normal breast from non-cancerous (number unstated, 0%)	IBC (23/28, 82%)	using the same technique targeting against IE. There is possibility for getting false-positive results
Mexico FFPE 53 for breast cancer; 45 for fibroadenoma Utrera-Barillas, D., et al, <i>Infect Agent Cancer</i> , 2013 [241]	qPCR (DNA) IE2 and PP65 NA	Breast tumor (2/27, 7%) One positive for both IE2 and PP65, the other only positive for PP65 Fibroadenoma (0/20, 0%)	NA	7% Almost no detection in any sample when using Real-time PCR
New Zealand Frozen Age range:25-88 for breast cancer, mean not stated Richardson, A.K., et al, <i>PLoS One</i> , 2015 [240]	qPCR (DNA) PP65 NA	Breast tumor (0/70, 0%) Paired breast from breast cancer patient (2/70, 3%)	HCMV IgG antibody: (49/70, 70%)	0% Almost no detection in any sample when using Real-time PCR
Egypt Fresh	Nested PCR (DNA)	Non-IBC breast tumor (67/91, 74%)	NA	74%

52 for non-IBC; 49 for IBC El-Shinawi, M., et al, <i>Ann Surg Oncol</i> , 2016 [237]	IE Sequencing and Blast search	IBC breast tumor (39/44, 89%)		We did not get specific PCR product when using the same technique targeting against IE. There is possibility for getting false-positive results
Egypt FFPE 54.6 for breast cancer Ahmed, R. A., et al, <i>Journal of Solid Tumors</i> , 2016 [242]	NA	NA	IHC (protein) Breast tumor (L: 47/107, 44%)	NA
Iran FFPE 35.2 for breast cancer; 45 for non-cancerous Bakhtiyrizadeh, S., et al, <i>Asian Pac J Cancer Prev</i> , 2017 [121]	Standard PCR (DNA) gB NA	Breast tumor (0/150, 0%) Fibroadenoma (2/150, 1%)	NA	0% Almost no detection in any sample when using standard PCR
Iran FFPE 42.5 for breast cancer; 39.5 for non-cancerous Mohammadizadeh, F., et al, <i>Infect Agent Cancer</i> , 2017 [238]	qPCR (DNA) Unpublished NA	Breast tumor (0/2, 0%) Only tested 2 samples as a confirmation for IHC result	IHC (Protein): Breast tumor (IE: 0/70, 0%) Paired breast from breast cancer patient (IE: 0/70, 0%)	0% Almost no detection in any sample when using real-time PCR or IHC staining for IE

			Normal breast from non-cancerous (IE: 0/26, 0%)	
Norway FFPE 55 for breast cancer Rahbar, A., et al, <i>Infect Agent Cancer</i> , 2017 [230]	NA	NA	IHC (Protein): IE detected for all breast tumor and paired breast from breast cancer patient, but at high grade in 77% breast tumor and 7% paired breast tissues ISH (DNA and RNA): Breast tumor (23/23, 100%)	100% Detection of DNA by ISH and protein by IHC in all samples, but with different grade of positive staining.
China FFPE 55 for breast cancer Cui, J., et al, <i>Cancer Biomark</i> , 2018 [231]	qPCR (DNA and mRNA) IE2 NA	Breast tumor (146/146, 100%) Adjacent non-cancerous breast (73/146, 50%) Metastatic sentinel lymph node (62/68, 91%) Non-metastatic sentinel lymph node (0/70, 0%)	Breast tumor (IE and L: 146/146, 100%) Adjacent non-cancerous breast (IE: 70/146, 48%; L: 78/146, 53%) Metastatic sentinel lymph node (IE and L: 63/68, 93%) Non-metastatic sentinel lymph node	100% Detected HCMV mRNA, DNA and protein In contrast to most studies, high detection even with real-time PCR

			(IE and L: 42/70, 60%)	
Egypt FFPE and frozen 48 for breast cancer; 41 for non-cancerous El Shazly, D. F., et al, <i>Clin Breast Cancer</i> , 2018 [233]	qPCR (DNA) CMV PCR kit NA	Breast tumor (11/61, 18%) Fibroadenoma (1/20, 5%) Adjacent non-cancerous breast (0/61, 0%)	IHC (Protein): Breast tumor (IE: 21/61, 34%; PP65: 49/61, 80%) Fibroadenoma (IE: 0/20, 0%; PP65 4/20, 20%) Adjacent non-cancerous breast (IE: 0/61, 0%; PP65: 15/61, 25%) IgG antibody: (61/61, 100%) IgM antibody: (0/61, 0%)	18% Lower detection by real-time PCR comparing to IHC 100% seropositivity, but not all samples can have HCMV protein or DNA detected
Iran FFPE 55 for breast cancer Sepahvand, P., et al, <i>Asian Pac J Cancer Prev</i> , 2019 [236]	Standard PCR (DNA), two rounds of PCR gB Sequencing and Blast search	Breast tumor (20/37, 54%) Fibroadenoma (10/35, 29%)	NA	54% Two rounds of standard PCR to have greater amplification
Iraq FFPE Age not specified Al-Nuaimi, B. N., et al, <i>Biochemical</i>	NA	NA	IHC (Protein): Breast tumor (E: 56/60, 93%; L: 37/60, 62%)	NA Positivity varies when detecting for different antigens

<i>and Cellular Archives</i> , 2019 [232]			Normal breast from non-cancerous (E: 2/10, 20%; L: 7/10, 70%)	
---	--	--	---	--

Abbreviations used: qPCR: quantitative real-time PCR; IHC: immunohistochemistry; ISH: in situ hybridization; FFPE: formalin-fixed paraffin-embedded; IBC: inflammatory breast cancer; IE: immediate early; E: early antigen; L: late antigen; gB: glycoprotein B; NA: not applicable.

There is evidence that multiple viruses including EBV, HPV, herpes simplex virus, human herpesvirus-8 and HCMV, are present in breast tumors and breast fibroadenoma specimens, but only HCMV is detected in normal breast tissues from women free of cancer [235]. The presence of HCMV DNA and/or proteins is detected in non-cancerous breast tissues including fibroadenoma, tumor adjacent non-cancerous breast, paired breast from breast cancer patient, and normal breast from women free of cancer (Table 1.2). However, for groups that detected very little or no HCMV viral presence in the breast tumors, there is also no detection in the non-cancerous tissues (Table 1.2). Some groups have shown that the detection rate for HCMV DNA and/or proteins in the breast tumors is higher than in the non-cancerous breast tissues (Table 1.2) [118, 231, 236, 244]. One of the examples is that 63% of normal breast tissues from women free of cancer and 97% of breast tumors show positive detection of HCMV proteins [118]. On the contrary, other studies show no significant difference in detection of HCMV in breast tumors and non-cancerous tissues, with a detection rate of 76% and 67%, respectively (Table 1.2) [232, 235].

A stronger association was observed between HCMV and inflammatory breast cancer (IBC) in comparison to non-IBC, where both the HCMV DNA detection in breast tumors and the IgG antibody titers were higher in the IBC patients [237, 244]. Furthermore,

multiple HCMV strains were detected in the breast tumors from IBC patients, but only one HCMV strain was found in non-IBC patient specimens [244].

HCMV DNA positivity in breast tumors is related to poor overall survival and low levels of relapse-free survival in breast cancer patients [243]. HCMV DNA and proteins are also abundantly expressed in sentinel lymph nodes [4, 231] and in brain tissue [245] from breast cancer patients. In addition, HCMV proteins are expressed in 60% of lymph nodes without metastases and in 94% of sentinel lymph node metastases when HCMV proteins are detected in all primary breast tumors [4]. These results suggest that HCMV might be associated with invasiveness and metastasis.

1.5.3 Association between HCMV and breast cancer patient characteristics

High-grade expression (>50% positively stained cells) of HCMV IE protein is negatively associated with ER and PR, with p values as 0.02 and 0.003, respectively [230]. The expression of HER2 is also reduced in samples that are positive for HCMV IE, although not reaching a level of statistical significance ($p=0.09$) [230]. Another study supports this finding, where the presence of HCMV late antigen in breast tumors is negatively associated with ER, PR and HER2 expression ($p=0.002$, 0.02, 0.005), respectively [242]. On the other hand, a positive relationship between HCMV antigen expression and HER2 overexpression is reported, and this is observed for both HCMV early antigen ($r=0.302$; $p<0.05$) and late antigen ($r=0.280$; $p<0.05$) expression [232]. Also, the detection of HCMV gB DNA is reported to be at a higher frequency in breast tumors of grade III comparing to grade II [236].

1.5.4 *In vitro* studies for the interaction between HCMV and breast cancer

Human MDA-MB-231 breast cancer cells express the IL-10 receptor, which can be bound by cmvIL-10 that is secreted from HCMV infected cells. Exposure of MDA-MB-231 cells to cmvIL-10 led to the activation of STAT3, which is a transcription factor that is strongly associated with enhanced metastatic potential and chemo-resistance [135]. cmvIL-10 also stimulates DNA synthesis and cell proliferation, as well as protecting MDA-MB-231 cells from etoposide-induced apoptosis [135]. Exposure of MDA-MB-231 cells to cmvIL-10 also enhanced cell invasion through a matrigel layer [5]. Expression of several genes that are important for metastasis is altered by cmvIL-10, including upregulation of MMP-3 and downregulation of metastasis suppressor 1. MMP-3 degrades extracellular matrix proteins such as collagen, while metastasis suppressor 1 regulates cytoskeletal rearrangements and is frequently lost in metastatic tumors [5]. MCF-7 human breast cancer cells also express IL-10 receptor, with exposure to cmvIL-10 leading to enhanced proliferation and increased expression of MMP genes, particularly MMP-10 [136].

Mesenchymal MDA-MB-231 breast cancer cells infected with HCMV showed repression of EMT genes and induction of MET genes, which depended on the expression of the HCMV early gene, leading to an epithelium-like cellular environment [132]. Expression of HCMV IE protein was observed in the infected MAD-MB-231 cells, with the cells possessing a flattened, cobblestone morphology in contrast to the normal elongated and spindle-like morphology. However, the late gene reporter was only observed in some of the IE expressing cells and cell death was not observed after 120 h of initial infection when the newly produced virus was typically released [132].

A recent report shows that infection of human breast epithelial cells with a clinical isolate of HCMV, strain DB, leads to oncogenic transformation [6]. HCMV early and late antigens were detected at the protein and transcription levels when the cells were infected. The infection led to the activation of STAT3, resulting in the upregulation of cyclin D1 and Ki67, both are important for cell proliferation [6]. Transformation of the HCMV infected human breast epithelial cells was evident by colony formation using the soft-agar assay, which is the most stringent test for transformation. Furthermore, the transformed cells injected into the mammary fat pads of NOD SCID Gamma mice developed tumors that were ER-/PR-/HER2- [6]. The genomic sequence of HCMV strain DB is highly similar to the genomic sequences of other previously available clinical strains, such as the Toledo, Merlin and JP strains [127]. Furthermore, these HCMV-infected human mammary epithelial cells show upregulated expression of several oncogenes, enhanced activation of pro-survival genes, and upregulated markers of cell proliferation and EMT [127]. However, it is unclear whether different HCMV strains cause different severity of the infection and if this affects oncogenicity [246].

1.6 Summary and thesis objectives

Some evidence suggests that HCMV infection is associated with breast cancer, but uncertainties exist, and the detailed mechanisms for such an association are still largely unknown. Although many laboratories have studied the presence of HCMV in human breast tumor samples, the results are inconsistent likely due to detection methods used and the demographic differences of the populations studied. My first aim in this thesis was to re-assess the findings from previous studies regarding detection of HCMV DNA in breast tumors, with the samples collected from a Canadian population and using a method that is

both highly sensitive and reliable. I will also correlate the presence of HCMV DNA to patient characteristics including tumor stage and receptor positivity of ER/PR/HER2.

My second aim of this thesis was to examine the direct effects of HCMV challenge on breast cancer cells and normal breast tissues. It is uncertain whether HCMV can productively infect breast cancer cells and what cellular responses are generated. The specific focus for this study will be on inflammation, which is a hallmark of cancer, through expression of inflammatory genes. Inflammatory mediators stimulated by CMV infection could potentially enhance breast cancer progression.

Currently, there are limited studies using *in vivo* animal models to investigate the effect of CMV infection on breast cancer progression. My final aim of this thesis was to investigate this issue using different mouse breast cancer models. Breast tumor growth, metastasis and inflammation in the mCMV infected and uninfected mice were analyzed. The different stages of CMV infection, including active, latency, and the intermediate in-transition phase, were also examined in these mouse models.

Overall, my hypotheses are that the presence of CMV DNA in breast tumors will be higher than in normal breast tissues. CMV-induced inflammation at the breast tumor site and in the breast cancer cells will aggravate breast tumor growth and metastasis.

Chapter 2: Methods

2.1 Reagents

All common chemicals and reagents were purchased from Sigma-Aldrich (Oakville, ON, Canada) or Thermo Fisher Scientific (Waltham, MA, USA) unless otherwise stated. Dulbecco's Modified Eagle Medium (DMEM), Roswell Park Memorial Institute (RPMI) 1640 medium, fetal bovine serum (FBS), penicillin/streptomycin and trypsin-ethylenediaminetetraacetic acid were from Life Technologies (Grand Island, NY, USA). Matrigel was purchased from BD Biosciences (Mississauga, ON, Canada). All primers were from Integrated DNA Technologies Inc. (Coralville, IA, USA). Other reagents and their sources are stated within the text as they appear.

2.2 Human breast tumors and breast adipose tissues

Breast tumors from 147 breast cancer patients were obtained during surgical removal of the tumors and immediately snap-frozen in liquid nitrogen and stored at -80 °C. Matching patient information was available for each sample including age, tumor size, presence of ER/PR/HER2 in tumor, tumor grade, lymph nodes metastasis and tumor recurrence. Fresh breast tissues from breast reduction surgery of non-cancerous patients were obtained. Each breast tissue had a small section ~1 cm³ snap-frozen in liquid nitrogen and stored at -80°C like the breast tumors. The remaining breast tissues were immediately processed for the establishment of tissue culture, with the procedures described in section 2.5.2. All patient samples were provided by Dr. Todd McMullen (Department of Surgery, University of Alberta, Edmonton, AB, Canada). The patient samples were obtained with the approval of the University of Alberta Health Research Ethics Board (Pro00018758) with written informed consent.

2.3 Cell lines

Human embryonic lung (HEL) 299 fibroblasts (CCL-137), mouse NIH/3T3 fibroblasts (CRL-1658), human MDA-MB-231 (HTB-26) and MCF-7 (HTB-22) breast cancer cells and BALB/c mouse derived 4T1 breast cancer cells (CRL-2539TM) were all purchased from American Type Culture Collection (Manassas, VA, USA). C57BL/6 mouse derived E0771 breast cancer cells (940001) were from CH3 BioSystems (Amherst, NY, USA). Cells were cultured in an incubator that was maintained at 37°C, 5% CO₂ and 95% humidity. The media used for culturing were either DMEM or RPMI 1640 with 10% FBS and 1% of penicillin/streptomycin unless otherwise stated. All cells used were at a low passage number.

2.4 CMV preparation

2.4.1 Virus propagation

2.4.1.1 HCMV

The HCMV used is a clinical isolate, Kp7 (from Dr. Jutta K. Preiksaitis, Department of Medicine, University of Alberta) [247]. The virus was propagated in HEL 299 fibroblasts that were cultured with low-glucose DMEM. Fibroblasts were grown in 9×75 cm² flasks and cultured in DMEM with 10% FBS until 80% confluent. The cells were then washed twice with phosphate buffered saline (PBS) and replaced with 4 mL of serum-free DMEM in each flask to facilitate better binding of the virus to the cells. HCMV was added to the cell culture at 0.1 multiplicity of infection (MOI) and incubated for 2 h. Six mL of DMEM with 2% FBS was then added to each flask and these were cultured overnight. The next day, cells were washed twice with PBS and replaced with DMEM containing 2% FBS. This process of medium change was repeated every 48 h until all cells were infected

with HCMV. The infected fibroblasts have a round morphology in contrast to the elongated shape of healthy fibroblasts.

After the cells were fully infected, they were scraped from the flask and pipetted into 50 mL conical tubes along with the culturing medium. All conical tubes were balanced in weight for the centrifugation process. The collected cells were centrifuged at 4000 rpm at 4°C for 30 min (CS-6R, Beckman, Santa Clara, CA, USA). The resulting supernatant was transferred to new 50 mL conical tubes and centrifuged at 10,000 ×g at 4°C for 2 h in an angled rotor centrifuge (J2-21M, Beckman, Santa Clara, CA, USA) to pellet the viral particles. Meanwhile, the resulting cell pellet in each conical tube was resuspended in 200 µL of serum-free DMEM and then combined in a 15 mL conical tube. The resuspended cells went through three freeze-thaw cycles in an ethanol/dry ice bath and then sonicated 3 × 30 sec (Vibra-Cell™, Sonics & Materials Inc., Newtown, CT, USA) with a 15 sec pause between each cycle to release viral particles from the cells. The suspension was then centrifuged at 4000 rpm at 4°C for 30 min to pellet cell debris. The resulting supernatant containing viral particles was used to resuspend the viral pellets obtained from the 10,000 ×g centrifugation after 2 h, which became the new viral stock. In order to obtain the maximum amount of virus, the cell pellet remaining in the 15 mL conical tube was resuspended in 200 µL of serum-free medium, followed by a repeated sonication and centrifugation process as described above. The resulting supernatant was combined with the new viral stock. The new viral stock was aliquoted and stored at -80°C.

2.4.1.2 mCMV

The mCMV used to infect the mouse models is RM427+, which has an insertion of the LacZ gene in the nonessential immediate-early 2 gene (gift from Dr. Edward Mocarski,

Stanford University, Stanford, CA, USA) [248]. This modified virus has the same properties as native mCMV, but the inserted LacZ gene allows visualization of an active infection since actively replicating virus produces β -galactosidase that converts its substrate, X-gal, into a blue product [248]. Preparation of mCMV stock follows similar techniques as described in section 2.4.1.1, except that NIH/3T3 mouse fibroblasts were used for viral propagation.

2.4.2 Determination of the viral titre

HEL 299 human fibroblasts or NIH/3T3 mouse fibroblasts were seeded at 4×10^4 cells per well in 96-well cell culture plates for testing HCMV or mCMV viral titre, respectively. Cells were cultured in low-glucose DMEM+10% FBS to become confluent, then washed three times with DMEM+1% FBS before viral infection. The viral stock was added to the fibroblasts at the following dilutions: $1:10^3$, $1:10^4$, $1:10^5$, and $1:10^6$. Each dilution was tested in triplicate wells. After 24 h, cells were washed three times with PBS and fixed with pre-cooled methanol for 10 min at -20°C , followed with three washes of PBS after which the cells were ready for staining.

2.4.2.1 Staining for HCMV IE antigen

Cells infected with HCMV were stained for the expression of HCMV IE antigen using the primary antibody (MAB810, Sigma-Aldrich, Oakville, ON, Canada), at a 1:500 dilution. The detection of IE was performed using the Histostain®-Plus Bulk Kit (Invitrogen, Carlsbad, CA, USA). Briefly, the fixed cells were incubated with 10% goat non-immune serum for 1 h at room temperature to block nonspecific staining and then incubated with the anti-IE antibody overnight at 4°C in a humidified chamber. On the next day, cells were washed three times with PBS and incubated with the biotinylated secondary

antibody for 1 h. After three washes of PBS, cells were incubated with streptavidin-horseradish peroxidase (HRP) conjugate for 10 min and then washed with PBS again. The AEC Single Solution kit (Invitrogen, Carlsbad, CA, USA) was used as the detection system. The reaction mixture contained AEC (3-amino-9-ethylcarbazole, diluted 1:10), a chromogenic substrate for HRP, that reacts with hydrogen peroxide (0.3%) and HRP to yield a red colored product as an indication of positive detection. Each IE antigen-positive nucleus was equated to one infection focus (IF) of virus and the total number was quantified throughout the entire well. The viral titre was determined as IFs per mL, with the average taken from all tested dose-response concentrations.

2.4.2.2 LacZ staining for mCMV RM427+

Cells infected with mCMV RM427+ were stained for the β -galactosidase activity from the inserted LacZ gene. The LacZ Detection Kit for Cells (Invitrogen, Carlsbad, CA, USA) was used for staining, following the manufacturer's instructions. Briefly, the staining solution that was composed of 4 mM potassium ferricyanide, 4 mM potassium ferrocyanide, 2 mM MgCl₂, 1 mg/mL X-Gal solution and PBS, was added to the fixed cells and incubated at 37°C for 2 h. The cells were checked every 30 min under a microscope for the development of blue cells. After color development, the cultures were washed three times with PBS and quantified for the number of blue cells as described in section 2.4.2.1, with each blue colored cell equating to one IF.

2.4.3 Generation of CMV negative control solutions

A filtered CMV (FCMV) negative control solution was generated by passing the HCMV or mCMV viral stock through a 0.05 μ m membrane filter (Millipore Sigma, Tullagreen, Carrigtwohill Co. Cork, IRL). The filtration apparatus was self-assembled and

sterilized by autoclave before use. The viral particles were eliminated through filtration, with the propagation medium retained, containing cytokines and growth factors.

An UV-inactivated negative control solution was generated by irradiating the HCMV or mCMV viral stock with a 230-volt ultraviolet (UV) lamp built within a biosafety cabinet. The virus was contained in a 35 mm cell culture dish with open lid for maximum exposure and placed 20 cm in distance from the lamp. CMV was irradiated with UV light over a range of time, including 5, 10, 20 and 30 min to determine the time required for effective viral inactivation. The irradiated CMV was added to cultured fibroblasts to examine for infectivity, with the procedures described in section 2.4.2. Thirty min effectively inactivated both HCMV and mCMV, with the results for mCMV illustrated as an example (Figure 2.1).

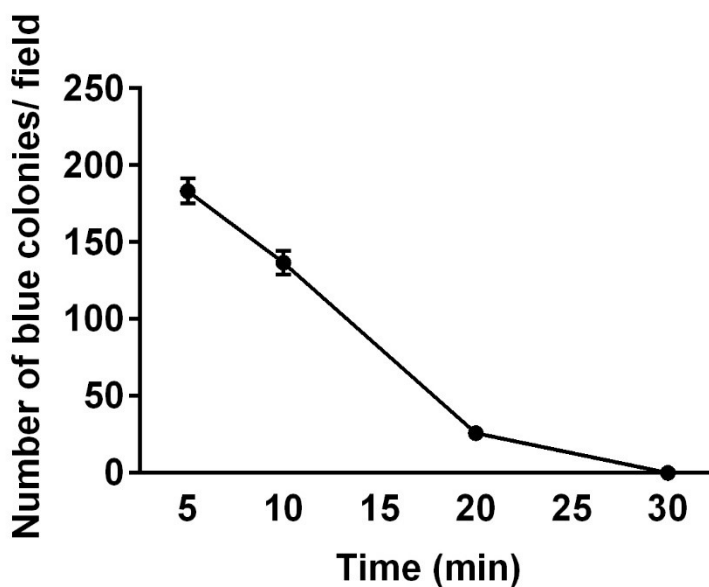


Figure 2.1. UV irradiation inactivates mCMV. mCMV was irradiated with UV light for 5, 10, 20, or 30 min before cultured with mouse NIH/3T3 fibroblasts for 24 h. The fibroblasts were stained for β -galactosidase activity and the number of blue colonies was determined as per microscopic field. No blue colony was observed for mCMV irradiated with 30 min of UV light. N=3.

All preparation procedures were performed on ice. All CMV negative control solutions were tested on fibroblasts of the matching species to ensure no infectivity before experimental use.

2.5 Cell and tissue cultures

2.5.1 Human breast cancer cells

Human MDA-MB-231 and MCF-7 breast cancer cells were seeded in 12-well plates at 10^5 cells/well and cultured with 1 mL of DMEM +10% FBS to grow until 80% confluent. The medium was replaced every 48 h, with the cells being washed twice with HEPES-buffered saline (HBS) between each change of medium and the start of the experiment. Before experimental treatments were added, the culturing medium was changed to 500 μ L of serum-free DMEM. Apart from the wells used for experiments, two additional wells were seeded to be able to quantify the total number of cells in each well prior to the start of the experiment, so that an accurate MOI could be calculated. The cells in these two wells were lifted using 0.05% trypsin and quantified in a Neubauer chamber, 0.100 mm depth, 0.0025 mm² (Hausser Scientific, Horsham, PA, USA). The volume of virus added to each experimental well was then calculated based on the following equation:

$$\frac{MOI \times Total\ number\ of\ cells\ per\ well}{Titre\ of\ virus}$$

An equal volume of serum-free DMEM, FCMV, or UV-inactivated virus was added to the corresponding wells as the negative control treatments.

2.5.2 Mammary adipose tissue culture

Human breast adipose tissues were obtained from patients undergoing breast reduction, as described in section 2.2. Tissues were cut into 1-2 mm³ pieces using sterilized

small scissors to increase the surface area and ensure viability throughout the culturing process. The tissues were cultured in 12-well plates, with ~15 small pieces of tissues per well in 1 mL of serum-free RPMI 1640 medium [249].

Mammary adipose tissues were also obtained from female C57BL/6 mice. Mice were euthanized by cervical dislocation and soaked in 95% ethanol for 2 min within a biosafety cabinet. All dissecting equipment were sterilized by autoclaving. Four large pieces of mammary adipose tissues were obtained from each mouse to generate six experimental wells. The tissues were cut and cultured as described above.

A pre-incubation of 48 h was required to allow the adipose tissues to equilibrate in culture. After 48 h, the tissues and medium were collected into a 1.5 mL microcentrifuge tube for each well and centrifuged at $1,000 \times g$ for 2 min at room temperature. The medium was discarded by pipetting through the floating layer of adipose tissues. The tissues were washed twice in the tube, with fresh serum-free RPMI medium. The tissues were then placed back into wells in a new 12-well culture plate with 500 μ L of serum-free medium per well prior to viral challenge.

2.5.3 Infecting cell and adipose tissue cultures with CMV

A time response curve was generated for cell and adipose tissue culture for the inflammatory responses after CMV challenge. For cells, a MOI of 2 was used for all time points to ensure maximum response. For adipose tissues, the amount of CMV added to each experimental well was determined after testing a range of viral titre on mouse adipose tissues, with 1.25×10^4 virus/mL generating an optimal expression of mCMV IE at the mRNA level (Figure 2.2). The time course established was 0, 3, 6, 12, 24, 36 and 48 h of

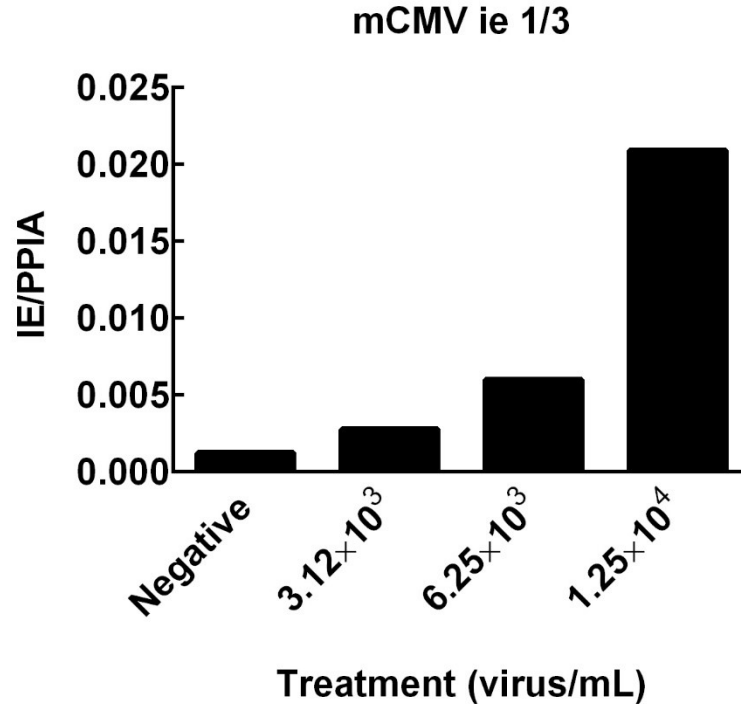


Figure 2.2. Mouse breast adipose tissues cultured with different amount of mouse CMV (mCMV). The mRNA expression of mCMV immediate early (IE) 1/3 gene was determined after 6 h of mCMV challenge. Results were expressed against the housekeeping gene peptidylprolyl isomerase A (PPIA). N=1.

HCMV challenge, with the virus added at the same time and samples collected at different endpoints.

A dose-response curve was generated for HCMV challenge in the cell culture, with MOIs of 0, 0.1, 1, and 2. Both the active HCMV and the UV-inactivated control were tested, with the gene expressions examined at the mRNA level 3 and 36 h post viral challenge.

CMV and negative control solutions were added to the cells and tissues in serum-free medium, which were DMEM and RPMI 1640, respectively. The culturing medium was removed after 2 h of viral challenge and the cells and tissues? washed three times with

serum-free medium to remove any viral particles that had not attached or entered the cell. The cultures were further incubated with 1 mL of medium containing 0.1% bovine serum albumin until the experimental endpoint.

For analysis at the mRNA level, the cells and tissues were collected, but the culturing medium was discarded. For cytokine secretion analysis, the medium was collected and weighed for the exact amount. The resulting cytokine expression were normalized to the total amount of protein obtained from the cells or tissues collected in each culture well.

2.5.4 Determination of HCMV IE expression in human breast cancer cells

The expression of HCMV IE antigen in human breast cancer cells was determined after 36 h of viral challenge at different MOI. The cells were washed three times with HBS and fixed with pre-cooled methanol for 10 min at -20°C. The percent of infection was determined by staining for the HCMV IE expression in the cells as described in section 2.4.2. Microscopic images were taken from five randomly chosen fields of view per well. For each field of view, the number of positively stained nuclei and the total number of nuclei were quantified. The percent of infection was calculated using the following equation and the result averaged from all five fields:

$$\frac{\textit{number of positively stained nuclei}}{\textit{total number of nuclei}} \times 100\%$$

2.5.5 Examination for productive infection of HCMV in cells

Human breast cancer cells were challenged with HCMV at MOI of 2 for 12, 36, 48, or 72 h. HEL 299 fibroblasts were infected in parallel by challenging with HCMV at 0.1 MOI. The cells were cultured in 96-well plates with DMEM containing 10% FBS until 80%

confluency, then washed three times with HBS, followed by the addition of HCMV in serum-free DMEM. The culturing medium was removed after 2 h of viral challenge and then washed with normal HBS at pH 7.4 or HBS at pH 3.0. The low pH treatment releases viral particles attached to the cell surface that have not yet entered the cell, therefore removing the input virus to ensure that only virus being made by the cells at each time point is assessed in this assay. Cells were washed three times with HBS at pH 3.0 or 7.4, each 20 sec, followed by five washes with HBS at pH 7.4 before continuing with the culturing process. Further incubation was performed with DMEM containing 1% FBS, without other medium changes. At the endpoints, cells along with the culturing medium were frozen and thawed three times, with vigorous pipetting in the culture wells during the last thawing phase to facilitate lysing of the cells and releasing of the viral particles. The collected cell lysates were then added to separate fresh wells of fully confluent HEL 299 fibroblasts that had been previously seeded in another 96-well plate. After 24 h of incubation, these fibroblasts were fixed and stained for expression of HCMV IE as described in section 2.4.2. The total number of IF in a well was quantified and expressed as virus/mL based on the volume of lysate added, representing the amount of infectious HCMV viral particles that are present in the lysate.

2.6 Mouse Models

2.6.1 Animal housing

Mice were housed in Animal Biosafety Level 2 biocontainment in the Health Sciences Laboratory Animal Services facility at the University of Alberta. Three to five mice were housed per cage, with housing conditions at 21°C, 55% humidity and a standard 12 h light/dark cycle. Standard laboratory diet and water were supplied to mice with free access. Cages were only opened in the biosafety cabinet, with the working area and outside

of cages wiped with 1% Virkon (Antec International Limited, Suffolk, UK) before and after each cage opening to avoid cross-infection between cages. All procedures were approved by the University of Alberta Animal Welfare Committee and followed guidelines from the Canadian Council of Animal Care.

2.6.2 Syngeneic orthotopic breast cancer model

Female BALB/c and C57BL/6 mice at 8 to 10 weeks of age were purchased from Charles River (Kingston, ON, Canada). The mice were housed for at least seven days upon arrival to acclimatize before starting the experiments.

Mouse breast cancer 4T1 cells, syngeneic to BALB/c mice, were cultured with RPMI 1640 medium + 10% FBS. The medium was changed every 48 h. Prior to injection, cells grown in culture were washed and collected by trypsinization using 0.05% trypsin. The collected cells were then washed three times through repeated centrifugation and resuspension in phenol red-free serum-free RPMI 1640 medium, with the final suspension at 4×10^5 cells/mL. An equal volume of Matrigel (BD Biosciences, Mississauga, ON), a mixture of basement membrane matrix proteins, was mixed with the cell suspension with a final concentration of 2×10^5 cells/mL. The resulting mixture was placed on ice until injection into the mouse mammary fat pad. The Matrigel solidifies at 37 °C, therefore keeping the cancer cells in place at the site of injection. The mice were anesthetized initially in a chamber with 5% isoflurane and then maintained at 2% isoflurane using a nose cone throughout the cancer cell injection. Each mouse was injected with 100 μ L of the prepared cell suspension, resulted in an injection of 2×10^4 cancer cells per mouse [250]. The orthotopic injection was made using a 27-gauge needle to inject right under the nipple of the fourth inguinal mammary fat pad, which was pre-wiped with 70% ethanol [250].

Another mouse breast cancer cell line E0771 (CH3 BioSystems), syngeneic to C57BL/6 mice was also cultured similarly with the same medium except that the medium was changed every 24 h to avoid cell lifting. The E0771 cells were resuspended at the concentration of 2×10^7 cells/mL, mixed 1:1 in volume with Matrigel to a final concentration of 1×10^7 cells/mL and 100 μ L was used for the final injection of 10^6 cells per mouse for the C57BL/6 strain.

2.6.3. Spontaneous breast cancer model

A spontaneous mouse breast cancer model was generated by breeding male mice that were hemizygous for B6.FVB-Tg (MMTV-PyVT)634Mul/LellJ with wild type female C57BL/6 mice [251, 252]. The breeding pairs were obtained from Dr. Ing Swie Goping (University of Alberta, Edmonton, AB, Canada). The generated transgenic mice carry the middle T oncogene under the transcriptional control of the mouse mammary tumor virus promoter/enhancer [251]. These mice spontaneously develop multiple breast tumors that are palpable by ~92 days of age [252]. Two distinct phases of tumor growth are observed in these models, with the early phase from 12-17 weeks and the late phase from 19-23 weeks, and the mean tumor volume reaching $\sim 5 \text{ cm}^3$ by 25 weeks [252]. Lung metastasis develops in these mice during the late phase of tumor growth [252].

2.6.3.1. Genotyping of transgenic mice

Ear notch samples were collected from weaned female mice at four weeks of age and DNA was extracted using the DNeasy Blood & Tissue Kit (Qiagen, Toronto, ON, Canada) according to the manufacturer's instructions. Briefly, one piece of ear notch sample was used for each extraction, placed into 1.5 mL microcentrifuge tube with 180 μ L Buffer ATL and 20 μ L proteinase K, and the tubes were shaken on a vortex mixer. The

samples were incubated at 56°C overnight to become completely lysed, then mixed for 15 sec, followed by the addition of 200 µL Buffer AL and 200 µL ethanol (100%) with mixing after each addition. The mixture was transferred into a DNeasy Mini spin column that sits in a 2 mL collection tube. The spin column was centrifuged for 1 min at 8000 rpm, next washed with 500 µL Buffer AW1 and centrifuged for 1 min at 8000 rpm, then washed with 500 µL Buffer AW2 and centrifuged for 3 min at 14,000 rpm, with the flow-through discarded after each centrifugation. The spin column was then transferred to a 1.5 mL DNase-free microcentrifuge tube to elute the DNA, with 200 µL Buffer AE added to the center of the spin column membrane and incubated for 1 min at room temperature after which it was centrifuged for 1 min at 8000 rpm. The samples were stored at -20°C until tested by PCR.

PCR was performed with 1 µL of the extracted DNA added to a 25 µL reaction volume containing 2X PCR Taq Master Mix (Applied Biological Materials, Richmond, BC, Canada). Two sets of primers were added simultaneously to the reaction. Internal control: sense 5'-CAA ATG TTG CTT GTC TGG TG-3' and anti-sense 5'-GTC AGT CGA GTG CAC AGT TT-3' (gives 200 bp product). PyVT: sense 5'-GGA AGC AAG TAC TTC ACA AGG G-3' and anti-sense 5'-GGA AAG TCA CTA GGA GCA GGG-3' (gives 556 bp product). PCR was performed using the following program: 1) initial denaturation for 30 sec at 98°C, 2) 35 cycles of denaturation for 10 sec at 98°C, annealing for 20 sec at 64°C, and elongation for 25 sec at 72°C, and 3) final elongation for 5 min at 72°C. The products and 100 bp ladder were loaded on a 2.0% agarose gel that was stained with ethidium bromide. Electrophoresis was performed at 100 V for 40 min and then the

gel was visualized with UV light. Female mice with samples that showed the presence of both bands at positions 200 bp and 556 bp were used for experiments.

2.6.4. Mouse infection with mCMV

Mice were randomly chosen for injection of mCMV at 10^6 IF, contained in 100 μ L of PBS and through intraperitoneal injection [248]. An equal volume of PBS, FCMV, or UV-inactivated virus was injected in other groups of mice as controls.

2.6.4.1. Verification of active mCMV infection in mice

An infection test was performed for each strain of mouse by injecting mice with mCMV or negative control solutions described above. The mice were euthanized four days post-injection. The kidneys were harvested and embedded in optimal cutting temperature (OCT) compound (Fisher Scientific International Inc., Ottawa, ON, Canada) and then snap-frozen in liquid nitrogen, followed by storage at -80°C . The tissues embedded in OCT were cryo-sectioned into 10 μm slices, mounted onto slides and stored at -80°C . The kidney slices were stained for β -galactosidase activity using the LacZ Detection Kit for Tissues (InvivoGen, San Diego, CA, USA), which converts the X-gal into a blue product if the virus containing a LacZ gene insertion has been actively replicating. The staining protocol for tissues is similar to cells, as described in section 2.4.2.2., except staining was performed for a longer time ranging from 2-4 h.

2.6.4.2. Establishment of active, intermediate and latent mCMV infection statuses in mice

BALB/c and C57BL/6 mice were infected for 4 days, 11 days or 10 weeks to generate an active, intermediate, or latent infection, respectively, prior to injecting 4T1 or E0771 breast cancer cells, respectively, into the mammary fat pad. The MMTV-PyVT mice

were infected at 5 weeks of age, allowing at least 10 weeks for the latent infection to establish before the spontaneous breast tumors became palpable.

2.6.5. Tumor growth and tissue collection

Tumor growth was monitored by taking orthogonal caliper measurements in two directions and estimating the tumor volume using $\text{width}^2 \times \text{length}/2$. The syngeneic-orthotopic models developed a single tumor per mouse and the experimental endpoint was 25 days post-cancer cell inoculation to achieve the estimated tumor volume of approximately 1000 mm³. The MMTV-PyVT mice spontaneously developed multiple tumors per mouse in all mammary fat pads with high intrinsic variability. Therefore, the experimental endpoint was when the largest tumor reached ~4000 mm³, which is the upper limit allowed by the ethics requirement. The MMTV-PyVT model had a large tumor size as the endpoint to ensure establishment of metastasis in these mice.

At the experimental endpoint, mice were euthanized with an intraperitoneal injection of 50 µL of Euthanyl (sodium pentobarbital, 240 mg/mL) (Bimeda MTC Animal Health Inc., Cambridge, ON). Blood was collected through cardiac puncture using a 1 mL syringe and a 23-gauge needle, both coated with ethylenediaminetetraacetic acid (EDTA) to prevent coagulation and then placed into a 1.5 microcentrifuge tube containing 50 µL of EDTA. The blood was then centrifuged at 13,000 rpm for 5 min to obtain the plasma, which was snap-frozen and stored at -80°C. Tumors were isolated, weighed and their morphological characteristics assessed by two independent observers who were blinded to the treatment group. The amount of blood in the tumor was categorized as pale, moderate or bloody, with the tumors being pale, pink or dark red, respectively. The number of lobes on the tumor was categorized as single tumor, multi-lobed (lobes started to form on the

original tumor) or fused small tumors (fusion of largely grown lobes). Further characterization of each tumor was made with respect to morphology including whether they were solid, soft, necrotic, disintegrated or fluid filled. Half of each tumor was snap frozen and the other half fixed in 10% neutral buffered formalin (pH=6.9). The salivary glands and spleens were immediately snap-frozen and stored at -80°C . Lungs and livers were stored and then analyzed for metastasis as described in the next section.

2.6.6. Metastasis quantification

Lungs from the BALB/c mice were isolated, and then stained with India ink (American MasterTech, Lodi, CA, USA) by intra-tracheal injection, leaving the metastatic nodules as white against the black lung [253]. The nodules observed on the surface of the lungs were counted, and then carefully isolated from the lung surface under a dissection microscope. The lungs and nodules were both snap frozen and stored at -80°C for further analysis. Livers and lungs from the C57BL/6 and the MMTV-PyVT mice were fixed with 10% formalin. The fixed samples were embedded in paraffin and 5 μm sections were prepared (Histology Core, Alberta Diabetes Institute, University of Alberta, Edmonton, AB, Canada). Sample slices were obtained from the front, middle, and back sections of the lungs for a relatively thorough representation. The micro-metastasis was determined by hematoxylin and eosin staining to identify the tumor nodules. The sample slides were dewaxed in three changes of xylene, with soaking for 10 min in each change. The samples were rehydrated using 100%, 80% and 50% ethanol by soaking for 5 min in each, following a decreased concentration gradient and then washed with distilled water for 5 min. The hydrated tissues were stained with hematoxylin (Sigma-Aldrich, St. Louis, MO, USA) for 3 min, rinsed with running tap water for 5 min, differentiated with 0.3% concentrated

hydrochloric acid in 80% ethanol by dipping rapidly for 12 times, rinsed with tap water for 2 min, and stained with eosin (Sigma-Aldrich, St. Louis, MO, USA) for 45 sec. The samples were then dehydrated by soaking for 5 min in each of the 50%, 80% and 100% ethanol, following an increased concentration gradient, and two changes of xylene. The slides were then dried and covered with Mounting Medium Xylene (Fisher Scientific Company, Kalamazoo, MI, USA), and sealed with a glass coverslip. Images were taken from five fields per section with 5X magnification lens and staining was quantified by ImageJ (National Institutes of Health, Bethesda, MD, USA) for the number of nodules per microscopic field and area of nodules relative to the corresponding lung area. The micro-metastasis in the liver was examined using the same technique.

2.7 Detection of CMV viral DNA

2.7.1 LightCycler (LC) PCR

This was performed with help from Dr. Xiao-Li Pang and her postdoctoral fellow Dr. Maria Eloisa Hasing (University of Alberta). The LC-PCR reaction mixture contained 5 μ L of DNA, 4 mM MgCl₂, 0.5 μ M of each primer, 0.2 μ M of each probe, and 2 μ L of the reagent from a LC-FastStart DNA Master hybridization probe kit (Roche Diagnostics, Laval, Québec, Canada) for a total of 20 μ L reaction volume. The primers used for detection of HCMV gB were as follows: forward: 5'-TACCCCTATCGCGTGTGTTTC-3' and reverse: 5'-ATAGGAGGCGCCACGTATTCT-3'. The hybridization donor probe with a fluorescein 3'-end label and the acceptor probe with a LC-Red 640 5'-end label were used in the LC-PCR reaction (TIB Molbiol LLC, New Jersey, NJ, USA) [254]. The reaction mixtures were loaded into the capillaries, then centrifuged and mounted onto the carousel, and placed into the LightCycler 480 Instrument II (Roche Diagnostics, Laval, Québec,

Canada). The thermal cycling conditions were as follows: 1) 10 min at 95°C and 2) 45 cycles of 15 sec of denaturing at 95°C, 10 sec of annealing at 55°C, and 10 sec extension at 72°C. Data were collected during the annealing period with a channel setting F2/F1 for real-time detection of the amplification. The specificity of the fluorescence signal was checked by a melting curve analysis, with $T_m=67.5^\circ\text{C}$ for the probes.

A positive standard curve was generated with a series of log dilutions containing 10^6 to 10^1 genome copies of HCMV, using purified viral DNA that was quantified by spectrophotometry, with absorbance at 260 nm [254]. An example of the standard curve is illustrated in Figure 2.3. The LC-PCR program compared results from the tested samples against the standard curve to determine the HCMV DNA level in a sample reaction.

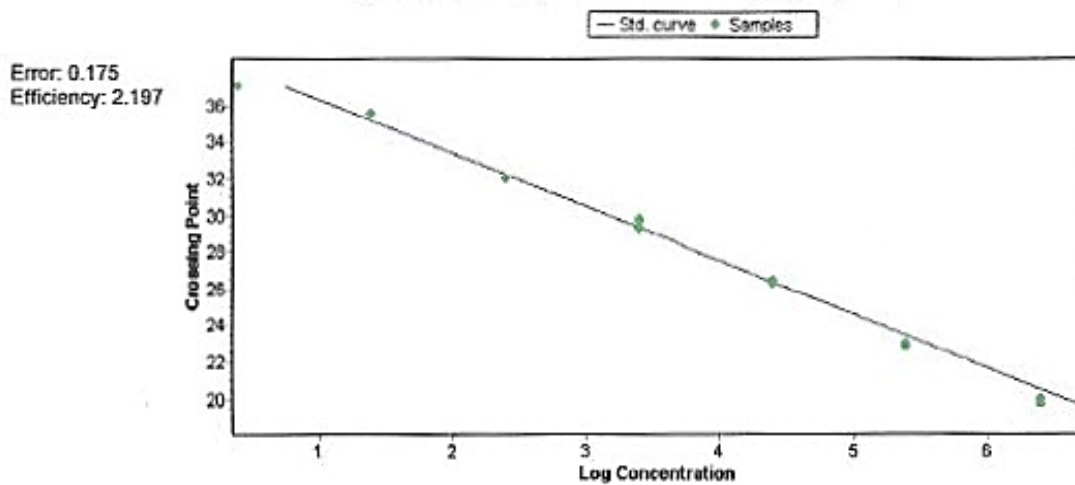


Figure 2.3. Positive standard curve for HCMV DNA detection using LC-PCR. Standard DNA from the HCMV glycoprotein B gene, in serial dilutions ranging from 10^1 to 10^6 copies, was amplified in the LC-PCR assay. The fluorescence intensity was plotted against cycle numbers. Concentration of samples were calculated based on the standard curve.

2.7.2 Nested PCR amplification and visualization

DNA was extracted from tissues using the DNeasy Blood & Tissue Kit (Qiagen, Toronto, ON, Canada) as described in section 2.6.3.1. Nested PCR was performed for the detection of the viral genome. The presence of HCMV DNA in human samples was

determined using primers specific to either the immediate early gene HCMV IE [244] or the late gene HCMV gB [255]. The presence of mCMV DNA in mouse samples was determined using primers specific to mCMV IE-1 [256] or mCMV gB [257]. The primer sets used in nested PCR are listed in Table 2.1. Each PCR reaction has a 50 μ L reaction volume, containing 2X PCR Taq Master Mix (Applied Biological Materials, Richmond, BC, Canada). The extracted DNA (150 ng) was amplified with the external primer set for the first round of amplification, then 2 μ L of the amplified product was used with the internal primer set for the second round of amplification. The PCR reaction was performed with an initial denaturation for 4 min at 94°C, followed by specific thermal cycling conditions that were individually listed for each primer set in Table 2.1 in the order of denaturation, annealing and elongation, and then a final elongation for 7 min at 72°C. Internal control was used for the analysis of mouse tissues, β -actin (gives 150-bp product): sense 5'-ATT GTG ATG GAC TCC GGT GA-3' and antisense 5'-AGC TCA TAG CTC TTC TCC AG-3'. The products were visualized on an agarose gel stained with ethidium bromide. For products >100 bp, 1.5% gel was used, and electrophoresis was performed at 100 V for 30 min. For products <100 bp, 3% gel was used and run for 1 h. The band size was determined relative to 100 bp DNA ladder.

2.7.3 Sequencing of PCR product

2.7.3.1 Re-extraction of DNA from agarose gel

PCR products were visualized on an agarose gel and bands with the expected size were cut out for re-extraction of the DNA using the MinElute Gel Extraction Kit (Qiagen, Toronto, ON, Canada). The gel slice was weighed and six volumes of Buffer QG were added to one volume of gel (100 mg gel \sim 100 μ L) and then incubated at 50°C for 10 min to completely dissolve the gel. An equal volume of isopropanol was added to the gel and mixed by

Table 2.1. Primer sequences for nested PCR.

	Thermocycling conditions (30 cycles)	Product size (bp)	Primer sequence
HCMV IE external	94°C-45 sec 55°C-45 sec 72°C-45 sec	373	Forward: 5'-GGTCACTAGTGACGCTTGTATGATGACCATGTACGGA-3' Reverse: 5'-GATAGTCGCGGGTACAGGGGACTCT-3'
HCMV IE internal	94°C-45 sec 50°C-45 sec 72°C-45 sec	293	Forward: 5'-AAGTGAGTTCTGTCCGGGTGCT-3' Reverse: 5'-GTGACACCAGAGAATCAGAGGA-3'
HCMV gB external	94°C-30 sec 58°C-30 sec 72°C-60 sec	149	Forward: 5'-GAGGACAACGAAATCCTGTTGGGCA-3' Reverse: 5'-GTCGACGGTGGAGATACTGCTGAGG-3'
HCMV gB internal	94°C-30 sec 52°C-30 sec 72°C-60 sec	96	Forward: 5'-ACCACCGCACTGAGGAATGTCA-3' Reverse: 5'-TCTTGCGTTTGAAAGAGGTA-3'
mCMV IE-1 external	94°C-30 sec 60°C-30 sec 72°C-30 sec	549	Forward: 5'-TGGATGAGAACCGTGTCTAC-3' Reverse: 5'-ATATCATCTTGCGTTGTCTT-3'
mCMV IE-1 internal	94°C-30 sec 60°C-30 sec 72°C-30 sec	310	Forward: 5'-TACAGGACAACAGAACGCTC-3' Reverse: 5'-CCTCGAGTCTGGAACCGAAA-3'
mCMV gB external	94°C-30 sec 53°C-30 sec 72°C-30 sec	298	Forward: 5'-TCATCAACTCGACGAAGCTC-3' Reverse: 5'-ATCTCGTCCAGGCTGAACAC-3'
mCMV gB internal	94°C-30 sec 53°C-30 sec 72°C-30 sec	235	Forward: 5'-CTGGGCGAGAACAACGAGAT-3' Reverse: 5'-CGCAGCTCTCCCTTCGAGTA-3'

Abbreviations used: HCMV: human cytomegalovirus; IE: immediate early; gB: glycoprotein B; mCMV: mouse cytomegalovirus.

inverting several times. The product was loaded onto the MinElute spin column and then centrifuged for 1 min at 17,900 ×g. The column was washed with 500 µL of Buffer QG

followed by 750 μL of Buffer PE through centrifugation and DNA was eluted into a clean microfuge tube with 10 μL of Buffer EB. The concentration of the eluted DNA was determined using the Nanodrop spectrophotometer ND-1000 (Thermo Scientific, Rockford, IL, USA). The DNA was further processed or stored at -20°C .

2.7.3.2 Cloning of PCR product into T-vector

PCR products <100 bp were cloned into vectors in order to perform DNA sequencing. The pUCM-T Cloning Vector Kit (Bio Basic Inc., Markham, ON, Canada) was used for cloning. The PCR product was generated by amplification with Taq DNA polymerase, which produced additional adenine at the 3' end that could be ligated to the T-vector with overhanging thymine. The ligation reaction was set up with 1 μL each of the 10X ligation buffer, 50% polyethylene glycol, pUCm-T vector (50 $\text{ng}/\mu\text{L}$), T4 DNA ligase and 0.2 pmol PCR product, and finally adjusted to 10 μL with sterile water. The reaction mixture was incubated overnight at room temperature. For transformation, 100 μL of competent *E. coli* cells were thawed on ice, followed by the addition of 5 μL ligation mixture. The samples were mixed gently and incubated on ice for 30 min. The mixture was heat-shocked at 42°C in a water bath for 1 min and then placed on ice for 2 min, after which 400 μL Super Optimal Broth was added and the mixture was shaken at 200 rpm for 1 h at 37°C . The mixture was spread out evenly onto an agar plate (10 mL of Luria Broth (LB), 10 μL of 100 mg/mL ampicillin, 10 μL of 200 mM isopropyl- β -D-thiogalactoside (IPTG), and 50 μL of 40 mg/mL X-gal). The plate was placed upward for 1 h at 37°C , then inverted to avoid condensation and the incubation was continued overnight. The incubation did not exceed 16 h to ensure ampicillin remained effective.

The developed colonies were screened for transformants. The pUCm-T vector contained a LacZ gene that encodes β -galactosidase, which converts X-gal into a blue product. Cloning of the foreign DNA fragment into the vector causes the reading frame of the LacZ gene coding sequence to be altered, disrupting its activity and the colonies produced should be white. Normally, both blue and white colonies will be present on the agar plate, representing non-recombinant and recombinant clones, respectively. However, if the recombinant had a DNA insertion that is small and has a sequence number that is the multiple of three, the activity from the LacZ gene may not be fully disrupted due to a small frameshift and the colony could remain blue. Therefore, at least ten colonies were chosen from each plate for sequencing. Each colony was picked up with a tooth stick and transferred into 5 mL of LB medium containing ampicillin, which was cultured overnight at 37°C with shaking at 200 rpm. Plasmid DNA was extracted from the liquid culture using the Column-Pure Plasmid Miniprep Kit (Applied Biological Materials, Richmond, BC, Canada). The sequence of the target clones from the extracted DNA was determined by M13 universal forward primer: 5'-GTAAAACGACGGCCAGT-3'. The analysis was performed using the Sanger DNA Sequencing service at the Molecular Biology Facility (University of Alberta, Edmonton, AB, Canada). The resulting sequences were aligned to the target gene using the CLC Sequence Viewer software (CLC bio, Aarhus, Denmark) to verify the product specificity. The sequences were further identified using the Basic Local Alignment Search Tool (BLAST) database.

2.8 Measurement of mRNA expression

2.8.1 mRNA isolation and reverse transcription

Tissues (20-50 mg) were homogenized in 1 mL of Trizol® (Invitrogen Life Technologies, Grand Island, NY, USA) contained in 2 mL microcentrifuge tubes with 5-

mm stainless steel beads, using the Qiagen TissueLyser II system (24-sample plates, 25 Hz, 5 min) (Qiagen, Toronto, ON, Canada). For cell culture experiments, cells were scraped from the plates with 500 μ L of lysis buffer provided by the Direct-Zol RNA MiniPrep Kit (Zymo Research Corporation, Irvine, CA, USA). The tissue homogenates or cell lysates were centrifuged at 4°C for 10 min at 1000 \times g to remove cellular debris, then the supernatants were obtained for RNA isolation. For adipose tissues, a 1 mL syringe with a 21-gauge needle was used to draw up the supernatant without disturbing the fat droplets floating on the surface that could interfere with RNA isolation. The Direct-Zol RNA MiniPrep Kit was used for RNA isolation. An equal volume of 100% ethanol was added to the collected supernatant and mixed thoroughly. The mixture was loaded onto the filter column inserted in a collection tube and then centrifuged at 4°C for 1 min at 10,000 \times g, leaving the nucleic acids bound to the column. Genomic DNA was removed by adding 2 U of DNase I dissolved in DNA digestion buffer directly to the column matrix and the samples were incubated for 15 min at room temperature. DNase I activity at 1 U is defined as an increase in the absorbance of a high molecular weight DNA solution at a rate of 0.001 A_{260} units/mL of the reaction mixture at 25°C. The column was then washed twice with 400 μ L of Direct-zol RNA Prewash, followed by 700 μ L of RNA Wash Buffer, each with 1 min centrifugation at 10,000 \times g at 4°C. An additional 2 min of centrifugation was performed for complete removal of the wash buffer and then the column was placed into an RNase-free tube. The RNA was eluted by adding 100 μ L of nuclease-free water to the column matrix, followed by centrifugation. The concentration and quality of the extracted messenger RNA (mRNA) were measured using the Nanodrop spectrophotometer ND-1000 (Thermo Scientific, Rockford, IL, USA). The $A_{260}/280$ ratio was \sim 1.98, confirming little

or no contamination with protein. The eluted mRNA was further processed or stored at -80°C.

The mRNA (500-800 ng) was then reverse transcribed to complementary DNA (cDNA) using 5X All-In-One Reverse Transcription MasterMix (Applied Biological Materials, Richmond, BC, Canada) that contained OneScript®, oligo deoxythymidine primers and reverse transcriptase random primers, dNTPs, RNase inhibitor and 5X reaction buffer. The thermocycler conditions used were as follows: 1) 25°C for 10 min, 2) 42°C for 60 min, 3) 95°C for 5 min, 4) Cooled to 4°C. The resulting cDNA was stored at -20°C.

2.8.2 Quantitative Real-Time PCR

The cDNA samples were assayed with quantitative Real-Time PCR (qPCR) for the expression of target genes. All reactions were examined in duplicate. Each reaction mixture contained 1 µL of cDNA, 12 µL of EvaGreen qPCR master mix (Applied Biological Materials, Richmond, BC, Canada) and 1 µL each of the 10 µM forward and reverse primers of the target genes that are listed in Table 2.2. The primers were designed using the Primer-BLAST website (National Center for Biotechnology Information, NIH, Bethesda, MD, USA). The reaction mixture was assayed using the Applied Biosystems 7500 real-time PCR System (Life Technologies, Grand Island, NY, USA). The thermocycling conditions for amplification were as follows: 1) 50°C for 2 min, 2) 95°C for 10 min, 3) 40 cycles at 95°C for 15 sec and 60°C for 1 min. Each cycle of amplification doubled the amount of transcript. Immediately after amplification, a melt curve analysis was performed to verify the specificity of the amplicon using the following program: 1) 95°C for 15 sec, 2) 60°C for 1 min, 3) 95°C for 15 sec. The amount of PCR product was

Table 2.2. Primer sequences of genes assayed by qPCR

Gene	Species	Primer sequence
mCMV gB	Mouse	Forward: 5'-AGGGCTTGGAGAGGACCTACA-3' Reverse: 5'-GCCCCGTCGGCAGTCTAGTC-3'
HCMV IE	Human	Forward: 5'-TGAGGATAAGCGGGAGATGT-3' Reverse: 5'-ACTGAGGCAAGTTCTGCAGT-3'
cmvIL-10	Human	Forward: 5'-TCGGTGATGGTCTCTTCCTC-3' Reverse: 5'-CGTCGCAATAAACCGTACCT-3'
GAPDH	Human/Mouse	Forward: 5'-TCCTGCACCACCAACTGCTT-3' Reverse: 5'-TCTTACTCCTTGGAGGCCAT-3'
PPIA	Human/ Mouse	Forward: 5'-GATGAGAACTTCATCCTAAA-3' Reverse: 5'-TCAGTCTTGGCAGTGCAGAT-3'
PPIA	Mouse	Forward: 5'-CACCGTGTTCTTCGACATCAC-3' Reverse: 5'-CCAGTGCTCAGAGCTCGAAAG-3'
HPRT	Human/ Mouse	Forward: 5'-AGATCCATTCCCTATGACTGT-3' Reverse: 5'-AATCAAGACATTCTTTCCAG-3'
ENPP2 (ATX)	Human/ Mouse	Forward: 5'-CATTTATTGGTGGAAACGCAGA-3' Reverse: 5'-ACTTTGTCAAGCTCATTTCC-3'
IL-1 alpha	Human	Forward: 5'-CTTCTGGGAAACTCACGGCA-3' Reverse: 5'-AGCACACCCAGTAGTCTTGC-3'
IL-1 beta	Human	Forward: 5'-AGATGAAGTGCTCCTTCCAGGAC-3' Reverse: 5'-TGCTGAAGCCCTTGCTGTA-3'
IL-6	Human	Forward: 5'-AGCCAGAGCTGTGCAGATGA-3' Reverse: 5'-CTGCAGCCACTGGTTCTGTG-3'
TNF-alpha	Human	Forward: 5'-CCCATGTTGTAGCAAACCCT-3' Reverse: 5'-TGAGGTACAGGCCCTCTGAT-3'
COX-2 (PTGS-2)	Human	Forward: 5'-ATGAGTGTGGGATTTGACCA-3' Reverse: 5'-ATTCCGGTGTGAGCAGTTT-3'
IL-10	Human	Forward: 5'-TACGGCGCTGTCATCGATTT-3' Reverse: 5'-TAGAGTCGCCACCCTGATGT-3'
LPAR1	Human	Forward: 5'-GACTGCCAGTGAGAGTGTGG-3' Reverse: 5'-TGAACACGCCCCAGAACTAC-3'
LPAR2	Human	Forward: 5'-CTGCTCATGGTGGCTGTGTA-3' Reverse: 5'-TACAGCCAGGACATTGCAGG-3'

Abbreviations used: mCMV: mouse cytomegalovirus; HCMV: human cytomegalovirus; cmv: cytomegalovirus; gB: glycoprotein B; IE: immediate early; ENPP2: ectonucleotide pyrophosphatase/phosphodiesterase family member 2; ATX: autotaxin; HPRT: hypoxanthine-guanine phosphoribosyltransferase; GAPDH: glyceraldehyde phosphate dehydrogenase; IL: interleukin; PPIA: peptidylprolyl isomerase A (cyclophilin A); TNF: tumor necrosis factor, COX: cyclooxygenase; PTGS: prostaglandin-endoperoxide synthase; LPAR: lysophosphatidic acid receptor

quantified at the end of each amplification cycle at 60°C by determining the fluorescence due to EvaGreen dye intercalated into the double-stranded DNA. The number of cycles needed for the sample to reach a particular fluorescent intensity threshold level, termed C_T , was used to assess the target gene expression level. The amount of transcript in a sample is inversely proportional to the resulting C_T value. The melting curve analysis measured the decrease in fluorescence from the EvaGreen dye as the double-stranded DNA dissociated at 95°C. The results for non-specific products or primer dimers are displayed as separate peaks from the product of interest on the dissociation curve, which is plotted as the first derivative of the rate of change in fluorescence as a function of temperature.

The relative amount of the target gene was determined by normalizing against the housekeeping genes glyceraldehyde 3-phosphate dehydrogenase (GAPDH), hypoxanthine-guanine phosphoribosyltransferase (HPRT), or peptidylprolyl isomerase A (PPIA; cyclophilin A). For human samples, all reference genes showed similar results and GAPDH was routinely used in the analysis. For mouse samples, PPIA was used due to a more stable expression across the samples.

2.9 Immunohistochemistry

Sample slides were prepared from the formalin-fixed and paraffin-embedded tissues as described in section 2.6.6. The samples were dewaxed in xylene and hydrated with a decreased concentration gradient of ethanol as previously described. The hydrated slides were fully covered with 10 mM citric acid (pH 6.0) and microwaved for 30 min in a Tender Cooker (Nordic Ware, Minneapolis, MN, USA) for antigen retrieval. The samples must remain hydrated throughout the process. The cooker was cooled to room temperature and then the slides were rinsed for 5 min with distilled water. The slides were then taken

out one at a time to avoid complete drying out of the tissue sections. The tissue sections were circled with a wax pen (Dako, Burlington, ON, Canada) and then immediately covered with 200 μ L of 9:1 methanol and 30% hydrogen peroxide for 10 min to block endogenous peroxidase activity. The slides were then washed by completely covering in PBS and placing on a shaker for 10 min. The primary antibodies used include rabbit anti-CD31 (ab28364, 1:80) from Abcam (Toronto, ON, Canada) and the rabbit anti-Ki67 (D3B5, 1:200) from Cell Signaling Technology (Whitby, ON, Canada). Staining was performed using Rabbit-specific HRP/DAB (ABC) Detection IHC Kit (Abcam, Toronto, ON, Canada) according to the manufacturer's instructions. Briefly, tissue sections were covered with the serum blocking solution and incubated at room temperature for 1 h to block background staining. The slides were drained and the tissue sections covered with primary rabbit antibody to incubate overnight in a humidified chamber at 4°C. The slides were washed three times with PBS, then incubated with biotinylated secondary antibody followed by the streptavidin-HRP conjugate solution, each for 30 min at room temperature and washed with PBS for three times after each incubation. The tissue sections were then covered with 3,3'-Diaminobenzidine (DAB) substrate solution and monitored under a light microscope for the development of the brown color. The reaction time was kept consistent between samples within a single experiment. The slides were washed with water and then counterstained with hematoxylin for 3 sec, followed by washing with running tap water for 5 min. For a blue hematoxylin staining, the slides were dipped once in saturated lithium carbonate solution (1.5% weight/volume), followed by washing with warm running tap water for 5 min. The slides were dehydrated by soaking in an increasing concentration gradient of ethanol and two changes of xylene, and then sealed with a glass coverslip as

described in section 2.6.6. Positive staining events for CD31 and Ki67 were selected and counted using ImageJ. The analysis was made using images taken with a 5X magnification lens and the illustration was taken with a 20X magnification lens. CD31 was quantified as the number of vessels per field and Ki67 as a percentage of positive cells. The results were averaged from 10 image fields for each sample.

2.10 Picro-Sirius red staining for collagen

Slides with sectioned breast tumor samples were hydrated as previously described in section 2.6.6. The slides were covered with 0.1% Sirius Red F3B (Sigma-Aldrich, Oakville, ON, Canada) dissolved in a saturated aqueous solution of picric acid (1.3% in water) and incubated for 1 h at room temperature on a shaker. The slides were then washed twice with 0.5% acetic acid, each for 5 min [258]. The samples were dehydrated and sealed as described in section 2.6.6. Collagen types I, III, and IV were stained as red against a pale orange background when visualized under a light microscope. Images were taken with a 5X magnification lens. The positively stained areas were identified using Adobe Photoshop (Adobe Inc., San Jose, CA, USA) and quantified using Image J software. The results were averaged from ten image fields for each sample.

2.11 Multiplex ELISA for cytokine/chemokine and matrix metalloproteinase (MMP) levels

Mouse breast tumor (20 mg) was homogenized in 200 μ L of radioimmunoprecipitation (RIPA) buffer (50 mM Tris-HCl (pH 7.4), 1% NP-40, 0.25% Na-deoxycholate, 150 mM NaCl, 1 mM EDTA, 1:100 dilution of protease inhibitor). Cell culture medium was collected and the cells were scraped from the culturing plate with 100 μ L of RIPA buffer. The tissue or cell lysates and the culturing medium were centrifuged at 10,000 \times g for 20 min at 4°C. The supernatants were collected into fresh tubes. The

protein concentration in the tissue or cell lysates was measured using the bicinchoninic acid (BCA) protein assay (Thermo Fisher Scientific, Rockford, IL, USA). Samples were diluted 1:10 with RIPA buffer and 10 μ L was loaded into the 96-well plate for the assay. A standard curve was set up on the same plate using 20, 10, 5, 2.5 and 1.25 μ g of albumin that were each dissolved in 10 μ L of RIPA buffer. The reagent A and reagent B from the BCA kit (Fisher Scientific) were mixed in 50:1 ratio, respectively, and 190 μ L of this mixture was added to each sample and standard well using a multi-well pipette. The samples were incubated at 37°C for 30 min and then measured for absorbance at 550 nm using the Easy Reader EAR 340 AT (SLT-Labinstruments, Austria). The protein concentration of samples was determined based on the standard curve generated with albumin. All protein lysates were adjusted to 1 mg/mL when performing protein expression analysis. Examination of protein expression in plasma was performed on undiluted sample.

A Mouse Cytokine/Chemokine Discovery array 31-plex (analytes listed in Table 2.3) and a Mouse MMP Discovery array 5-plex (MMP-2, MMP-3, MMP-8, pro-MMP-9, and MMP-12) were performed by Eve Technologies Corp (Calgary, AB, Canada).

2.12 Measurement of ATX activity

ATX activity was measured by the detection of choline release from LPC [249]. Fifteen μ L of plasma was mixed with 15 μ L of buffer A (100 mM Tris-HCl, pH 9.0; 500 mM NaCl; 500 mM MgCl₂; and 0.05% v/v Triton X-100), then incubated at 37°C for 30 min. Next, 30 μ L of 8 mM C14:0-LPC dissolved in buffer A was added to the mixture and incubated at 37°C for 3 h. In a 96-well plate, each sample was pipetted at 20 μ L per well in duplicate, followed with addition of 90 μ L of buffer C (88 μ L buffer B (100 mM Tris-

Table 2.3. Analytes quantified by the Mouse Cytokine/Chemokine Discovery array 31-plex

Analyte	Full name
Eotaxin (CCL11)	Eotaxin
G-CSF	Granulocyte colony-stimulating factor
GM-CSF	Granulocyte-macrophage colony-stimulating factor
IFN γ	Interferon gamma
IL-1 α	Interleukin 1 alpha
IL-1 β	Interleukin 1 beta
IL-2	Interleukin 2
IL-3	Interleukin 3
IL-4	Interleukin 4
IL-5	Interleukin 5
IL-6	Interleukin 6
IL-7	Interleukin 7
IL-9	Interleukin 9
IL-10	Interleukin 10
IL-12 (p40)	Interleukin 12 p40 subunit
IL-12 (p70)	Interleukin 12 p70 subunit
IL-13	Interleukin 13
IL-15	Interleukin 15
IL-17A	Interleukin 17A
IP-10 (CXCL10)	Interferon gamma-induced protein 10
KC (CXCL1)	Keratinocyte chemoattractant
LIF	Leukemia inhibitory factor
MCP-1 (CCL2)	Monocyte chemoattractant protein 1
M-CSF	Macrophage colony-stimulating factor
MIG (CXCL9)	Monokine induced by gamma interferon
MIP-1 α (CCL3)	Macrophage inflammatory protein 1-alpha
MIP-1 β (CCL4)	Macrophage inflammatory protein 1-beta
MIP-2 (CXCL2)	Macrophage inflammatory protein 2
RANTES (CCL5)	Regulated on activation, normal T cell expressed and secreted
TNF- α	Tumor necrosis factor-alpha
VEGF	Vascular endothelial growth factor A

HCl, pH 8.5, and 5 mM CaCl₂), 0.7 μ L of 10 mM Amplex Red (Invitrogen Life Technologies, Grand Island, NY, USA), 0.1 μ L of 1000 U/mL horseradish peroxidase, 1.2 μ L of 300 U/mL choline oxidase). After 5 min, the formation of choline was measured

using Fluoroskan Ascent FL Fluorometer (Thermo Fisher Scientific, Vantaa, Finland) at Ex 544/Em 590 nm. The measured activity was expressed as an activity/mL of plasma.

2.13 Statistical analysis

Results other than patient characteristics of human specimens and tumor characteristics in the MMTV-PyVT model are expressed as means \pm standard error of the mean (SEM). Student's t-test, one-way analysis of variance (ANOVA), two-way ANOVA or Chi-square analysis were used as appropriate and analysis is indicated in each figure legend. $P < 0.05$ was considered significant as evaluated and graphed using GraphPad Prism 6 (GraphPad Software, La Jolla, CA, USA).

The statistical analysis for tumor characteristics in the MMTV-PyVT model was performed by Ana Paula Belon and Jesus Serrano-Lomelin (University of Alberta). Changes in the number of tumors by blood content, type of tumors, and morphology (severity characteristics) across infection status (with/without mCMV infection) were estimated by Chi-square analysis (and Fisher's exact test when applicable). An additional binary logistic regression model was used to assess the odds ratio of severity characteristics between the with/without mCMV infection groups as suggested by the results of the Chi-square analysis. The Chi-square analysis and the logistic models were performed using SPSS version 25.0 [259] and p-values of <0.05 were considered to be statistically significant.

Chapter 3: Detection of HCMV genome and viral transcripts in human breast tumors and normal breast adipose tissues

3.1 Introduction

The role of HCMV infection in breast cancer has been debated over the past decades. It is unclear whether HCMV is an oncogenic virus that leads to breast cancer. Evidence from epidemiological studies has shown an association between HCMV infection and breast cancer [226-228]. It has been demonstrated recently that a clinical isolate, HCMV strain DB, causes an oncogenic transformation of human breast epithelial cells [6]. However, the results are inconsistent for whether HCMV DNA, RNA, and/or proteins are present in the breast tumor specimens. Laboratories across the world have used various detection methods to examine HCMV viral presence in breast cancerous and non-cancerous tissues, with the percent of positive detection ranging from 0 to 100% (Table 1.1 and 1.2) [4, 118, 121, 230, 231, 233-241, 243-245]. Although HCMV DNA and/or proteins can be detected in normal breast tissues from women free of cancer, there is evidence that the detection rate is lower comparing to breast tumors [117, 212, 217, 225]. On the other hand, some studies have shown no significant difference between these two types of samples in terms of HCMV detection positivity [213, 216].

Evidence has shown detection of HCMV DNA and proteins in metastatic sentinel lymph nodes and brain tissues of breast cancer patients, suggesting an association with metastasis [4, 231, 245]. Furthermore, HCMV DNA positivity in breast tumors is related to poor overall survival and low levels of relapse-free survival in breast cancer patients [224].

Most of the studies were done in regions with high HCMV seroprevalence, such as China, Iraq, Iran, and Egypt (Table 1.1 and 1.2) [151, 152]. Therefore, it is important to investigate this issue in a population that has relatively lower HCMV seroprevalence, such

as the Canadian patient population. The discrepancy in results from different laboratories could be due to the highly variable detection methods used, including IHC staining for viral antigens and PCR amplification for different viral genes. PCR is commonly used for the detection of HCMV DNA in human breast tumors, but it gives the most variable results when comparing between different studies (Table 1.1). Therefore, an evaluation of the PCR technique targeting the HCMV genome in human tissue samples should be performed to identify an optimal detection method.

In this chapter, I assessed the sensitivity and specificity of the HCMV PCR detection methods that are currently available, including LC-PCR and nested PCR. LC-PCR uses fluorescent hybridization probes that allows for highly specific PCR reaction and real-time quantification of the product [185]. Nested PCR enhances the sensitivity on top of the standard PCR by having two rounds of reactions using two different sets of primers, where the second set of primer is amplifying a shorter sequence that is within the product generated by the first round of PCR. It is important to establish a reliable and optimal detection method for the presence of HCMV DNA in human specimens. This was achieved in this study, with the details discussed in this chapter.

The detection of HCMV genome was performed on locally obtained breast tumors and normal breast tissues from women free of cancer as a representation of the Canadian population. I hypothesized that the HCMV DNA positive detection in breast tumors from our patient population will be relatively lower comparing to previous studies that were performed in countries with high HCMV seroprevalence. However, the presence of HCMV DNA in breast tumors would be higher than in normal breast tissues. I also hypothesized that the presence of HCMV DNA in breast tumors is associated with worse prognosis.

3.2 Detection of HCMV gB DNA using LightCycler Real-time PCR (LC-PCR) and nested PCR

Human breast adipose tissue that was actively infected with HCMV in culture for 24 h was extracted for DNA, which was used as the HCMV positive control. A serial dilution of the extracted DNA was prepared, including the original stock and at 1:10, 1:10², 1:10³, 1:10⁴ and 1:10⁵ dilutions. The negative control was prepared using DNA extracted from human MDA-MB-231 breast cancer cells. The HCMV gB DNA level was examined in these positive and negative control samples using LC-PCR and nested PCR for parallel comparison, providing differences in specificity and sensitivity of these two assays. The LC-PCR was able to detect HCMV gB DNA up to 1:10² dilution of the HCMV positive control, with an estimation of two copies of the viral genome in the reaction based on calculations using a previously established standard curve (Figure 3.1a). On the other hand, a band at the 96 bp position on the gel, representing the HCMV gB gene, was detected up to 1:10⁵ dilution when using nested PCR (Figure 3.1b). This showed that the nested PCR detection has a 1000-fold greater sensitivity in comparison to LC-PCR. Both methods showed no detection of HCMV gB DNA in the negative control sample (Figures 3.1, 3.2). Furthermore, no bands were observed for the nested PCR product of the negative control, indicating that the reaction appeared to be specific with no cross-contamination between the samples (Figure 3.1b).

3.3 Determination of nested PCR specificity using different viral genes for detecting HCMV DNA in human specimens

Presence of the HCMV viral genome in the human breast tumors and normal breast tissues was examined by nested PCR, targeting either the gB or IE genes. The positive (1:10 dilution) and negative controls established in section 3.2 for HCMV were used in the

a)

Sample	PCR cycle number	Expected Concentration (copies/ μ L)	Calculated Concentration (copies/ μ L)
Standard 1800 copies	29.72	1800	1480
Standard 180000 copies	22.96	180000	180000
HCMV original	32.26	Unknown	200
HCMV 1:10	33.10	Unknown	104
HCMV 1:10 ²	38.18	Unknown	2
HCMV 1:10 ³	Undetermined	Unknown	Undetermined
HCMV 1:10 ⁴	Undetermined	Unknown	Undetermined
HCMV 1:10 ⁵	Undetermined	Unknown	Undetermined
Negative control	Undetermined	Unknown	Undetermined

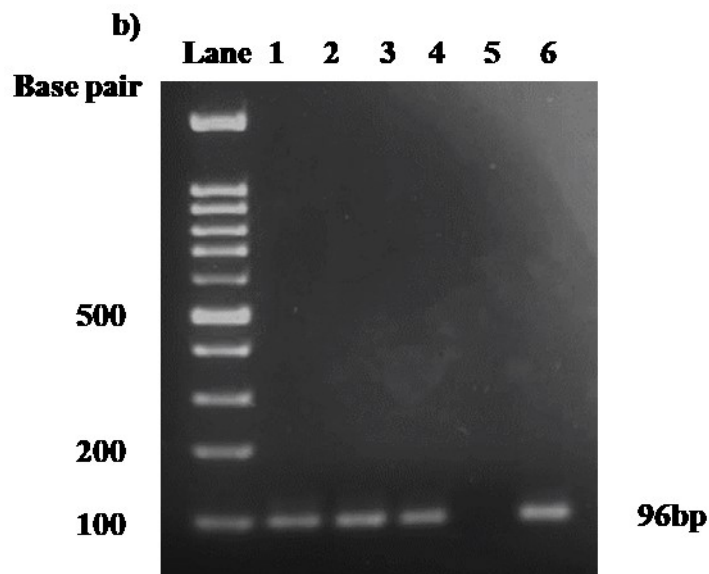


Figure 3.1. The detection limit of LightCycler PCR (LC-PCR) and nested PCR for HCMV glycoprotein B (gB) DNA. HCMV positive control was prepared in serial dilutions ranging from 1 to 1:10⁵. The samples were examined for expression of HCMV gB DNA using LC-PCR (a) and nested PCR (b). The calculated concentration in panel a) was determined by the LC-PCR program based on the previously established HCMV standards. In panel b), the samples illustrated in lanes 1-6 are as follows: 100 base pair (bp) DNA ladder, HCMV 1:10³, 1:10⁴, 1:10⁵, negative control, positive control (HCMV 1:10).

assessments. For each round of PCR amplification, a reaction mixture that was free of DNA was included to confirm no contamination during the experimental procedure. No bands were observed on the gel for any of these control mixtures.

For the detection of HCMV gB in human breast tumor samples, the PCR product either showed no band or a single band at the 96 bp position similar to the positive control (Figure 3.2a). The observed bands showed a similar appearance across the patient samples, with single bands at similar intensity (Figure 3.2a). Therefore, one of the bands was randomly chosen for sequence analysis. The DNA re-extracted from the gel was cloned into the T-vector, with ten of the generated clones randomly chosen and sequenced. All ten resulting sequences showed alignment to the UL55 genomic sequence that encodes HCMV gB, with four of these clones illustrated as examples in the sequence alignment map (Figure 3.2b). This indicates that the PCR products observed at the 96 bp position were not false positive from other genes of similar length.

On the other hand, the detection of HCMV IE DNA in human breast tumor samples showed unclear results. As expected, the HCMV positive control showed a single band at position 293 bp on the gel (Figure 3.3a). Multiple bands were observed in the negative control sample, although the products were <200 bp (Figure 3.3a). The human breast tumors showed highly variable results across the samples and with multiple bands. Some samples appeared to have a product of 293 bp, but it was not the most intense band (Figure 3.3a). Seven patient samples were randomly chosen, with the observed ~293 bp bands re-extracted for the DNA products. The samples were sequenced and aligned to the HCMV IE genomic sequence, but none of the seven tested samples were aligned with IE (Figure 3.3b). The resulting sequences were identified using the BLAST database, with all found

to be from the human genomic sequence. Therefore, the detection of HCMV IE using nested PCR produced non-specific products and led to false positive results.

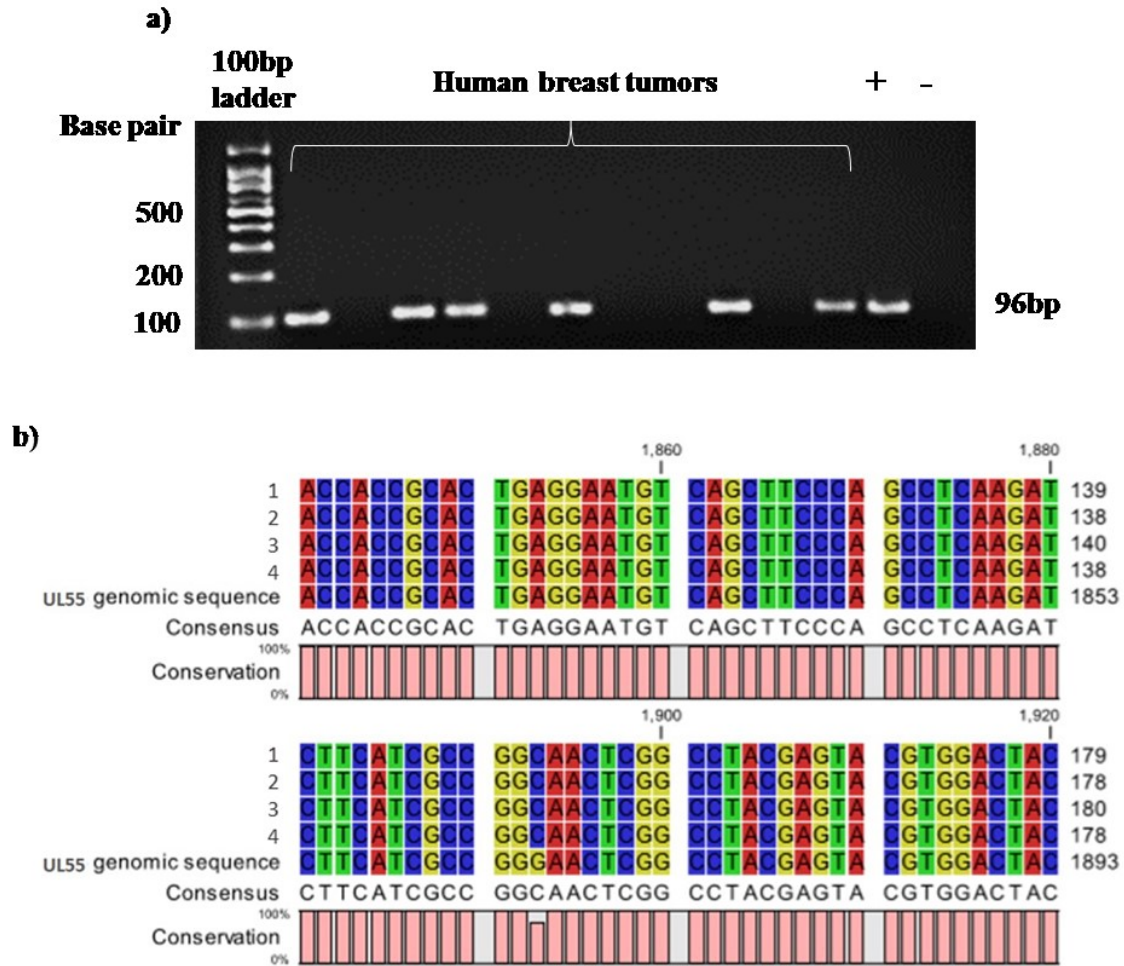


Figure 3.2. Specificity of HCMV glycoprotein (gB) DNA detection using nested PCR. PCR products for amplified HCMV gB gene from human breast tumor samples were visualized on 3% agarose gel stained with ethidium bromide, resulting with a band at 96 bp for a positive detection (a). The PCR product at 96 base pair (bp) position was re-extracted from the gel and cloned for Sanger DNA sequencing, with the results aligned to UL55 genomic sequence that encodes HCMV gB (b). Ten samples were analyzed, all UL55. Four of the samples were randomly chosen and illustrated in the sequence alignment map (b).

3.4 Incidence of HCMV gB detection in human breast tumors and normal breast tissues at the DNA level

Breast tissue samples from ten women free of cancer and breast tumors from 147 breast cancer patients were analyzed for the detection of HCMV gB DNA using nested PCR, resulting in 30% and 40% positivity, respectively (Table 3.1). The difference in positivity of detection was not statistically significant between these two groups (Table 3.1).

Table 3.1. Detection of HCMV glycoprotein B DNA in human breast tumors and breast tissues

Sample type	Total sample number	Number of HCMV-	Number of HCMV+	Percent HCMV+	P-value
Breast tissue	10	7	3	30%	0.74
Breast tumor	147	88	59	40%	

P-value calculated by Chi-square analysis.

The HCMV gB DNA detection in breast tumor samples was sub-analyzed in relation to available patient characteristics, including age (average age=55 for both HCMV+ and HCMV-), survival, chemotherapy treatment, recurrence, lymph node metastasis, distant metastasis, tumor grade, tumor stage and expression of ER/PR/HER2 receptors. No statistical significance was observed in any of these characteristics when comparing patients with breast tumors that were positive or negative for HCMV gB (Table 3.2 and 3.3). However, there was a trend ($p < 0.06$) that HER2 negative tumors had a higher incidence of HCMV gB detection than those that were HER2 positive (Table 3.3).

Table 3.2. Patient characteristics for breast tumors analyzed.

	Total sample number	Number of HCMV-	Number of HCMV+	Percent HCMV+	P-value
Alive					
Yes	118	69	49	42%	0.36
No	24	17	7	29%	
Recurrence					
Yes	49	31	18	37%	0.72
No	93	55	38	41%	
Chemotherapy					
Yes	87	52	35	40%	0.86
No	55	34	21	38%	
Lymph node metastasis					
Yes	91	55	36	40%	0.85
No	40	25	15	38%	
Distant metastasis					
Yes	18	9	9	50%	0.31
No	123	77	46	37%	
Tumor grade					
Low	45	31	14	31%	0.19
High	87	49	38	44%	
Tumor stage					
I	36	21	15	42%	0.19
IIA	27	20	7	26%	
IIB	40	25	15	38%	
IIIA	9	3	6	67%	
IIIB	10	8	2	20%	
IV	18	9	9	50%	

P-values calculated by Chi-square analysis.

Table 3.3. Cellular receptor positivity for breast tumors analyzed.

	Total sample number	Number of HCMV-	Number of HCMV+	Percent HCMV+	P-value
Cellular receptors					
ER -	18	13	5	28%	0.30
ER +	109	62	47	43%	
PR -	52	32	20	39%	0.71
PR +	75	43	32	43%	
HER2 -	96	52	44	46%	0.06
HER2 +	31	23	8	26%	
Combination of all three receptors					
ER+/PR-/HER2-	24	11	13	54.2	0.42
ER-/PR-/HER2+	12	9	3	25.0	
ER+/PR+/HER2-	66	37	29	43.9	
ER+/PR-/HER2+	11	9	2	18.1	
ER+/P-/HER2+ (Triple-positive)	7	4	3	42.3	
ER-/PR-/HER2- (Triple-negative)	5	3	2	40.0	

P-values calculated by Chi-square analysis. Abbreviations: HCMV: human cytomegalovirus; ER: estrogen receptor; PR: progesterone receptor; HER2: human epidermal growth factor receptor 2.

3.5 mRNA expression of HCMV IE was not detected in human breast tumors and breast tissues

The expression of HCMV IE was examined at the mRNA level in the same set of human breast tumors (n=147) and normal breast tissues from women free of cancer (n=10). The HCMV positive and negative controls were included in each round of qPCR analysis. The HCMV positive control resulted in an amplification cycle number of ~22 and a single peak in the melting curve at 86.5°C (Figure 3.4 and 3.5). All the tested patient samples showed undetermined or >35 amplification cycle numbers (Figure 3.4). The samples that

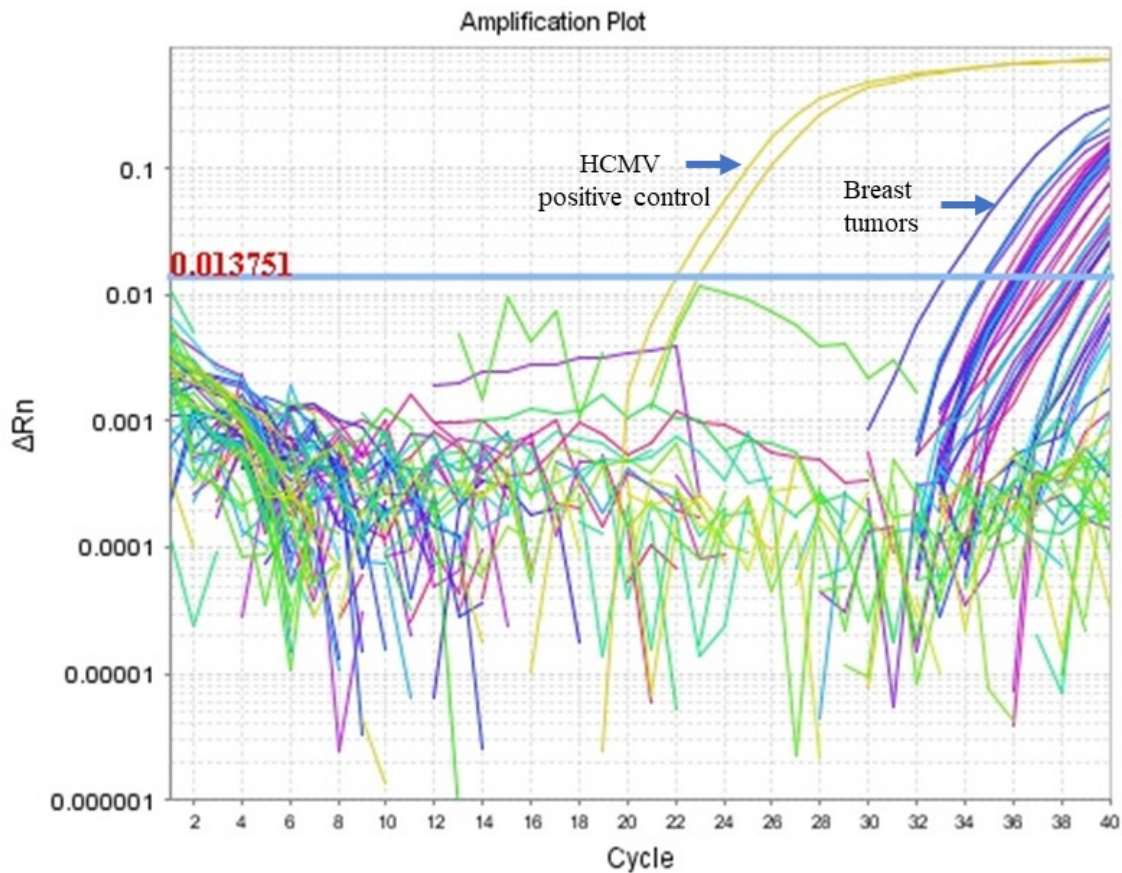


Figure 3.4. mRNA expression of HCMV immediate early (IE) gene in human breast tumor samples. The expression of IE transcript was determined by Quantitative Real-time PCR, with the resulting amplification plot illustrated. The HCMV positive control was depicted in yellow. A total of 147 breast tumors and 10 breast tissues were analyzed, with results from one round of experiment (n=40) illustrated as example.

Melt Curve

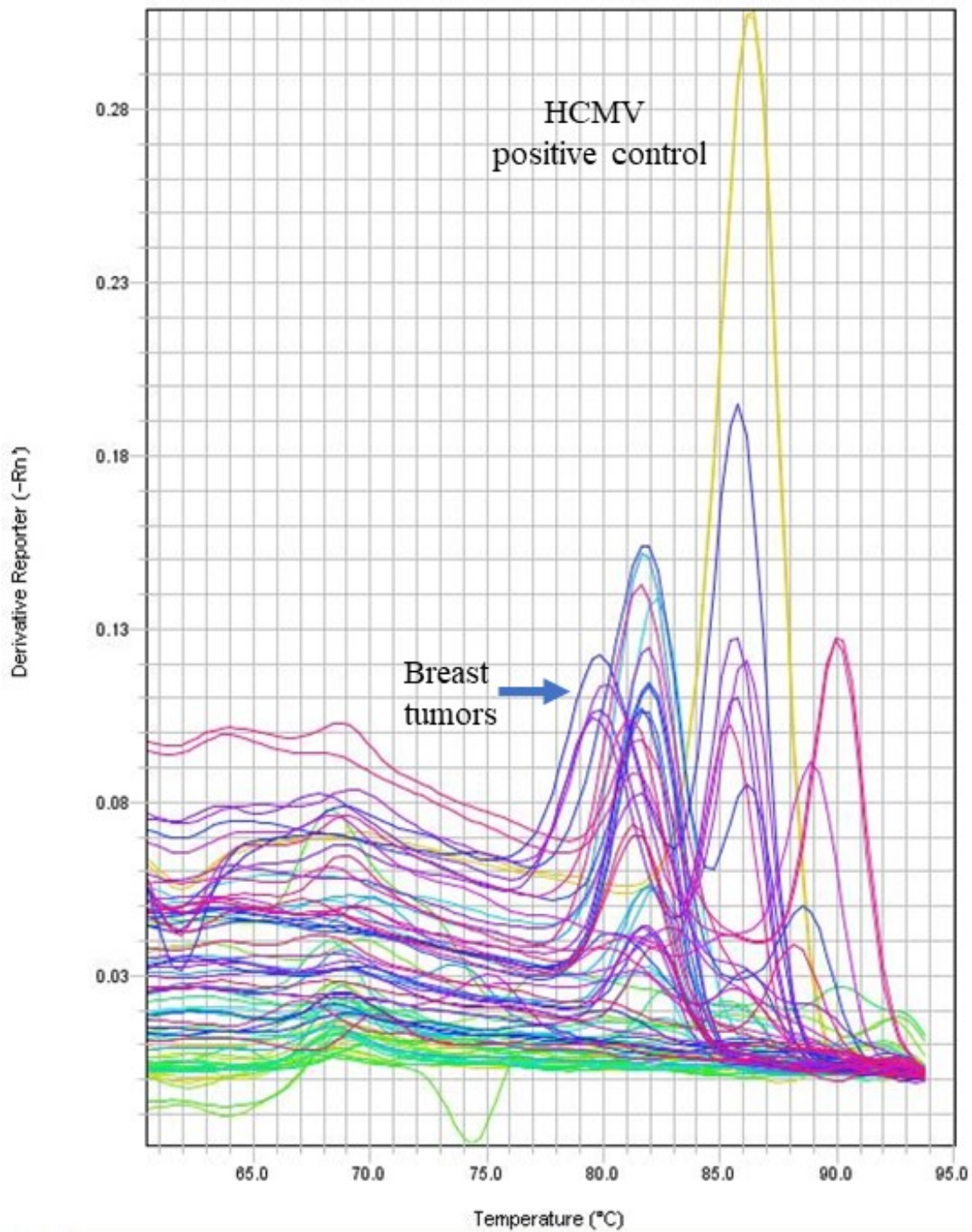


Figure 3.5. mRNA expression of HCMV immediate early (IE) gene in human breast tumor samples. The expression of IE transcript was determined by Quantitative Real-time PCR, with the resulting melt curve illustrated. The HCMV positive control was depicted in yellow. A total of 147 breast tumors and 10 breast tissues were analyzed, with results from one round of experiment (n=40) illustrated as example.

have shown a value for amplification did not show a single peak that matches with the positive control on the melt curve (Figure 3.5). These results indicate that the mRNA expression of HCMV IE was not detected in any of the patient samples analyzed.

3.6 Discussion

The detection of HCMV gB DNA by nested PCR was determined to be both sensitive and specific. Although LC-PCR is very specific with the use of hybridization probes and allows for real-time quantitative analysis of the viral load, the sensitivity is outcompeted by nested PCR with a 1000-fold difference. Several studies showing very little or no detection of HCMV DNA in breast tumors have used detection methods that are similar to LC-PCR, which involve real-time analysis that we have shown is not the most sensitive detection method [233, 238-241]. However, there are two studies that have used qPCR but detected HCMV DNA in all patient samples that were analyzed [4, 231]. All of these samples are also positive for HCMV proteins when analyzed using IHC, which suggest that there could be a high level of HCMV viral presence in these samples that reaches the qPCR detection limit (Table 1.2). The problem with nested PCR is its specificity and the possibility of getting false positive results. In fact, we showed that the nested PCR targeting against HCMV IE gene resulted in false positives after performing Sanger DNA sequencing on the resulting PCR products. This nested PCR method involving the same primers and PCR conditions is described by another laboratory, where they detected HCMV IE DNA from 53.1% (26 out of 49) of the breast tumors from non-inflammatory breast cancer patients when the HCMV seropositivity is 65% (32 out of 49) [244]. They show that HCMV DNA is not detected in normal breast tissues from women free of cancer (number of samples and seropositivity unspecified) [244]. In a later study,

these same authors updated the positive detection of HCMV IE DNA in breast tumors of non-inflammatory breast cancer patients to 74% (67 out of 91) and inflammatory breast cancer patients to 89% (39 out of 44) [237]. By following the exact detection method described, we were not able to obtain specific PCR products to make a reliable conclusion. However, the specimens we used were snap-frozen and stored at -80 °C until the time of DNA extraction, whereas fresh samples are used in the El-Shinawi et al study [237, 244]. There is a possibility that the viral DNA was better preserved when extraction was made from fresh tissues. A suggestion for the discrepancy in results could be that the HCMV DNA amount available in the analyzed samples are different, where non-specific reactions could overpower the target gene amplification if the level of viral genome present is very low. This is likely since the gels illustrated in the El-Shinawi et al study also showed some non-specific bands, although they are very faint compared to the target gene product [244]. This is also supported in our study, where the HCMV positive control containing a high level of viral DNA generated a PCR product that showed a single strong band on the gel at the expected position, in contrast to the multiple bands observed for the analyzed human specimens. Nevertheless, the use of nested PCR targeted against HCMV IE DNA is not a reliable method for examining our patient samples. In our study, the product from nested PCR targeting against HCMV gB DNA is confirmed to be specific. PCR products that were inserted into the clones and randomly chosen for DNA sequencing were all found to be the HCMV gB gene, indicating that the observed PCR product on the gel only contained the HCMV gB sequence.

Our results showed a 40% positivity for HCMV DNA detection in breast tumors that were obtained from the local population, which is at the low end when compared to

other studies (Table 1.1). This could be due to the difference in HCMV seropositivity for the patient populations studied, where the infection rate is greater than 80% for regions such as South America, Africa, and Asia but only 40-70% in North America [151]. However, a limitation that lies within our study is that we do not have the HCMV seropositivity information for each of the patients we obtained the specimens from. These patients could be infected by HCMV, but we were just not able to detect the viral genome in the tissue samples. This is especially important if the viral infection is latent and only very few copies of the viral genome are present in the individual. Latency is likely the case since HCMV IE mRNA was not detected using qPCR in any of our samples. The difficulty for detecting HCMV DNA during latency is expected based on our previous experience working with latently infected mice. We examined various organs including lungs, spleens, livers, and kidneys of latently infected mice, but could only detect the mCMV DNA in one or two organs of each mouse [260]. Nevertheless, it is evident that in the patient population we studied, the detection of HCMV DNA was not observed in majority of the breast tumors analyzed.

In our study, 30% of the normal breast tissues from women free of cancer showed positive detection of HCMV DNA, which was not significantly different from the 40% detection in breast tumors. This indicates that the viral genome can be retained in both the normal breast tissues and the breast tumors. Currently, we only have ten normal breast tissues from women free of cancer, which is markedly low comparing to the number of breast tumors analyzed. Increasing the sample size would provide a more representative analysis with stronger statistical power, but the current results showed no evidence for a higher detection rate of HCMV DNA in breast tumors compared to breast tissues from non-

cancerous women. This is against our hypothesis and several studies where they showed a difference between the two types of tissues when examining for the presence of HCMV IE DNA and/or proteins [118, 232, 244]; however, there is one study supporting no difference in the rate of detection [235]. It is important to take into consideration that we have shown nested PCR targeting against HCMV IE DNA could lead to false-positive results that are unreliable, therefore challenging some of the previous findings [244]. Therefore, the results from our study only represent detection of HCMV gB DNA in the human specimens.

We were not able to find a statistically significant association between the presence of HCMV gB DNA in the breast tumors to any of the patient characteristics. This could be due to the uneven distribution of the sample size in different characteristic categories that were compared. We did observe a trend for a higher incidence of HCMV DNA detection in breast tumors that are HER2- compared to those that are HER2+, regardless of the ER/PR hormone receptor positivity. HER2+ breast tumors account for 15-20% of all breast cancer cases; therefore, the majority of breast cancer patients are HER2- [90]. Therefore, it is important to have further understanding of the relationship between HER2 expression and HCMV viral presence in breast tumors. HER2 activation stimulates signalling pathways such as the PI3K/AKT pathway that promotes cancer progression and its overexpression is associated with worse prognosis [93, 94]. It is surprising that HCMV in breast tumors shows a trend for negative association with HER2 expression, since we hypothesized that HCMV infection is associated with worse breast cancer outcomes. However, HER2 negative breast tumors can also be triple-negative, which is a highly aggressive type of breast cancer. Unfortunately, we only had five triple-negative breast tumors in the study, which is not representative for this type of breast cancer. Other studies

have shown HCMV to be correlated with negative expressions of ER, PR, and HER2 in breast tumors, although the presence of HCMV was indicated by IHC staining of viral proteins [230, 242]. Therefore, it is possible that our analysis could reach statistical significance with increased sample size in categories that are currently having low number of samples.

The patient information available for our breast tumor specimens only provides whether metastasis has occurred or not in the patient, but not when it occurred or the severity of the secondary tumors. These are interesting for investigation since it could be that instead of causing the breast cancer cells to metastasize, HCMV infection is promoting metastasis through the process of oncomodulation [128, 129]. Another limitation is that our current patient information only indicates whether the individual has ever been treated with chemotherapy, but not the length of treatment or if adjuvant therapy was provided. In addition, HCMV DNA presence in human specimens should be analyzed by having the samples grouped according to patient age when greater sample size is available. This is important since HCMV infection rate increases with age and the age range for breast cancer patients is very broad [150].

We have focused on the detection of HCMV at the DNA level using nested PCR, which is convenient and sensitive, but HCMV proteins can also be detected using IHC as an indication for viral presence. The combination of both methods could decrease false negative results, therefore can be performed in future analysis. The nested PCR method we have used has a limitation for not able to provide information on which specific cell types carried the viral genome in the analyzed tissues. The breast tumors are composed of multiple cell types, such as breast cancer cells, fibroblasts, endothelial cells, lymphocytes,

dendritic cells and macrophages. The study that used IHC as the detection method suggested that HCMV proteins are found to be associated with cancer cells [231]. If fresh tumor samples were available, more detailed analysis could be performed using multi-color flow cytometry, with antibodies targeted against HCMV antigens and the specific cell types to investigate the viral localization. The most important question is whether breast cancer cells can be infected with HCMV and what are the responses of the cancer cells to that infection. I will investigate this question *in vitro*, with the details discussed in the next chapter.

Chapter 4: CMV infection in breast cancer cells and breast adipose tissues

4.1 Introduction

HCMV has a broad cell tropism and is commonly found in fibroblasts, epithelial cells, endothelial cells, smooth muscle cells, and macrophages of the infected individuals [159]. It is shown that HCMV proteins are detected in breast tumors and within the cancer cells [231]. Also, expression of HCMV IE protein was observed in the infected MDA-MB-231 cells, although there was limited detection of viral late genes and a delayed cell death comparing to other HCMV susceptible cells that were infected [132]. These results suggest that HCMV does not lead to a productive infection in breast cancer cells, where infectious viral particles are not reproduced [132].

The HCMV viral transcripts and proteins such as IE, regulate not only viral replication but also cellular mechanisms that could play a role in tumor progression, such as production of inflammatory mediators [261]. HCMV infection normally stimulates upregulation of inflammatory mediators such as IL-6, IL-7, IL-11 and COX-2 in the infected cells [218, 219]. Other cytokines that are immunosuppressive factors such as TGF β , IL-10 and viral encoded cmvIL-10 are also produced upon HCMV infection [134, 215]. It is important that tumor-promoting inflammation is a hallmark of cancer [30]. HCMV-induced production of IL-6 is associated with tumor development in salivary gland cancer [222]. Furthermore, a correlation was found between HCMV and overexpression of COX-2 in breast cancer [223]. Inflammation in breast cancer involves crosstalk between breast cancer cells and tumor-associated breast adipose tissues through a vicious signaling cycle driven by ATX/LPA [31]. Currently, it is unknown whether HCMV stimulates production of inflammatory mediators in breast cancer cells and the mechanisms that are potentially involved.

In the previous chapter, I found that HCMV DNA is detected more often in HER2-negative breast tumors than HER2-positive breast tumors, although not reaching statistical significance with the current sample size. However, this led to the question of whether breast cancer cells with different receptor positivity would respond differently to challenge with HCMV. In this study, we examined the effects of HCMV challenge in the triple-negative MDA-MB-231 and the ER/PR positive MCF-7 breast cancer cells.

Previous reports have shown that exposure of MDA-MB-231 and MCF-7 breast cancer cells to cmvIL-10 enhanced cell proliferation and migration [135, 136]. However, the cells were not directly challenged with infectious HCMV. The laboratory strains of HCMV that are extensively passaged in fibroblasts are mutated and result in the loss of broad cell tropism [163]. We use a clinical isolate of HCMV, Kp7, that is at a low passage number. This ensures a broad cell tropism of the isolate, that can then be used to examine its infectivity in breast cancer cells.

In this study, we examined whether HCMV can fully replicate and produce new infectious viral particles in breast cancer cells, with a comparison between MDA-MB-231 and MCF-7 cell lines. The HCMV-challenged breast cancer cells were examined for expression of viral transcripts and inflammatory genes. The HCMV-induced inflammation was also studied in cultured human adipose tissues for a representation of the responses at the breast local site. I hypothesized that production of HCMV viral transcripts will stimulate transcription of inflammatory genes in the viral-challenged breast cancer cells and adipose tissues, which could contribute to promoting breast cancer progression and metastasis.

4.2 Human breast cancer cells challenged with HCMV expressed low levels of IE protein

The number of MDA-MB-231 and MCF-7 breast cancer cells expressing HCMV IE protein was low after 36 h of initial HCMV challenge, with the IE-positive cells <1% (Figure 4.1). The percent of IE-positive cells increased as the viral challenge increased in MOI, but without ever exceeding 1% positivity in both cell lines (Figure 4.1a,b). However, HCMV challenge at a MOI of 2 produced the highest percent of IE expressing cells, therefore, it was used for future analysis. Breast cancer cells challenged with the FCMV control did not express IE antigen, indicating that FCMV is an effective negative control and the breast cancer cells were not previously infected with HCMV (Figure 4.1c).

4.3 Human breast cancer cells were not productively infected by HCMV

MDA-MB-231 cells showed no production of infectious viral particles after HCMV challenge. A viral amount of <1500 virus/mL was determined for the MDA-MB-231 cell lysates collected after 12 and 36 h of initial viral challenge, when normal HBS (pH=7.4) was used for cell washing to remove the input virus. This was decreased to ~500 virus/mL after 48 and 72 h of initial viral challenge (Figure 4.2a). When HBS at pH 3.0 was used for the washing process, the 72 h time point showed a significant increase in infectivity comparing to the 12 h time point (Figure 4.2a). However, the viral titre determined for the lysates collected at the 72 h time point was ~500 virus/mL, which is low. Furthermore, no significant differences were observed across all time points examined ($p=0.07$, Figure 4.2a).

On the other hand, HEL 299 cell lysates collected after 12 and 36 h of initial viral challenge, prior to the 48 h typically required to produce virus, was determined to have a remaining infectious viral amount of ~5000 virus/mL when normal HBS (pH=7.4) was used for cell washing to remove input virus from the medium (Figure 4.2b). The infectious

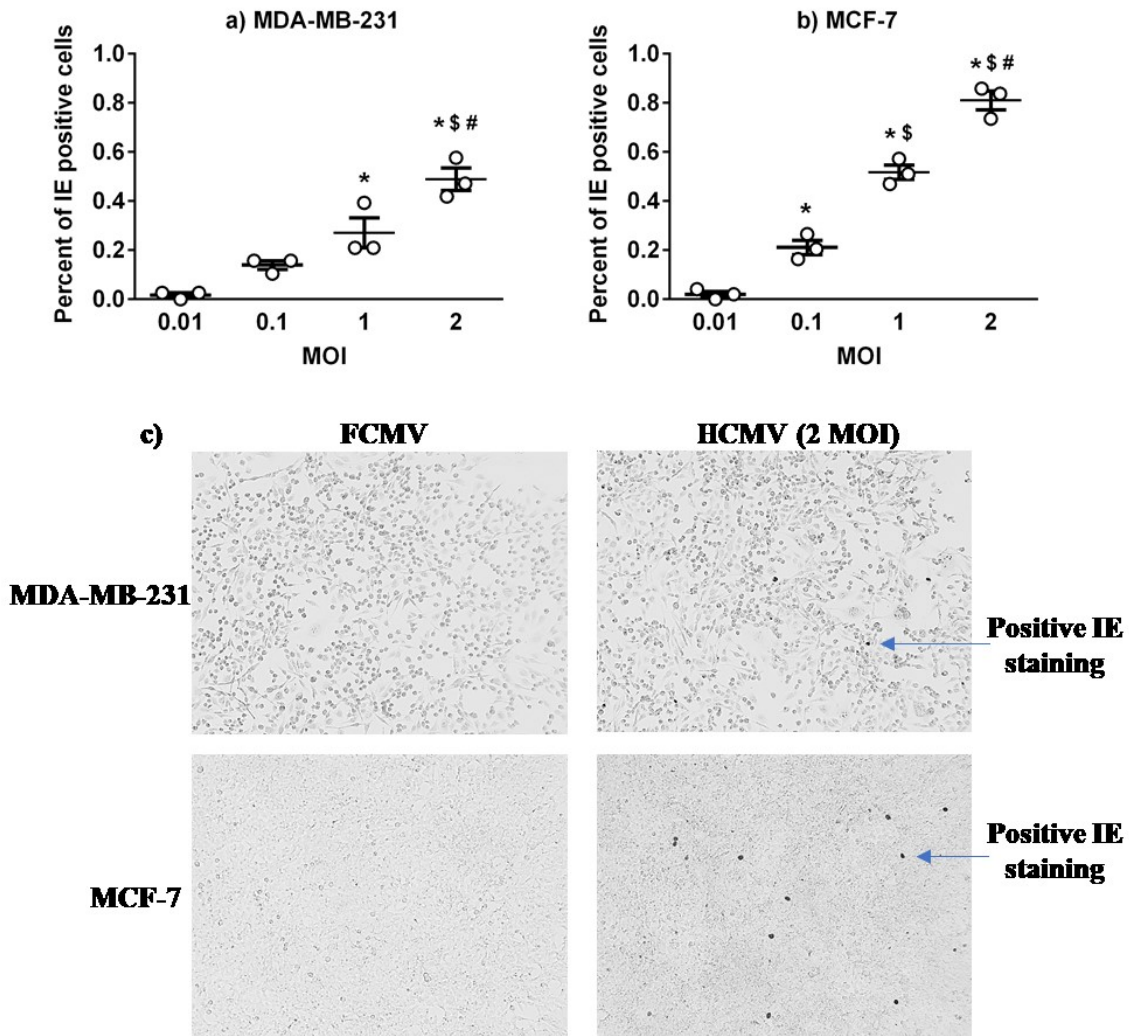


Figure 4.1. HCMV challenge of human breast cancer cells leads to a low number of cells expressing HCMV IE antigen. Human breast cancer cell lines MDA-MB-231 (a) and MCF-7 (b) were challenged with HCMV at MOIs of 0.01, 0.1, 1, and 2 for 36 h, then stained for HCMV IE using anti-IE antibody. Cells positively stained for IE were expressed over the total number of cells as a percentage, quantified in 5 randomly chosen fields. N=3. P-values were calculated by one-way ANOVA. *=p<0.01 compared to 0.01 MOI; \$=p<0.01 compared to 0.1 MOI; #=p<0.05 compared to 1 MOI. Representative images of stained cells infected with filtered control (FCMV) and HCMV at MOI of 2 were taken with 20X magnification lens (c).

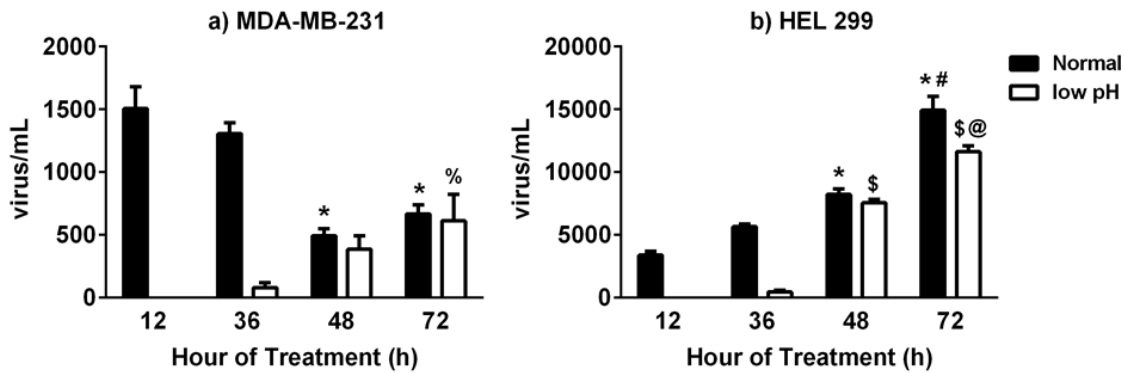


Figure 4.2. HCMV does not productively infect human breast cancer cell line MDA-MB-231. Examination for productive infection when cells were challenged with HCMV for 12, 36, 48, or 72 h, with MOI of 2 for MDA-MB-231 breast cancer cells (a) and 0.1 MOI for HEL-299 fibroblasts (b). Cells were either washed with normal (pH=7.0) or low pH (pH=3.0) HBS after 2 h of HCMV challenge, with the low pH wash ensuring removal of the input virus to evaluate the amount of virus produced by the cells. Cell lysates and supernatants were collected at each treatment time point and re-added to fresh HEL 299 fibroblasts for 24 h, followed by HCMV IE antigen staining for infectivity. Results were expressed as virus/mL. N=3. P-values were calculated by two-way ANOVA and Tukey's post-hoc test. A significant difference was observed for the hour of treatment in b) ($p=0.0001$) but not in a) ($p=0.07$). $*$ = $p<0.05$ compared to 12 and 36 h normal wash; $\$$ = $p<0.0001$ compared to 12 and 36 h low pH wash; $\#$ = $p<0.01$ compared to 48 h normal wash; $@$ = $p<0.05$ compared to 48 h low pH wash; $\%$ = $p<0.05$ compared to 12 h low pH wash.

virus was eliminated when HBS at pH=3.0 was used for cell washing to remove viral particles that were bound to the cell surface receptors (Figure 4.2b). HCMV infection in HEL 299 fibroblasts was productive after 48 h of initial viral challenge, with the viral amount determined as ~7500 virus/mL, regardless of the wash solution used for viral removal (Figure 4.2b). The amount of new virus produced was significantly increased after 72 h of initial viral challenge, with ~14000 virus/mL and 10000 virus/mL for cells washed with HBS at pH=7.0 and pH=3.0, respectively (Figure 4.2b). For HEL 299 fibroblasts, a statistically significant difference was observed between the different time points after viral challenge ($p=0.0001$, Figure 4.2b).

4.4 HCMV challenge stimulated expression of viral genes at the mRNA level in human breast cancer cells

The MDA-MB-231 breast cancer cells showed increased mRNA expression for HCMV IE (Figure 4.3a) and cmvIL-10 (Figure 4.3b) after challenge with HCMV for 3 h. The increase in expression of IE persisted until 6 h post-challenge, but with a lower expression compared to 3 h (Figure 4.3a). The increase in cmvIL-10 expression was no longer significant after 3 h (Figure 4.3b).

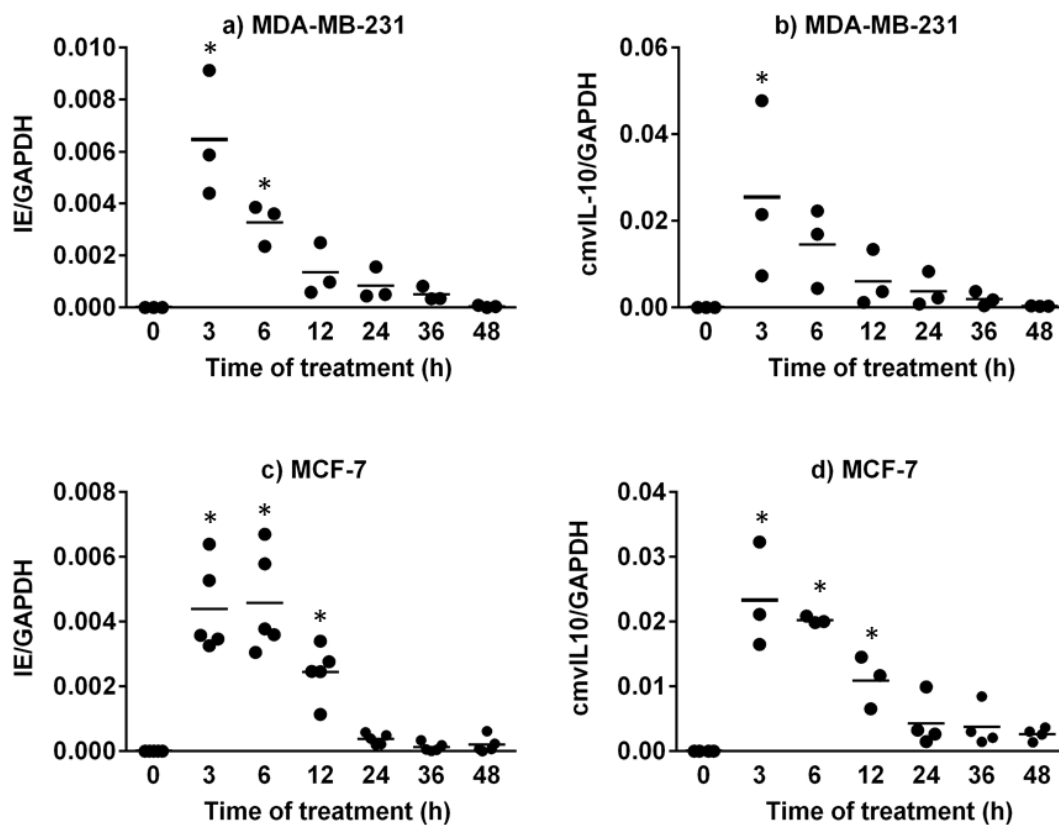


Figure 4.3. HCMV-challenged breast cancer cells showed increased expression of viral genes at the mRNA level during initial infection. Human MDA-MB-231 and MCF-7 breast cancer cells were challenged with HCMV at MOI of 2. Cells were collected at various timepoints after the viral challenge and analyzed for the mRNA expression of HCMV immediate early (IE) and cmvIL-10 viral genes. N=3-5. P-values were calculated by one-way ANOVA, with $*=p<0.05$.

The increase in mRNA expression of IE and cmvIL-10 was also observed in the MCF-7 breast cancer cells where both showed an increase starting at 3 h post-challenge (Figure 4.3c,d). These increases continued up to 12 h post-challenge and were no longer observed after 24 h (Figure 4.3c,d).

4.5 HCMV challenge stimulated expression of cytokines and inflammatory mediators at the mRNA level in human breast cancer cells

The mRNA expression for IL-1 β , IL-6, PTGS-2 and LPAR2 were significantly increased in the MDA-MB-231 breast cancer cells that were challenged with HCMV for 36 h compared to those without viral challenge (0 h) (Figure 4.4a-d). These increases were no longer significant at 48 h post-challenge, and there was a significant decrease in mRNA expression for IL-1 β when compared to the 0 h cells (Figure 4.4a). For IL-1 β , IL-6 and PTGS-2, the increase observed at 36 h was very marked (Figure 4.4a-c). However, a more gradual change was observed for LPAR2, with a trend of increase starting after 6 h and reaching significance by 24 and 36 h (Figure 4.4d). The expression of TGF β -1 was also analyzed but no significant differences were observed among any time points (Figure 4.4e). The expression of IL-10 and LPAR1 were low in these breast cancer cells and resulted in unreliable amplification cycle numbers that were greater than 33.

The same set of genes was analyzed in the MCF-7 breast cancer cells that were challenged with HCMV using the same conditions. No significant differences were observed in any of the tested genes, except for IL-6, which showed increased expression after 36 h of viral challenge compared to 0 h (Figure 4.5). However, a trend for increased IL-6 and PTGS-2 expression at the early time points was observed (Figure 4.5b,c). The MCF-7 breast cancer cells showed greater variability between independent experiments

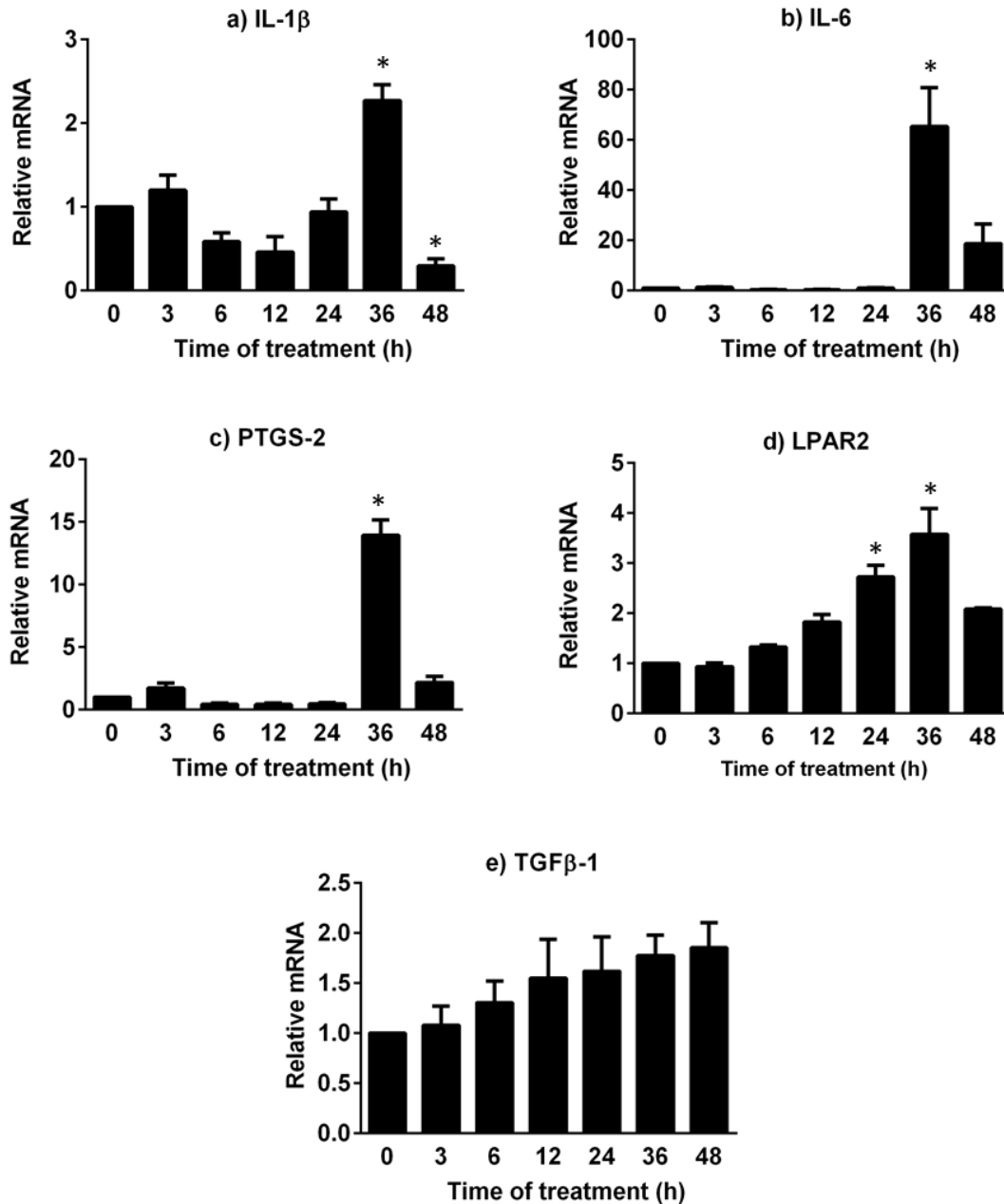


Figure 4.4. MDA-MB-231 breast cancer cells challenged with HCMV showed increased expression of cytokines and inflammatory mediators at the mRNA level. Cells were challenged with HCMV at MOI of 2 and collected at various timepoints for mRNA expression analysis. The expressions of IL-10 and LPAR1 were also tested but resulted in low detection. N=3. The mean and SEM are shown for each treatment time and p-values were calculated by one-way ANOVA. *= $p < 0.05$ compared to 0 h treatment. Abbreviations used: IL: interleukin; PTGS: prostaglandin-endoperoxide synthase; LPAR: lysophosphatidic acid receptor; TGF: transforming growth factor.

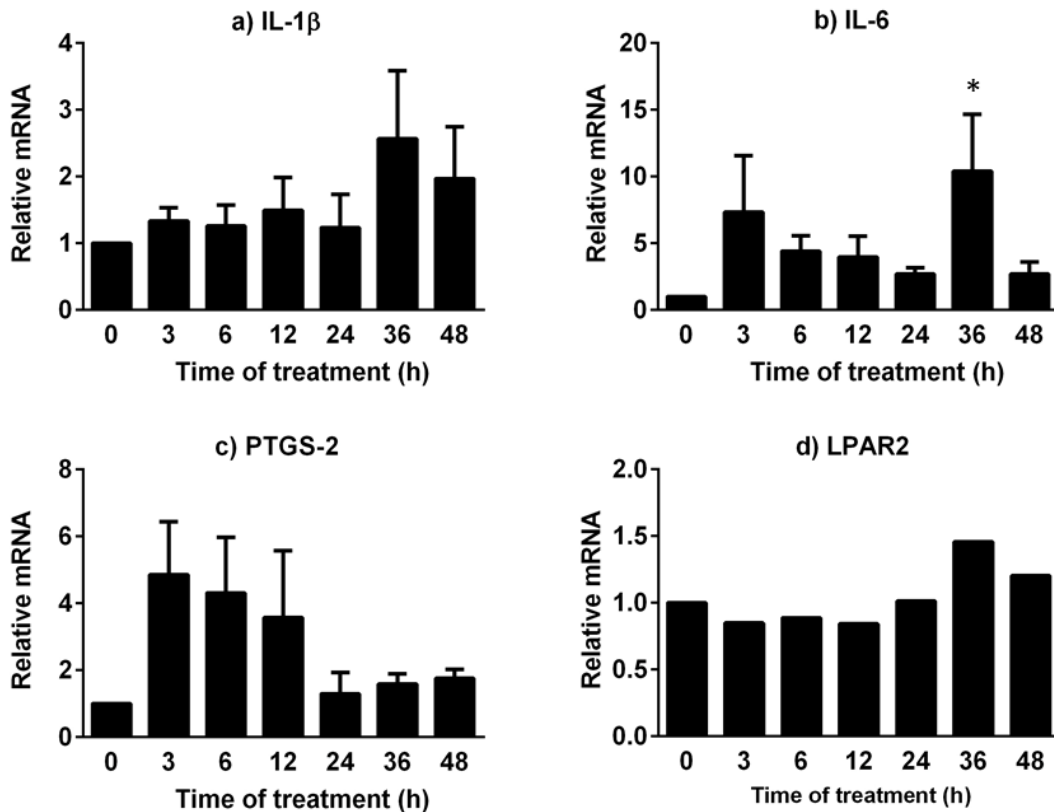


Figure 4.5. MCF-7 breast cancer cells challenged with HCMV showed increased expression of IL-6 but not other inflammatory mediators at the mRNA level. Cells were challenged with HCMV at MOI of 2 and collected at various timepoints for mRNA expression analysis. The expressions of IL-10 and LPAR1 were also tested but resulted in low detection. N=5. The mean and SEM are shown for each treatment time and p-values were calculated by one-way ANOVA. *=p<0.05 compared to 0 h treatment. Abbreviations used: IL: interleukin; PTGS: prostaglandin-endoperoxide synthase; LPAR: lysophosphatidic acid receptor.

compared to the MDA-MB-231 cells, which could contribute to the lack of statistical significance.

4.6 UV-inactivated HCMV did not stimulate mRNA responses in breast cancer cells

UV-inactivated virus that retains the whole viral particle but cannot infect cells due to its damaged DNA was used as a control for whether mRNA responses are stimulated due to viral gene transcription. The mRNA expression of HCMV viral genes and cytokines

in MDA-MB-231 breast cancer cells challenged with HCMV were increased following a dose response. The IE gene was expressed when challenged with 0.1 MOI of HCMV and reaching a significant difference with MOI of 2 when analyzed 3 h post-challenge, but the same response was not observed in cells challenged with UV-inactivated virus (Figure 4.6a). A similar lack of response to UV-inactivated virus was observed for the other viral gene, cmvIL-10, where 1 MOI of HCMV was sufficient to cause a significant difference (Figure 4.6c). As expected, both IE and cmvIL-10 showed low expression at 36 h post-challenge, with no statistical significance observed (Figure 4.6 b,d). The expression of IL-1 β was not significantly changed after 3 h of HCMV challenge (Figure 4.6e), but after 36 h, significant increases were observed for the HCMV challenge at MOIs 1 and 2 (Figure 4.6f). This is compatible with the previous results observed in Figure 4.5a. The UV-inactivated virus did not stimulate a significant change in mRNA expression of viral gene or inflammatory mediators for any time points or MOI tested (Figure 4.6).

4.7 mRNA expression of cytokines and inflammatory mediators in cultured breast tissues challenged with HCMV

It appears that the mRNA expression of IL-6 and PTGS-2 was increased in cultured human breast tissues challenged with HCMV for 12, 24, and 48 h, compared to the FCMV-challenged controls (Figure 4.7a,b). A decreased mRNA expression of ATX appears to occur at 12 and 24 h post-challenge, which goes back to the basal level by 48 h (Figure 4.7c). However, we only have results from two samples at the current stage, therefore, more experiments are required to confirm statistical significance.

A similar analysis was performed using mouse breast tissues challenged with mCMV, and an additional time point at 6 h was included. The responses in cultured mouse

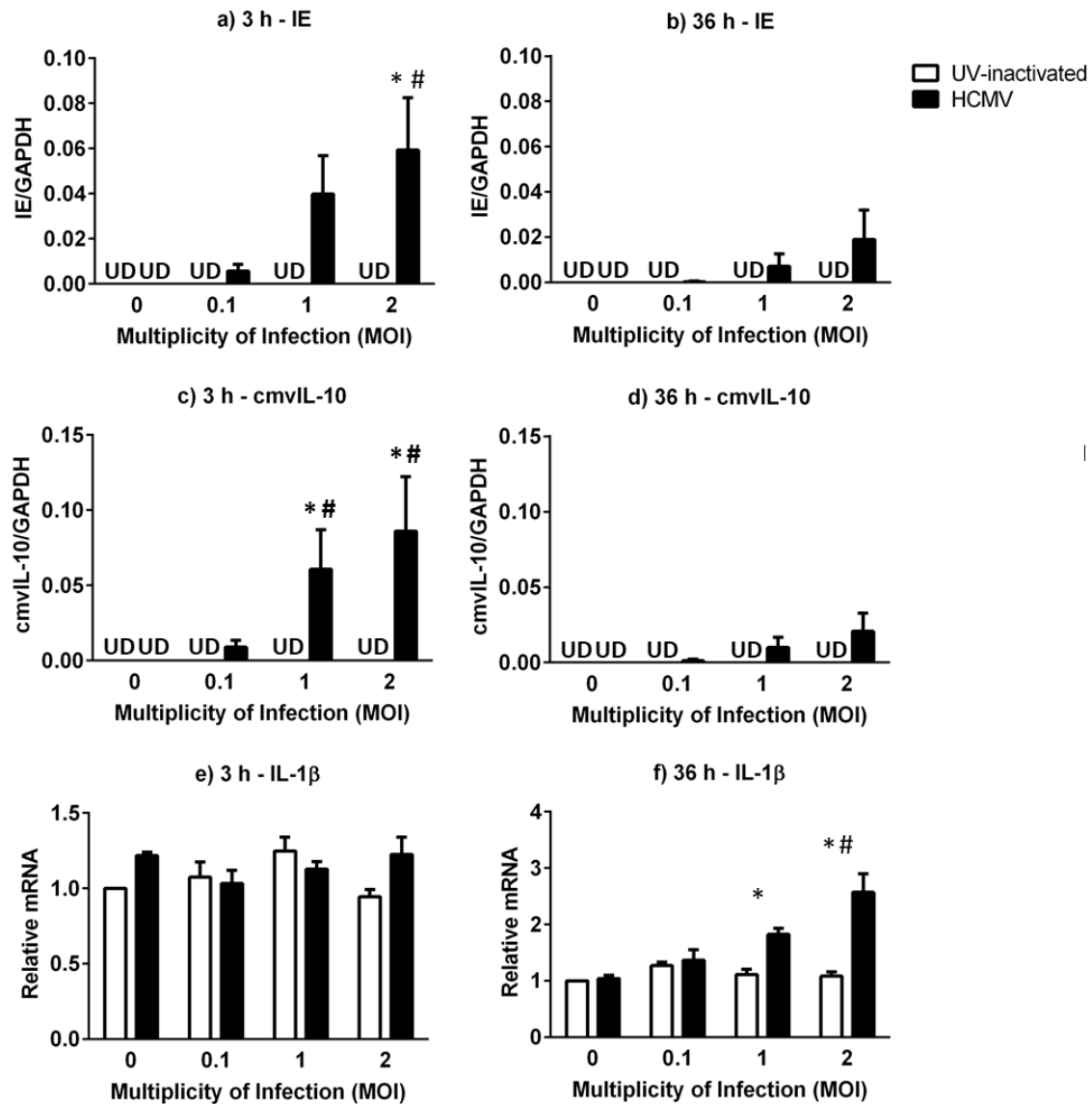


Figure 4.6. UV-inactivated virus did not stimulate mRNA expressions of viral genes and cytokines in breast cancer cells. MDA-MB-231 breast cancer cells were challenged with UV-inactivated virus or HCMV at MOIs of 0, 0.1, 1 and 2. Cells were collected at 3 and 36 h post-challenge for mRNA expression analysis. N=3. No detection of IE or cmvIL-10 was observed for cells challenged with UV-inactivated virus (a-d). The mean and SEM are shown for each MOI. P-values were calculated by two-way ANOVA and Tukey's post-hoc test. *= $p < 0.05$ compared to 0 MOI; #= $p < 0.05$ compared to UV-inactivated. Abbreviations used: UD: undetectable; IE: immediate early; cmv: cytomegalovirus; IL: interleukin.

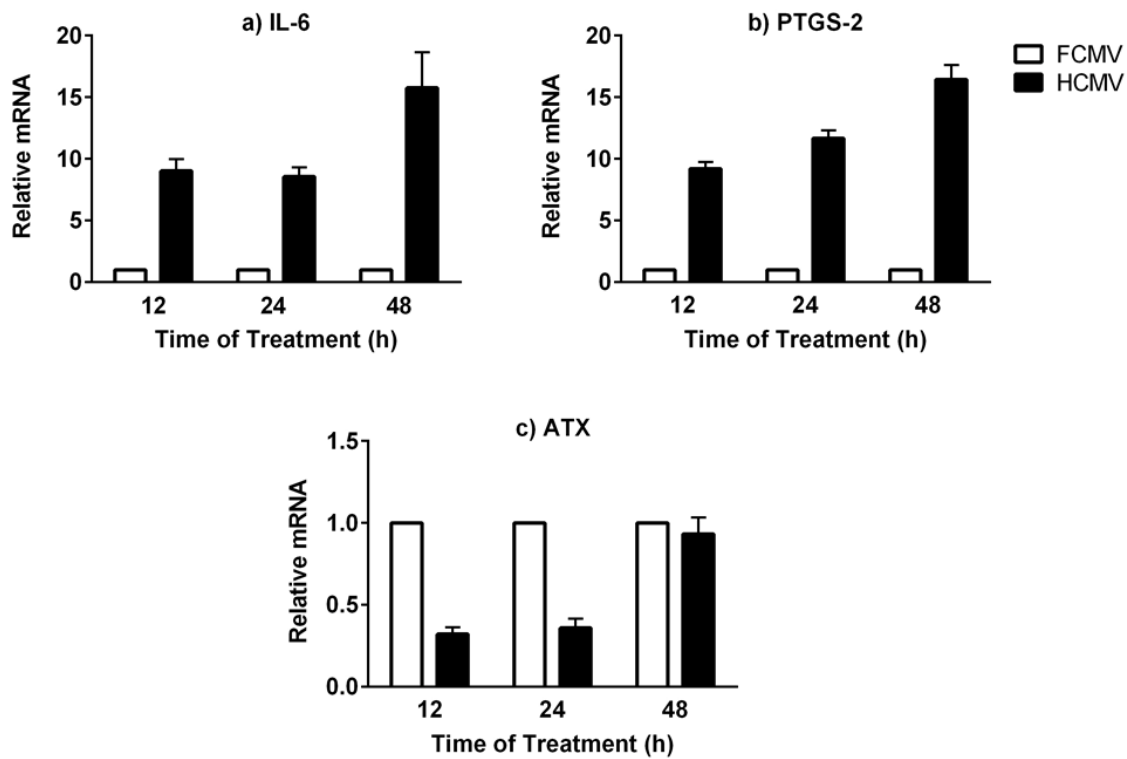


Figure 4.7. mRNA expressions of cytokine and inflammatory mediators in human breast adipose tissues challenged with HCMV. The cultured tissues were collected at various timepoints for mRNA expression analysis. Results are normalized to FCMV-challenged control at each time point. N=2. No statistical analysis was performed at this point. Abbreviations used: IL: interleukin; PTGS: prostaglandin-endoperoxide synthase; ATX: autotaxin.

breast tissues could be more rapid compared to those observed in cultured human breast tissues, which occurred by 12 h post-challenge (Figure 4.8). There was a tendency for increased expression of IL-6, PTGS-2 and ATX at 12 h, while IL-10 showed a tendency for decreased expression (Figure 4.8). The expression of IL-6 and PTGS-2 appeared to decrease by 48 h in the mouse breast tissues, which were not observed in the human breast tissues within the examined time range (Figure 4.8 a,b).

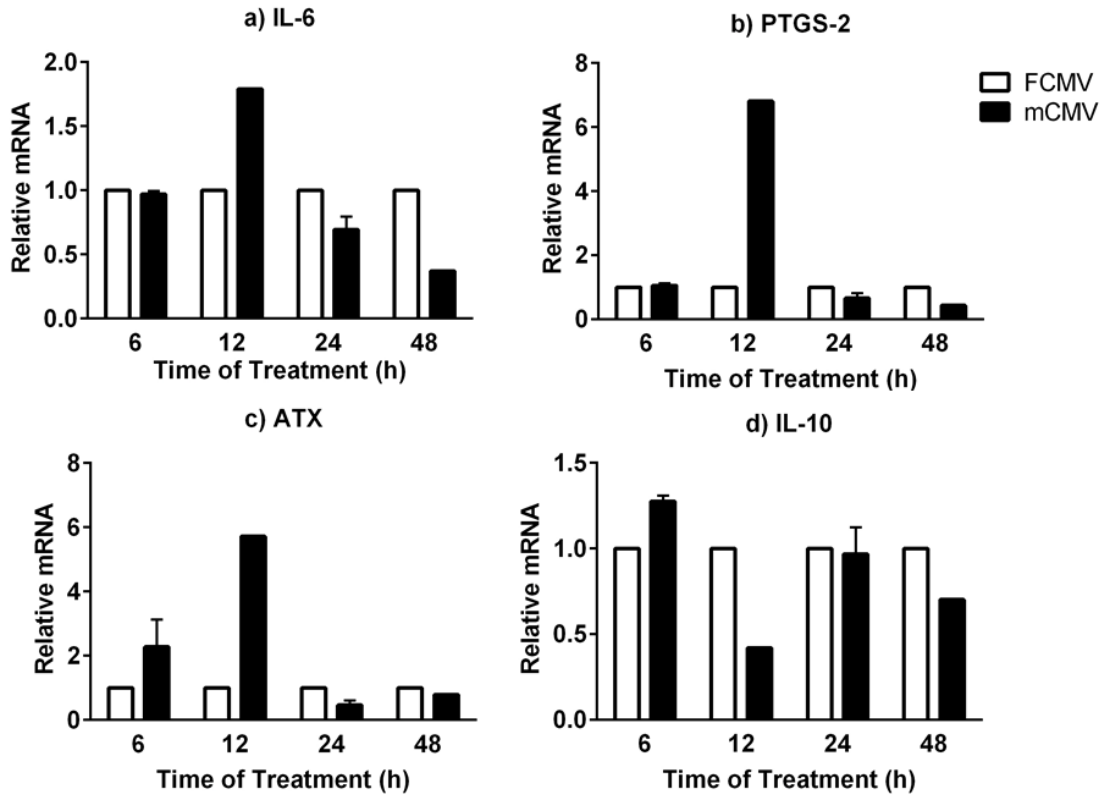


Figure 4.8. mRNA expressions of cytokines and inflammatory mediators in mouse breast adipose tissues challenged with mCMV. The cultured tissues were collected at various timepoints for mRNA expression analysis. Results are normalized to FCMV-challenged control at each time point. N=1-3. No statistical analysis was performed at this point. Abbreviations used: IL: interleukin; PTGS: prostaglandin-endoperoxide synthase; ATX: autotaxin.

4.8 Discussion

The HCMV-challenged breast cancer cells showed expression of HCMV IE antigen only in a very limited number of cells. The maximum amount of HCMV we added to the breast cancer cells was at MOI of 2, which is 2 infectious units per cell, but only less than 1% of the cells were positively stained for HCMV IE in the nucleus. One possible suggestion is that the amount of viral entry into breast cancer cells is limited. CMV has a broad cell tropism, where it can enter the cells through interaction with different receptors, such as integrins, EGFR and PDGFR- α , depending on the cell type [166, 167, 262]. It is

known that HCMV extensively passaged in cultured fibroblasts or the laboratory strains of HCMV have lost the ability to enter cells such as epithelial cells and macrophages. This is due to the mutations in the HCMV open reading frames that encode constituents of a glycoprotein complex (gH-gL-UL128-UL130-UL131) present in the virion envelope, which is important for viral entry [160]. In our experiments, we used a clinical isolate of HCMV that is maintained at a low passage number; therefore, cell entry should not be affected by mutation. However, the exact mechanism for HCMV entry into breast cancer cells is unclear and remains to be investigated. The low expression of IE antigen could also be explained by restrained production of HCMV viral proteins in breast cancer cells, which is likely since we did not observe a productive infection of the virus in the HCMV-challenged breast cancer cells.

Productive infection was observed in the HEL 299 fibroblasts that were challenged with HCMV, as expected. However, this was not observed in the MDA-MB-231 breast cancer cells even with a much higher MOI of HCMV added (MOI of 0.1 vs. 2). Although evidence of infectious virus was detected in the test fibroblasts that were cultured with lysates from HCMV-challenged breast cancer cells, the amount was very limited and statistically insignificant. These were probably due to the input viruses that remained or that production of virus was at a slow and minimal level. Input viruses that did not enter the cell but attached to the cell surface still possess infectivity. These viruses were not sufficiently removed when cells were washed with HBS at physiological pH, since infection was mostly eliminated when HBS at pH 3.0 was used for cell washing. The low pH condition allows unbinding of ligand from its receptor, therefore, led to removal of viral particles from cell surface receptors [263]. For HEL 299 fibroblasts, a significant amount

of new virus was produced starting at 48 h post HCMV challenge. There is a possibility that a longer time is required for HCMV to reproduce in the breast cancer cells, since cell lysing was not observed in MDA-MB-231 breast cancer cells challenged with HCMV for 120 h [132]. However, the breast cancer cells replicate very rapidly, and prolonged incubation led to overconfluent cells that would lift from the plate. Therefore, we conclude that HCMV did not productively infect breast cancer cells within the 72 h time frame.

A limitation of the study is that we do not know the amount of virus that has entered the cells. This could be determined by examining the level of HCMV DNA in the viral-challenged cells at various timepoints using LC-PCR that was described in section 2.7.1. In Chapter 3, we have shown detection of HCMV DNA in human breast tumors, with a trend for higher incidence of detection in tumors that are HER2 negative. It is uncertain whether HER2 expression directly affects the amount of viral DNA in the breast cancer cells. The MDA-MB-231 and MCF-7 breast cancer cells investigated in this study are both HER2 negative; therefore, it could be interesting if a comparison can be made to breast cancer cells that are HER2 positive.

Despite the low number of cells expressing HCMV IE antigen, transcription of viral genes was stimulated in MDA-MB-231 and MCF-7 breast cancer cells that were challenged with HCMV. The HCMV IE gene and the viral encoded homolog of IL-10, *cmvIL-10*, were both increased in expression at the mRNA level. The increases were observed at the initial stage after viral challenge, with a maximum expression at 3 h (1 h after removal of input virus), which is expected since both genes are immediately transcribed when HCMV enters a susceptible cell [192]. However, the increased expression was no longer observed at later hours, providing additional evidence that new viruses were

not produced to initiate further infection within the time range of our experiment. The expression of viral genes was more persistent in MCF-7 cells, which lasted to 12 h post viral challenge. This indicates that the transcription cycle of HCMV differs in different cancer cell lines, although the mechanism was unclear. The MCF-7 cells should be analyzed in parallel with the MDA-MB-231 cells for the level of HCMV DNA expression at various time points after viral challenge.

The mRNA of IE and *cmvIL-10* were only expressed at the early time points in response to the input virus and was not maintained due to lack of new stimulation, but there is evidence that viral transcription is required for stimulating gene expression of inflammatory mediators in the HCMV-challenged breast cancer cells. In HCMV susceptible cells like fibroblasts, the infection was shown to upregulate a variety of cytokines due to the activity of IE proteins and/or induction of cellular transcription factors like NF- κ B [264]. We found increased mRNA expression of cytokines and inflammatory mediators in the HCMV-challenged breast cancer cells after 36 h, which could be in response to the previous transcription of viral genes and IE antigen expression. This was not observed in breast cancer cells challenged with the UV-inactivated virus, where the viral particles are still intact but have lost the ability to initiate viral gene transcription in the host cells. This indicates that the observed responses were not due to HCMV binding to the cellular receptors but that they require viral entry and viral transcription. The upregulated mRNA expression of cytokines and inflammatory mediators did not persist, which is compatible with the observation that viral transcripts also did not persist. However, when in context of a tumor, the HCMV-induced inflammation in breast cancer cells could trigger further signalling responses in the surrounding cells, therefore leading to a long

term effect that promotes tumor progression and metastasis [30, 62, 63]. In fact, other cells in the tumor microenvironment such as fibroblasts and macrophages are susceptible to CMV infection [159]. It is possible that the effect of CMV infection on these cells are more evident than in the breast cancer cells. Therefore, an interplay between these cells and breast cancer cells in terms of CMV infection and stimulation of inflammation is interesting for future investigation.

The increased mRNA expression of inflammatory genes in our HCMV-challenged MDA-MB-231 breast cancer cells are compatible with previous findings in other cell types where HCMV infection upregulated expression of cytokines, including IL-1 β [265], IL-6 [266], and PTGS-2 [267]. Also, the increased expression of LPAR2 would increase LPA signaling of inflammation, since LPA binds to LPAR for activation of signaling pathways involved in cancer progression [53]. With tumor-promoting inflammation as a hallmark of cancer, it can be suggested that HCMV challenge of breast cancer cells could promote breast cancer cell growth and metastasis [30]. However, the expression of cytokines and inflammatory mediators have not been tested at the protein level. This can be analyzed in the collected culturing media for the level of functional cytokines and inflammatory mediators that were secreted from the cells.

We have observed a difference in the mRNA expression profiles of the two breast cancer cell lines examined. This could be due to the different basal levels of gene expression in the two cell lines, for example, uninfected MCF-7 cells express very little IL-6. This is especially important since our results were expressed as a relative value against cells that were not challenged with HCMV or were treated with the negative control, resembling the wild type cells with a basal level of gene expression. We found that a very

low percentage of the breast cancer cells were positive for HCMV IE antigen after viral challenge. If the viral entry can be increased, there could be a stronger response generated in the cells and thus it would be easier to observe the changes stimulated by HCMV. There is evidence that overexpression of PDGFR- α would increase HCMV entry into cells that are normally low or non-permissive for HCMV [268]. The breast cancer cells examined in this study expressed very little PDGFR- α but can be transfected for overexpression [269]. PDGFR- α is also interesting since its activation stimulates signalling pathways that promote cancer progression and metastasis [270]. This could be helpful for the purpose of study by maximizing the effects of HCMV challenge in breast cancer cells.

In Chapter 3, we have shown that HCMV DNA is not only detected in breast tumors, but also in normal breast tissues. The breast adipose tissue is a major site of inflammation and HCMV infection could enhance this effect [31]. Currently, our study consists of a limited number of cultured human adipose tissues due to the availability of patient samples; therefore, we can only describe what appears to have occurred. There is a trend for increased mRNA expression of cytokines and inflammatory mediators including IL-6 and COX-2 in HCMV-challenged human breast adipose tissues. Similar responses occurred when mouse breast adipose tissues were challenged with mCMV after 12 h, but not for other time points. This suggests different expression profiles between the two species. It is to our surprise that a trend of decreased ATX expression was observed for human adipose tissues challenged with HCMV after 12 and 24 h, since our previous work with ATX shows that it drives inflammation in the breast tissues [31, 249]. However, this should be further investigated by extending the time frame of experiment, since the ATX expression was increased to a similar level as the negative control treated tissues by 48 h. On the other

hand, the ATX results observed in mouse tissues were compatible with our expectation, with a trend of increased expression at 6-12 h post CMV challenge. Our current investigation is on independently cultured normal breast tissues from non-cancerous women. For better understanding of how the CMV-induced inflammation in the breast tissues would interplay with the breast cancer cells during a cancerous condition, co-culture of the breast tissues and breast cancer cells should be considered for future investigation. This is important since our lab has shown that the tumor-associated breast adipose tissues play a crucial role in tumor-promoting inflammation that leads to breast tumor progression and metastasis [31].

These *in vitro* models allowed us to study the effect of HCMV infection directly in breast cancer cells and breast tissues. However, the host systemic effect to HCMV infection could not be studied in culture. Therefore, it is important to establish *in vivo* models where the effect of CMV infection on breast cancer progression can be studied with regards to active and latent infections. We have, therefore, established several mouse breast cancer models with mCMV infection for this purpose, which will be discussed in the next chapter.

Chapter 5: The effect of mCMV infection on breast tumor growth and metastasis in mice

Components of Chapter 5 have been published as:

Yang, Z., Tang, X., Meng, G., Benesch, M.G.K., Mackova, M., Belon, A.P., Serrano-Lomelin, J., Goping, I.S., Brindley, D.N., and Hemmings, D.G., *Latent cytomegalovirus infection in female mice increases breast cancer metastasis*. *Cancers (Basel)*, 2019. **11(4):447**

5.1 Introduction

Our results from the previous chapters showed an association between HCMV and breast cancer. Next, we investigated the role of CMV infection on breast tumor growth and metastasis using mouse models. CMV infection is species specific, therefore, mCMV was used to infect the mice. Three mouse models were established using immunocompetent mice, so mCMV infection would not lead to severe symptoms, which represents the majority of the CMV-infected population in human beings. Two of the mouse models were with orthotopic injection of the syngeneic breast cancer cells and the other model was of transgenic mice with spontaneous breast tumor growth. The BALB/c and C57BL/6 mice were inoculated with the syngeneic 4T1 or E0771 breast cancer cells in a mammary fat pad, respectively. The transgenic mice used were B6.FVB-Tg (MMTV-PyVT)634Mul/LellJ, on a C57BL/6 background and referred to as the MMTV-PyVT model [251, 252].

The initial stage of CMV infection produces a strong innate immune response. This is followed by an adaptive immune response, and both are important in the host's defense against CMV [210]. In most cases, CMV infection will become latent, with the viral genome retained in the host but very little or no viral transcription observed [175]. However, CMV can be reactivated under conditions that involve inflammation and stress [180, 181]. The active and latent stages of CMV infection stimulates the host immune responses differently; therefore, all stages should be considered when examining the effect of CMV infection on breast tumor progression. We established mouse models of breast cancer with different mCMV infection statuses at the time of tumor inoculation or development to examine the different effect between active infection and latency on breast tumor growth and metastasis.

HCMV proteins and DNA are abundantly expressed in sentinel lymph nodes [231] and in brain tissues [245] from breast cancer patients, suggesting that HCMV infection might be associated with invasiveness and metastasis. This was investigated further in our mouse models of BALB/c mice inoculated with 4T1 breast cancer cells and the MMTV-PyVT mice with spontaneous tumor development since both are known to be metastatic.

Apart from the finding that CMV viral particles are present in cancerous tissues, there is other evidence showing CMV to be involved in cancer progression. CMV infection fulfills many of the criteria for hallmarks of cancer, such as activating invasion and metastasis, tumor-promoting inflammation and inducing angiogenesis [137]. Examples include salivary gland cancer, where HCMV infection increased production of the inflammatory cytokine IL-6, leading to an association with tumor development [222]. A correlation is also found between HCMV IE protein and overexpression of COX-2 in breast tumors of breast cancer patients [223].

In this chapter, I have investigated the consequences of mCMV infection on breast tumor progression and metastasis in the established mouse models. The effect of mCMV infection on inflammation was investigated in these mice and specifically in the breast tumors. The presence of mCMV DNA and mRNA was also investigated in various mouse tissues, including but not limited to the breast tumors. I hypothesized that mCMV-infected mice will show enhanced inflammation that contributes to promotion of breast tumor progression and metastasis.

5.2 Active infection of mCMV was detected in mice 4 days post-infection

We demonstrated that injection of mCMV at 10^6 IF was able to produce an active infection for all mouse models used in the experiments, including C57BL/6, BALB/c, and

MMTV-PyVT mice. The PBS, FCMV, and UV-inactivated control solutions were also tested in mice to verify non-infectivity. Two test animals were used for each infection or control test. The mice were sacrificed four days after infection and organs were stained for the activity of β -galactosidase, a product of the LacZ gene, which was inserted into the immediate-early 2 region of the mCMV genome. This modified virus has the same properties as native mCMV but the production of β -galactosidase allows an active infection to be visualized by the conversion of its substrate, X-gal, into a blue product when the virus is actively replicating [248]. Positive staining was observed in the kidneys collected from mice infected with active mCMV, but not in those injected with control solutions like FCMV (Figure 5.1). In addition, transcripts for mCMV IE 1/3 and gB were both detected in the salivary glands and kidneys of mice actively infected for four days, with the amplification cycle number ranging from 20 to 24. These transcripts were not detected in the control-treated mice, with the cycle numbers unable to be determined. We also determined that the β -galactosidase activity and viral transcripts were no longer detectable when mice infected with active mCMV were studied at 11 days or 10 weeks post-infection, indicating that the infection was transiting to or becoming latent. No physical illnesses or behavioral changes were observed for the mCMV-infected mice compared to the control-treated mice.

5.3 mCMV infection had no significant effect on breast tumor growth

The effects of active, intermediate and latent mCMV infection on breast tumor growth was determined by infecting mice with mCMV or by treatment with negative control solutions 4 days, 11 days or 10 weeks, respectively, prior to inoculation of the syngeneic breast cancer cells into the mammary fat pads of BALB/c and C57BL/6 mice. Volumes of the breast tumors in mCMV-infected

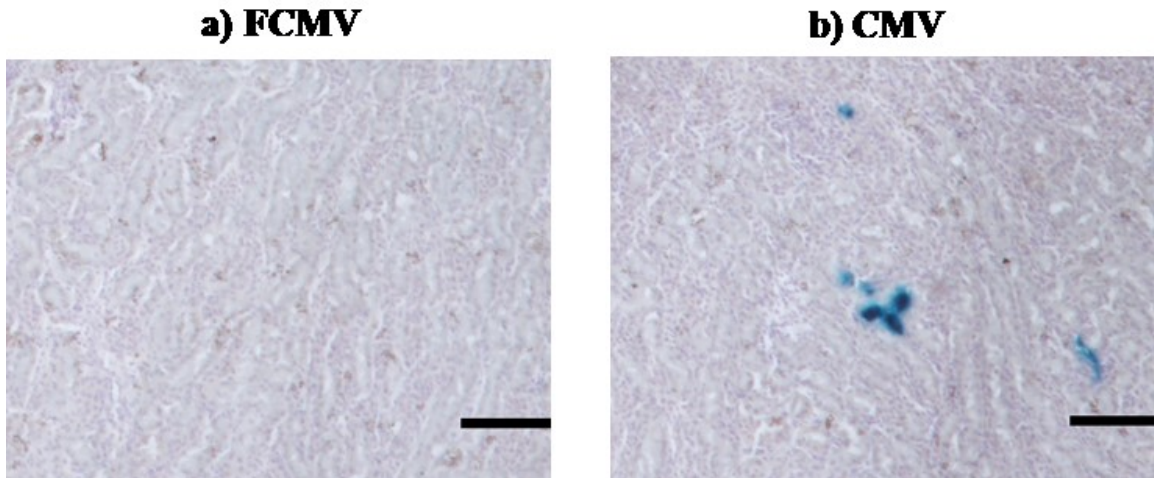


Figure 5.1. Verification of active infection 4 days post mCMV injection in mice. LacZ activity detected by staining for β -galactosidase, representing an active infection, in kidney tissues from FCMV (a) and CMV (b) treated C57BL/6 mice. Development of blue colonies indicates positive detection of active mCMV infection. Similar results were obtained in the BALB/c and MMTV-PyVT mice. Images taken with a 20X magnification lens. Scale=100 μ m.

BALB/c mice were not significantly different throughout tumor development compared to control-treated mice regardless of the length of the pre-existing infection (Figure 5.2a-c). In the C57BL/6 mice, there were no differences in tumor volume in those with an intermediate or latent infection (Figure 5.2e,f). However, mice with an active infection prior to injection of breast cancer cells had a reduced overall estimate of tumor volume on days 15 and 17, which was significant on post-hoc testing (Figure 5.2d).

It can be difficult to measure the tumor volumes accurately, especially if the tumors are soft and filled with fluid. Therefore, tumor mass measurements are normally more accurate. With one exception, the masses of the breast tumors at the endpoint in the BALB/c and C57BL/6 mice were not significantly different between mCMV-infected or control-treated mice in the active, intermediate, or latent models (Figure 5.3 and Figure 5.4a,b). The exception was that latently infected BALB/c mice had an increased tumor

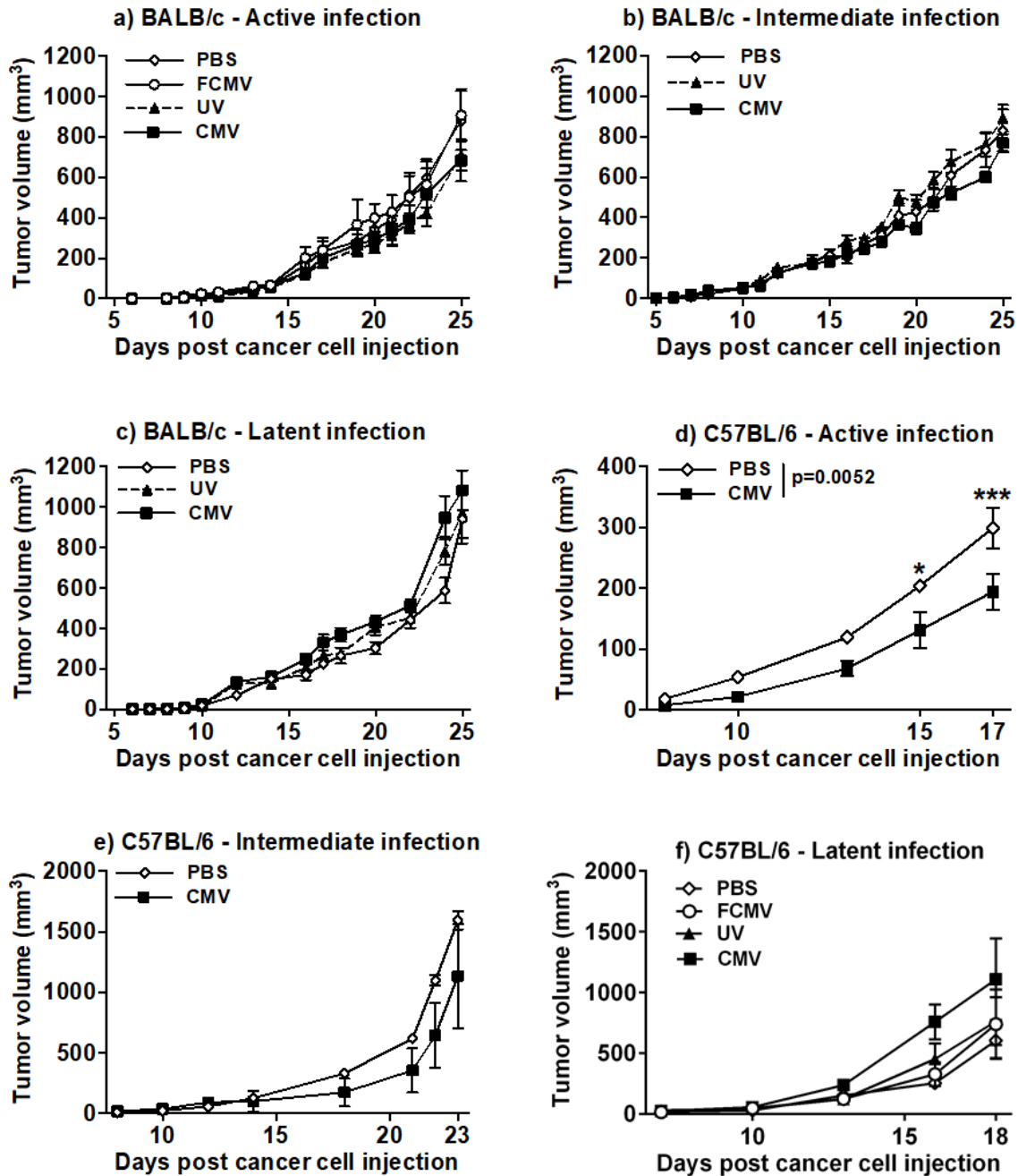


Figure 5.2. Estimated volume of breast tumors developed over time in BALB/c and C57BL/6 mice with and without active, intermediate or latent mCMV infections. Estimated breast tumor volume by caliper measurement for BALB/c with active (a), intermediate (b) or latent (c) infections and C57BL/6 with active (d), intermediate (e) or latent (f) infections. N=5-6 for each group. P-values calculated by two-way ANOVA, ***p<0.001, *p<0.05.

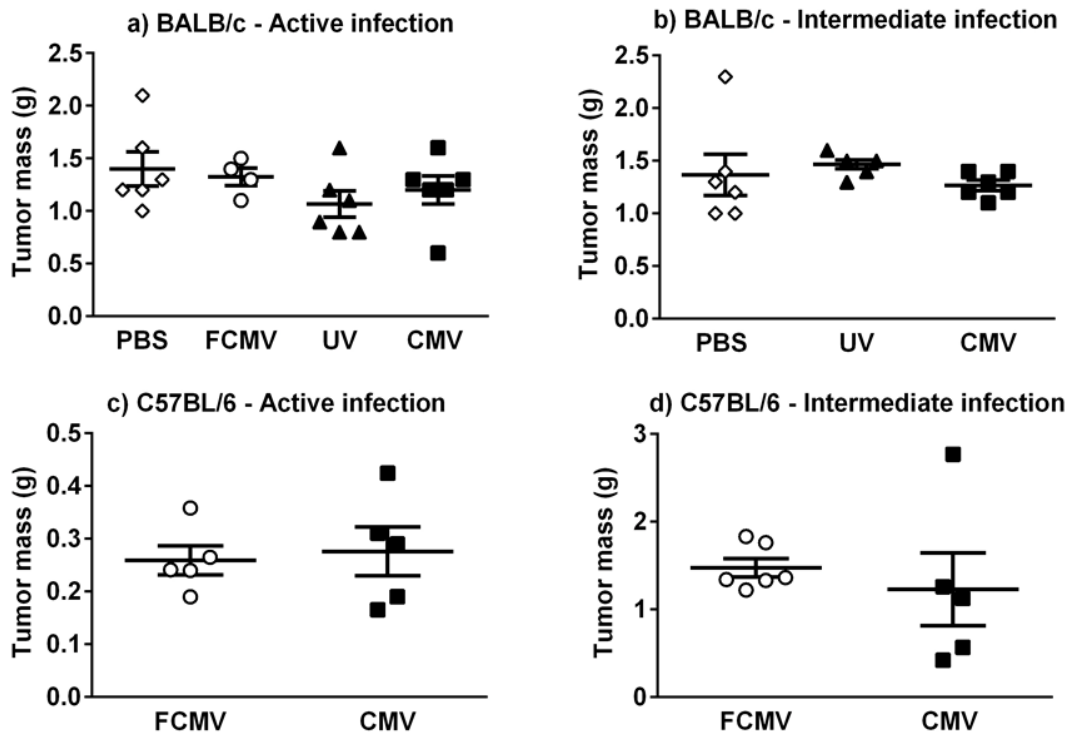


Figure 5.3. Breast tumor mass was not significantly affected in mice with active or intermediate mCMV infections. Breast tumor mass taken at endpoint for BALB/c with active (a) or intermediate (b) infections and C57BL/6 with active (c) or intermediate (d) infections. N=5-6 for each group. P-values calculated by one-way ANOVA (a, b) or Student's t-test (c, d), all with no significant differences.

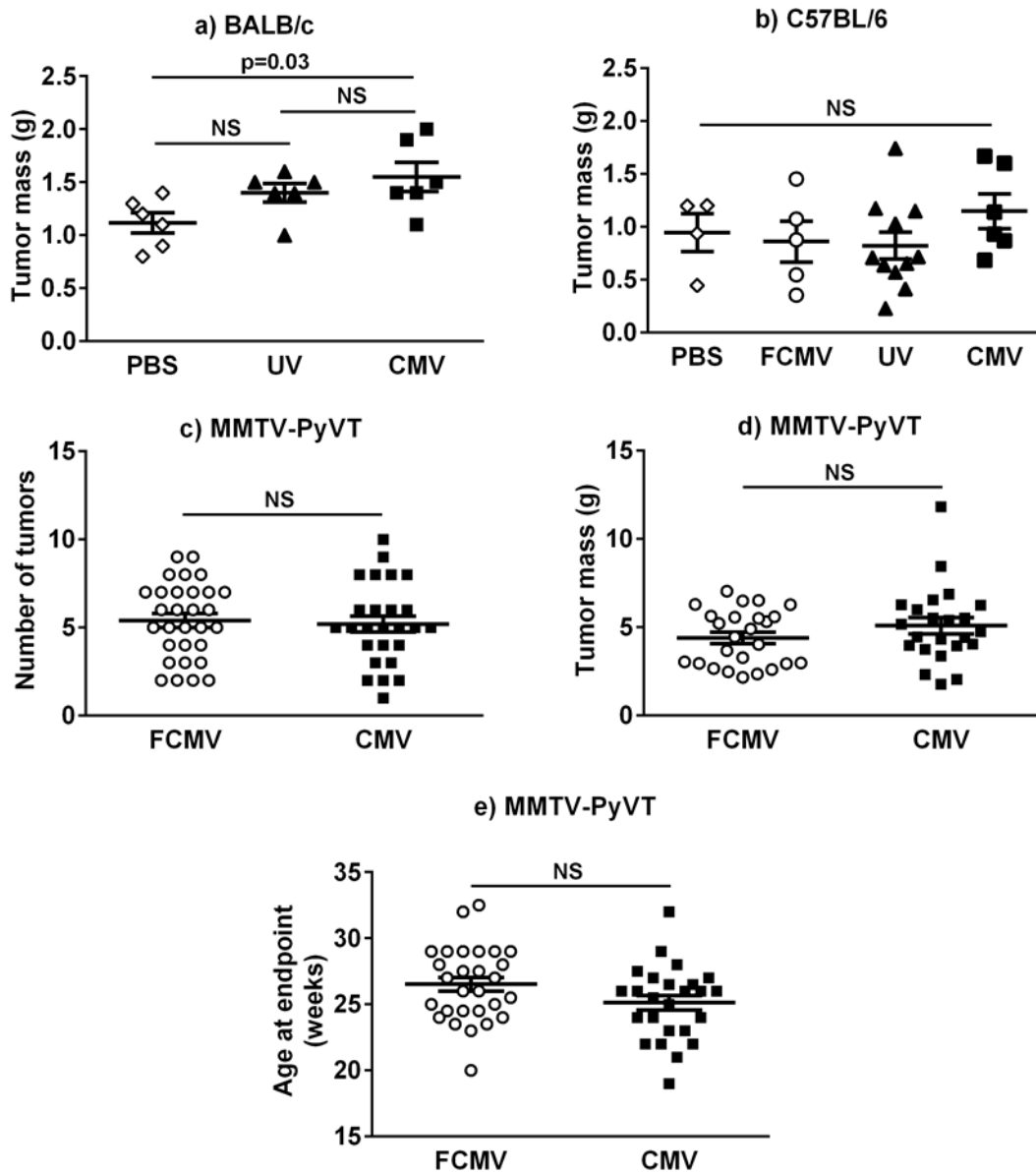


Figure 5.4. Latent mCMV infection has minimal effects on breast tumor mass. Breast tumor mass was measured at the endpoint in the latent infection models of BALB/c (a) and C57BL/6 (b) mice, $n=6$ and $n=4-11$, respectively. Control mice were injected with PBS, UV-inactivated CMV (UV) or a solution where active CMV was filtered out (FCMV). For MMTV-PyVT mice, the total number (c) and total mass (d) of all breast tumors developed per mouse were quantified for 25 mice treated with a filtered control solution (FCMV) and 23 mCMV-infected mice. The age of these mice at the experimental endpoint was illustrated (e). P-values were calculated by one-way ANOVA (a, b) or Student's t-test (c, d) with $p < 0.05$ considered to be significant. NS=not significant.

mass compared to the PBS-treated group, but there was no significant difference compared to the control treatment where mCMV was inactivated by UV exposure (Figure 5.4a).

We then studied MMTV-PyVT mice, which are on a C57BL/6 background, to provide a spontaneous model of breast cancer that better resembles the human situation. mCMV or FCMV was injected at 5 weeks of age to allow at least 10 weeks to develop a latent mCMV infection before the spontaneous tumors became palpable. The number of tumors per individual mouse was highly variable, as expected in this model, with a range from one to ten tumors (Figure 5.4c). The total burden of tumor mass per mouse (Figure 5.4d) and the average volume, mass or density of tumors (Table 5.1) did not differ statistically between the FCMV and mCMV-infected groups at the experimental endpoint. The time required for mice to reach the experimental endpoint was highly variable and not significantly different between the experimental groups (Figure 5.4e).

Table 5.1. Average tumor volume, mass and density in MMTV-PyVT mice with and without latent mCMV infection.

Variables	n	Mean \pm SD	95% CI	p-value
Tumor Volume (mm³)				
FCMV	133	957 \pm 947	795, 1120	0.064
CMV	104	1202 \pm 1077	993, 1411	
Tumor Mass (mg)				
FCMV	133	0.84 \pm 0.85	0.70, 0.99	0.164
CMV	104	1.01 \pm 0.96	0.82, 1.20	
Tumor Density (mg/mm³)				
FCMV	133	0.90 \pm 0.29	0.85, 0.95	0.789
CMV	104	0.89 \pm 0.33	0.82, 0.95	

5.4 Latent mCMV infection of MMTV-PyVT mice changed the breast tumor phenotypes

Each breast tumor in the MMTV-PyVT mice was examined for different phenotypes, which included the blood content categorized as pale, moderate or bloody tumors (Figure 5.5a); the tumor type characterized as single tumors, multilobed or fused small tumors (Figure 5.5b); and tumor morphology characterized as solid, soft, necrotic, disintegrated or fluid filled tumors (Table 5.2). Although an mCMV infection did not affect the total tumor burden per mouse (Figure 5.4c,d), it did change the tumor phenotypes. On average, each mouse had one tumor that had a pale appearance. In the FCMV control mice, equal numbers of tumors per mouse were characterized as moderate or very bloody. By contrast, more tumors in each mCMV-infected mouse were very bloody (dark red) as opposed to containing a moderate amount of blood (pink) (Figure 5.5a). Very few or no

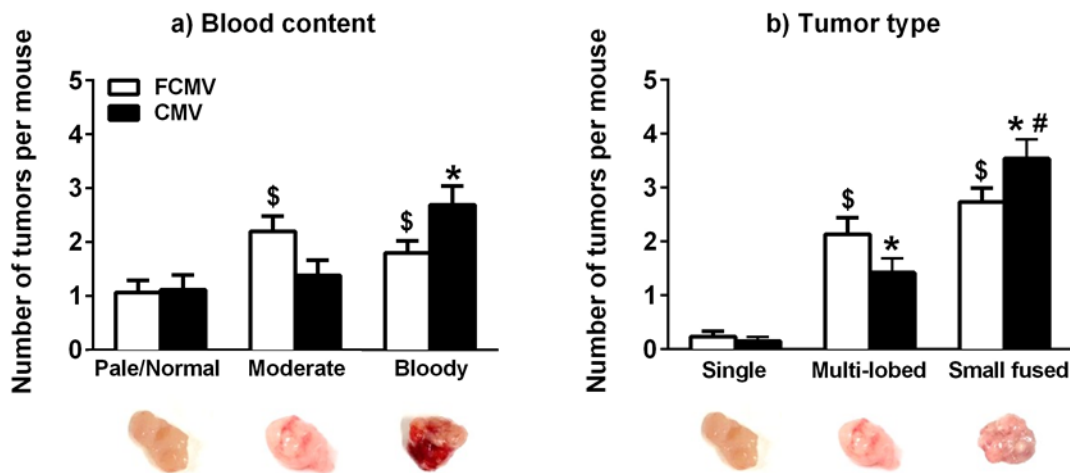


Figure 5.5. MMTV-PyVT mice latently infected with mCMV developed more breast tumors with severe phenotypes associated with metastasis. Tumors were categorized as pale/normal, moderate or bloody (a) or as a single tumor, multi-lobed or fused small tumors (b) in 25 control mice treated with a filtered control solution (FCMV) or 23 mCMV-infected mice. The mean number and SEM for each type of tumor per mouse are shown and p-values were calculated by two-way ANOVA and Tukey's post-hoc test. A significant interaction between treatment and phenotype was found in a) ($p=0.009$) and b) ($p=0.01$). \$= $p<0.05$ compared to pale/normal or single tumor in the FCMV group; *= $p<0.05$ compared to pale/normal or single tumor in the mCMV group; #= $p<0.05$ compared to multi-lobed in the CMV group.

Table 5.2. Severity of tumors in MMTV-PyVT mice with and without latent mCMV infection.

Variables	FCMV		CMV		p-value
	n	%	n	%	
Blood Content					0.005
Pale	34	25.6	22	21.1	
Moderate	56	42.1	27	26.0	
Bloody	43	32.3	55	52.9	
Tumor Type					0.006
Single	5	3.8	3	2.9	
Multi-Lobed	61	45.9	28	26.9	
Fused	67	50.4	73	70.2	
Morphology					0.303
Solid	10	7.5	7	6.7	
Soft	56	42.1	32	30.8	
Necrotic	23	17.3	17	16.4	
Disintegrated	12	9.0	15	14.4	
Fluid Filled	32	24.1	33	31.7	

* Based on Chi-square analysis (homogeneity test)

tumors were characterized as a single tumor. The numbers of multilobed and fused small tumors in each FCMV control mouse were not significantly different. By contrast, a significantly greater proportion of fused small tumors were found in each mCMV-infected mouse compared to multilobed tumors (Figure 5.5b). When analyzing all tumors, we determined that tumors with more severe phenotypes such as high blood content ($p=0.005$) or fused small tumors ($p=0.006$) were more often found to be from the mCMV-infected mice. This was not the case with tumors that were solid, soft, necrotic, disintegrated or fluid-filled ($p=0.303$) (Table 5.2). In addition, the odds ratio of having a fused small tumor combined with high blood content was 2.22 times higher (95% CI 1.29, 3.84; $p=0.004$) in the mCMV-infected group compared to the FCMV controls.

The observed increase in the proportion of very bloody breast tumors in the mCMV-infected MMTV-PyVT mice was further investigated by assessing the number of blood vessels by staining for the endothelial marker, CD31. Eight mice from each group were chosen randomly, and the largest tumor at the endpoint from each mouse was used for analysis. These large tumors were bloodier with more fused lobes, regardless of treatment. The average number of blood vessels observed in the stained sections of the breast tumors from the mCMV-infected mice was significantly increased compared to those from the FCMV control mice (Figure 5.6a,b).

The amount of collagen was significantly lower in the breast tumors of mCMV-infected MMTV-PyVT mice compared to the controls (Figure 5.6c,d). This could have reflected an increased collagen degradation, but there were no significant differences in the expression of MMP-2, MMP-3, MMP-8 (a collagenase), pro-MMP9 and MMP-12 in the tumors (Figure 5.7).

These combined results establish that, although latent mCMV infection of MMTV-PyVT mice did not affect the tumor load, there was a difference in the tumor phenotype that could modify metastasis.

We also characterized the tumors from the C57BL/6 and BALB/c mice that were injected orthotopically with E0771 or 4T1 breast cancer cells, respectively. In these cases, there were no obvious differences in the tumor phenotypes for mCMV-infected and uninfected mice of either strain. The breast tumors from BALB/c mice that were actively

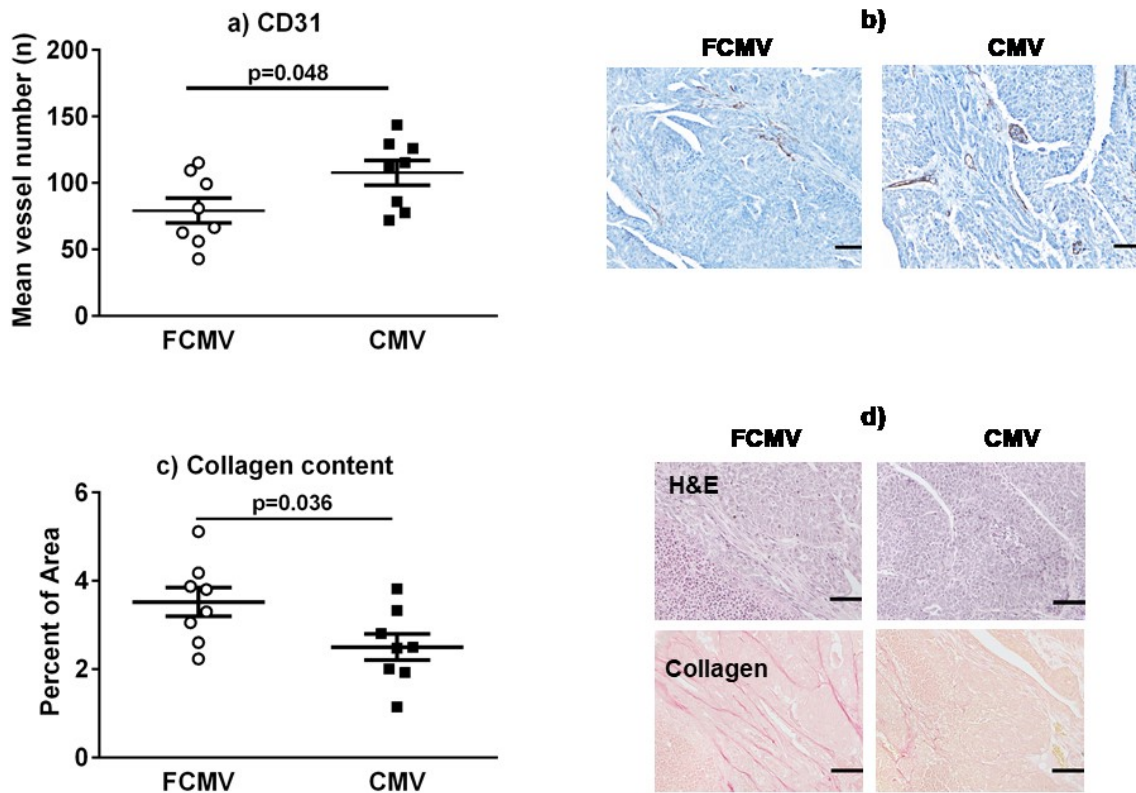


Figure 5.6. Tumors from MMTV-PyVT mice latently infected with mCMV had increased microvasculature and decreased collagen content. The number of blood vessels was assessed by CD31 staining in sections from the largest breast tumors from n=8 mice in each group (a), with representative images of stained sections (b). Collagen was quantified as percent of total area in sections from the same set of breast tumors (c). Representative matched sections taken from the same area of the breast tumors were stained with H & E for detection of nuclei (d, top) and for collagen using Sirius red (d, bottom). Images were taken with 20X magnification lens. Scale=100 μ m. P-value was calculated using a Student's t-test.

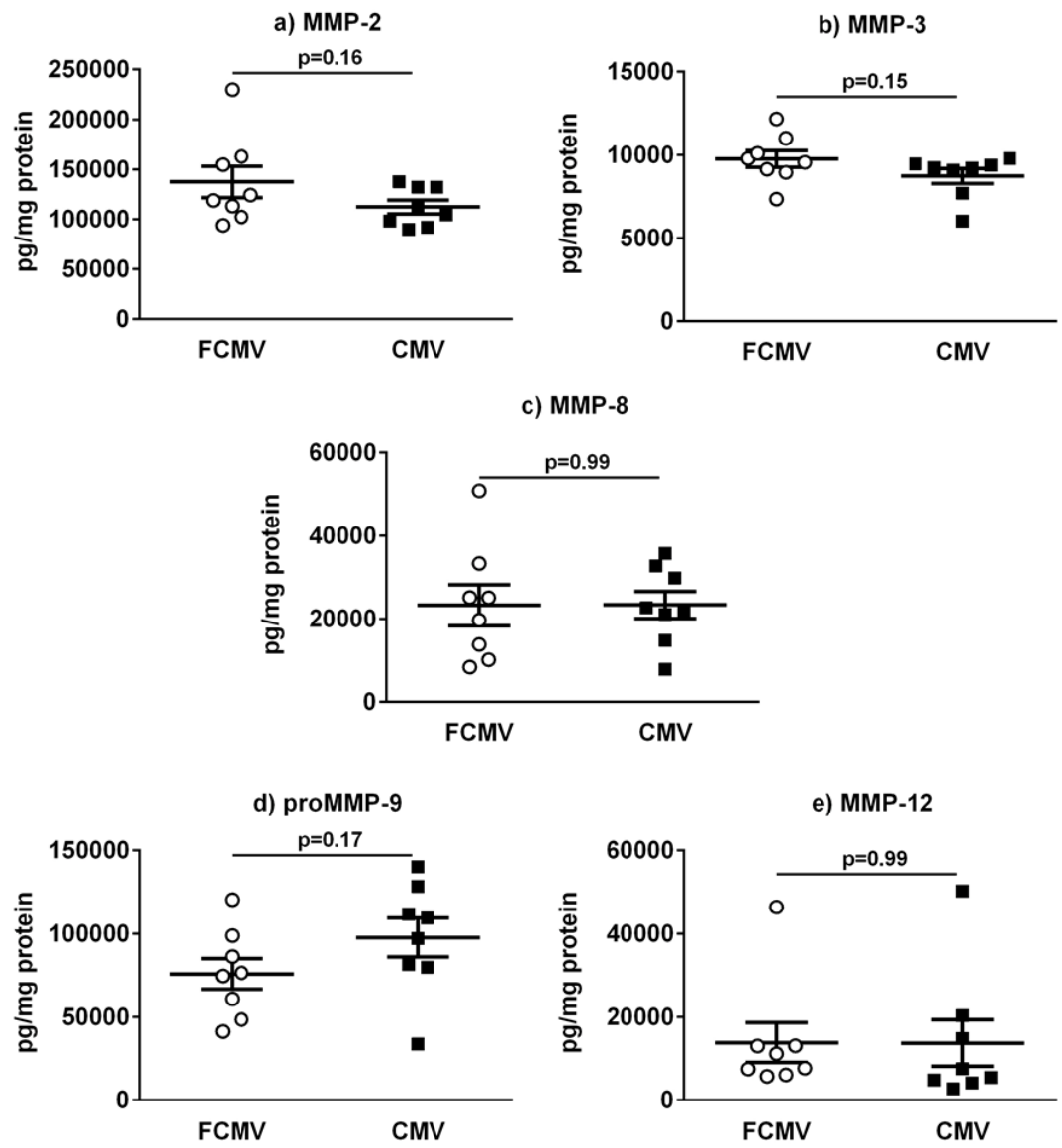


Figure 5.7. Expressions of matrix metalloproteinase (MMP) in breast tumors were not affected by mCMV infection in the MMTV-PyVT mice. Breast tumor levels of MMP-2 (a), MMP-3 (b), MMP-8 (c), proMMP-9 (d), and MMP-12 (e). N=8. P-values were calculated by Student's t-test. P-values >0.05 is determined as not significant.

infected with mCMV were stained for CD31 and for collagen content. There were no significant differences between the UV-inactivated control and the actively infected mice (Figure 5.8).

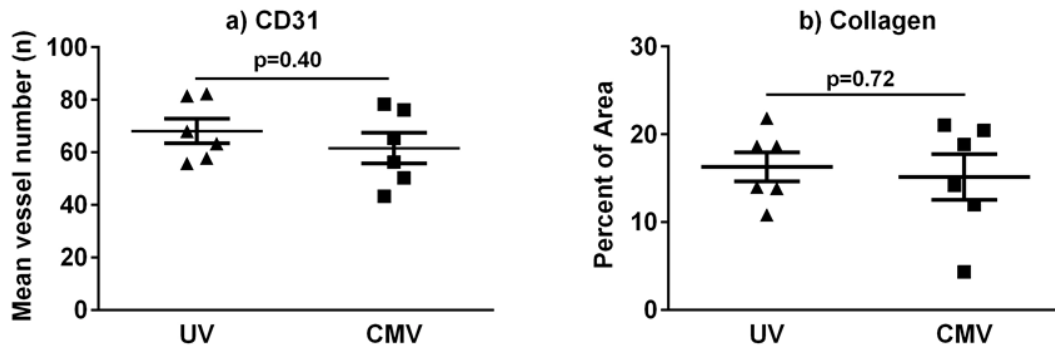


Figure 5.8. Tumors from BALB/c mice actively infected with mCMV or UV-inactivated control showed no differences in the expressions of CD31 and collagen content. The number of blood vessels was assessed by CD31 staining (a) and collagen was quantified as percent of total area (b) in breast tumors. N=6 for each group. P-values were calculated by Student's t-test. P-values >0.05 is determined as not significant.

5.5 Lung metastasis was increased in latently infected BALB/c and MMTV-PyVT mice

The number of metastatic nodules on the lung surface was determined for BALB/c mice. Mice with an active or intermediate mCMV infection prior to the introduction of the cancer cells showed no significant effect on lung metastasis compared to the control groups (Figure 5.9a,b). However, latently infected BALB/c mice showed a 3-fold increase in the number of lung metastatic nodules when compared to the PBS and UV-inactivated control groups (Figure 5.9c,d).

Macro-metastatic nodules were not observed on the lungs from the MMTV-PyVT mice, but sectioned lungs stained positively for micro-metastasis. The latent infection of MMTV-PyVT mice with mCMV resulted in 2-fold more lung nodules compared to the

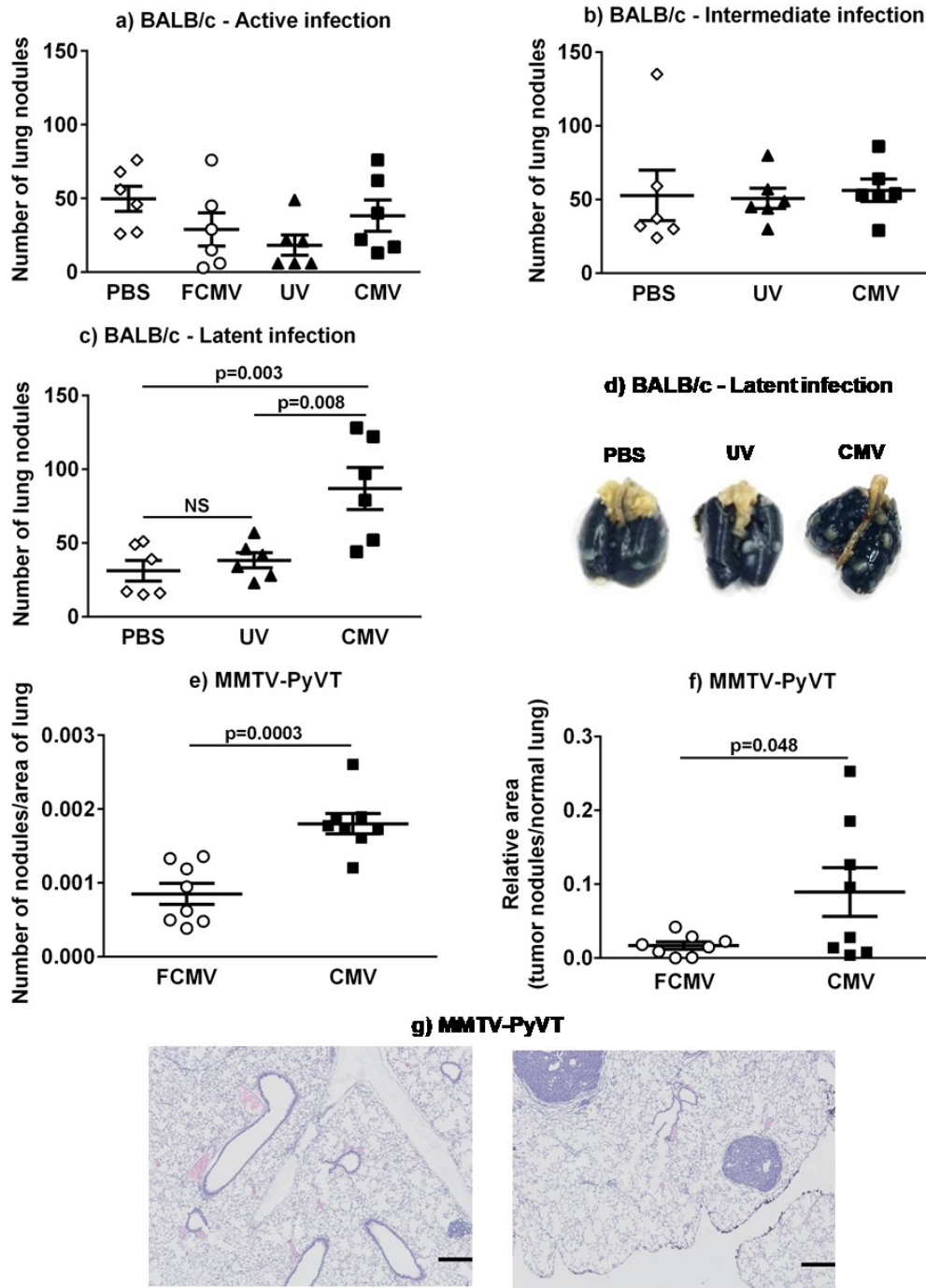


Figure 5.9. Lung metastasis was increased in mice latently infected with mCMV, but not in active or intermediate infection models. The numbers of large lung nodules in the BALB/c active (a), intermediate (b) and latent (c) infection models were quantified (n=6), with representative lungs depicted for the latent model (d). Lung micro-metastasis in the MMTV-PyVT model (n=8, each with sections cut from top, middle, and bottom of the lung), was assessed by staining with H & E and analyzed as the number of nodules per area of lung (e) and area of nodules per lung area (f). Representative stained lung sections were illustrated with 5X magnification lens (g). Scale=280 μ m. P-values were calculated by one-way ANOVA (a-c) or Student's t-test (e, f). NS=not significant.

control mice (Figure 5.9e,g). These nodules were also larger in the mCMV-infected group, and they occupied a 6-fold greater area of the lungs (Figure 5.9f,g).

The injection of E0771 cells into the mammary fat pads of C57BL/6 mice did not produce obvious macro- or micro-metastasis in the lungs (Figure 5.10a). No significant micro-metastases were detected in the liver from any experimental mice tested (Figure 5.10b).

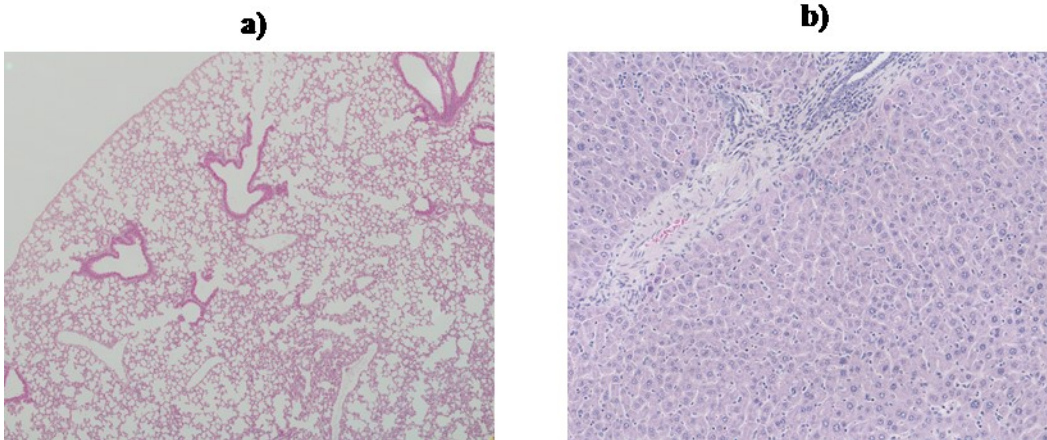


Figure 5.10. Negative detection of micro-metastasis. Lungs from C57BL/6 mice (a) and livers from MMTV-PyVT mice (b) latently infected with mCMV were sectioned and stained with H & E for micro-metastasis. N=5-8. Representative stained sections were illustrated with 5X magnification lens. Scale=280 μ m.

5.6 Mice latently infected with mCMV showed enhanced cell proliferation in lung metastatic nodules but not in primary breast tumors

Cell proliferation was determined in the lung metastatic nodules and breast tumors from the active and latent models of the MMTV-PyVT and BALB/c mice by staining for Ki67. There was a 2-fold increase in the percentage of Ki67-positive cells in the metastatic nodules of MMTV-PyVT mice that were latently infected with mCMV compared to the FCMV control mice (Figure 5.11a,b). A significant increase in Ki67 positivity in lung nodules was also observed in the latently infected BALB/c mice compared to both the PBS

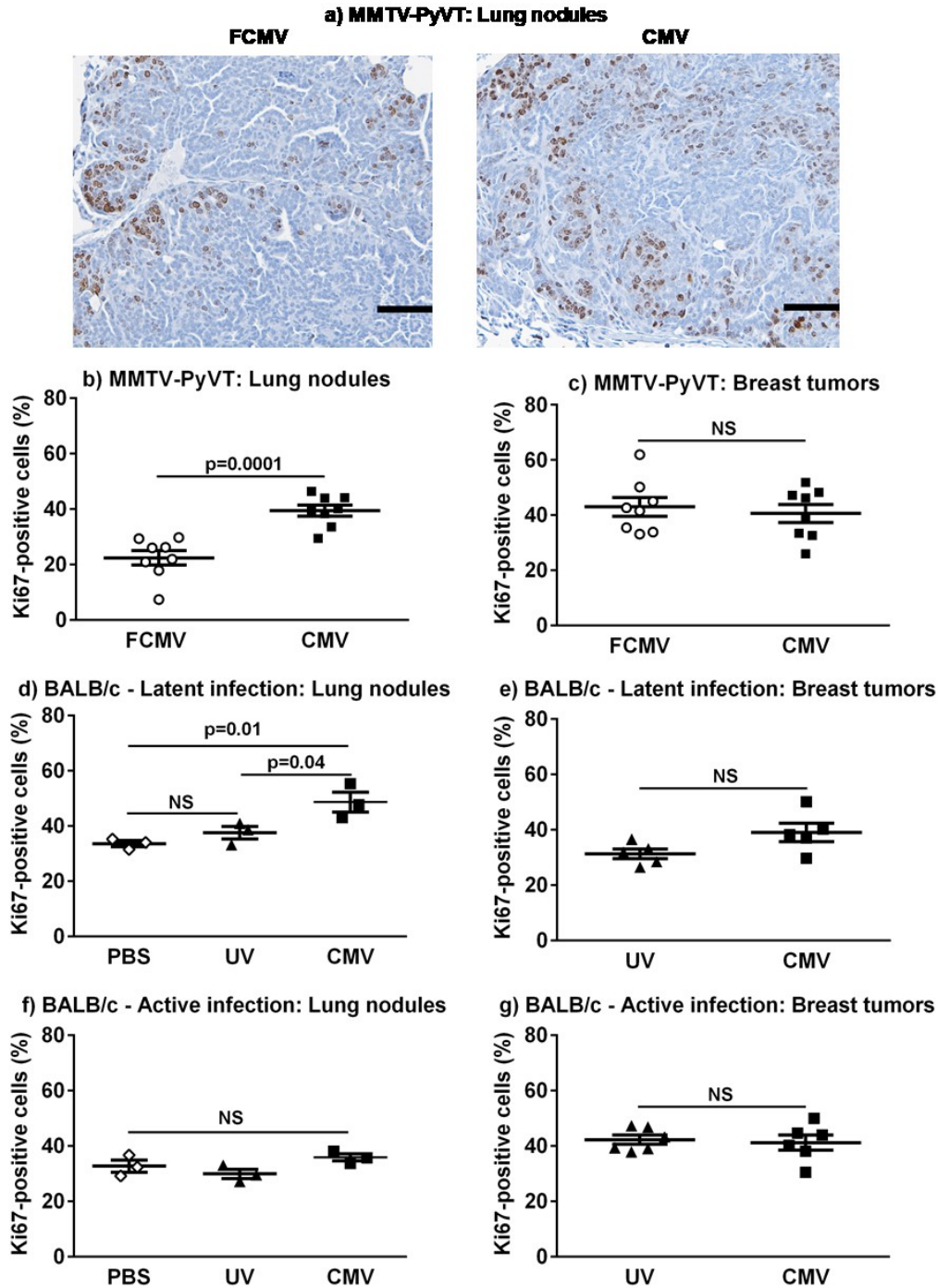
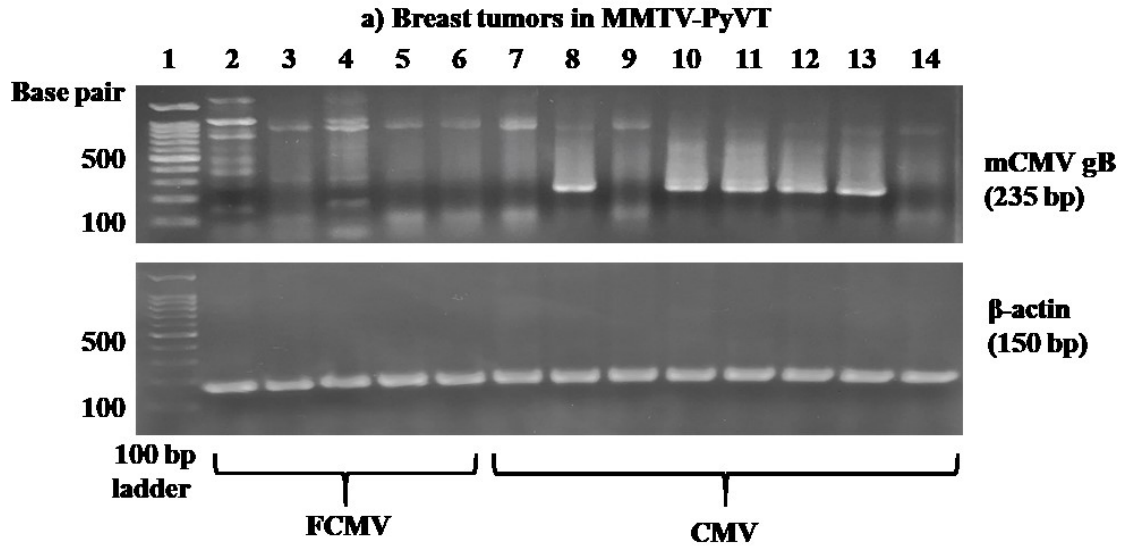


Figure 5.11. Enhanced cancer cell proliferation in lung metastatic nodules but not in the breast tumors in mice latently or actively infected with mCMV. Lung metastatic nodules (b, d, f) and breast tumors (c, e, g) were stained for Ki-67 to assess cell proliferation in latently infected MMTV-PyVT (a, b, c) and actively or latently infected BALB/c mice (d, e, f, g). Representative stained sections of lung nodules from MMTV-PyVT mice are illustrated (a). The image was taken with 20X magnification lens. Scale=100 μ m. P-values were calculated by Student's t-test (b, c, e, g) or one-way ANOVA (d, f). NS=not significant.

and UV controls (Figure 5.11d), but this difference was not observed in the actively infected model (Figure 5.11f). By contrast, there was no significant difference in the percentage of Ki67-positive cells in breast tumors between the controls and actively or latently infected mice in all models tested (Figure 5.11c,e,g).

5.7 mCMV DNA but not mRNA was detectable in tissues, metastatic nodules and tumors from mice latently infected with mCMV

The presence of the viral genome was detected by measuring mCMV gB DNA expression in the tissues. Salivary glands, spleens, lungs, lung metastatic nodules and breast tumors from mice latently infected with mCMV were examined. A sample was considered positive for viral gB DNA with the detection of a 235 bp band after a nested PCR amplification of the gene, with β -actin as the internal control showing a 150 bp band. A representative gel of the breast tumor samples from MMTV-PyVT mice is shown in Figure 5.12a and the results for positive detection in each mouse model summarized in Figure 5.12b. The detection of mCMV gB DNA specifically in each type of tissue for every mouse was delineated in Table 5.3. Apart from 2/6 animals in the C57BL/6 model and 1/23 in the MMTV-PyVT model, there was positive detection of DNA for mCMV gB in at least one type of tissue, nodule or tumor examined from each animal (Table 5.3). BALB/c mice had macro-nodules on the surface of the lungs that were separated from the underlying lung tissue. Half of these lung nodules from the BALB/c mice were positive for viral gB DNA compared to the 5/6 positive underlying lung tissues (Figure 5.12b). Macro-nodules were not present on the lungs of the C57BL/6 or MMTV-PyVT mice. Viral DNA for gB was detected in the lung tissues from 83% of the MMTV-PyVT mice but only 20% of the C57BL/6 mice (Figure 5.12b). Viral DNA was detected in 50% and 26% of breast tumors from the BALB/c and the MMTV-PyVT mice, respectively, but none from the C57BL/6



b) Summary table

	BALB/c		C57BL/6		MMTV-PyVT	
	Positive/total	% positive	Positive/total	% positive	Positive/total	% positive
Salivary gland	5/6	83	2/5	40	15/23	65
Spleen	ND	ND	3/5	60	6/10	60
Lung	5/6	83	1/5	20	19/23	83
Lung nodule	3/6	50	NA	NA	NA	NA
Breast tumor	3/6	50	0/5	0	6/23	26

ND=Not done, NA=Not applicable

Figure 5.12. DNA for mCMV glycoprotein B (gB) was detected in MMTV-PyVT mice latently infected with mCMV. Representative gel showing detection of DNA for mCMV gB in breast tumors from five filtered control (FCMV; lanes 2-6) and eight mCMV-treated (lanes-7-14) MMTV-PyVT mice (a). Lane 1=100 bp ladder. Positive detection of mCMV gB DNA was identified by a band at 235 base pairs (bp). Beta-actin (150 bp) was used as an internal control. The number of tissues, nodules or breast tumors positive for mCMV gB DNA from each animal model was summarized in Panel b.

Table 5.3. Detection of mCMV glycoprotein B DNA in specific tissues, nodules or tumors from each mouse in all animal groups.

BALB/c

Mouse ID (CMV)	Salivary gland	Spleen	Lung	Lung nodule	Breast tumor
1	+	ND	+	+	+
2	+	ND	+	+	+
3	+	ND	+	-	+
4	+	ND	-	-	-
5	+	ND	+	-	-
6	-	ND	+	+	-

C57BL/6

Mouse ID (CMV)	Salivary gland	Spleen	Lung	Breast tumor
1*	-	-	-	-
2	+	+	+	-
3	+	+	-	-
4	-	+	-	-
5*	-	-	-	-

Detection of mCMV glycoprotein B at the DNA level is depicted as “+” with no detection depicted as “-”. No detection in any of the tissues tested in the mouse is identified with *. ND=Not done.

Table 5.3. Continued. Detection of mCMV glycoprotein B DNA in specific tissues, nodules or tumors from each mouse in all animal groups.

MMTV-PyVT

Mouse ID (CMV)	Salivary gland	Spleen	Lung	Breast tumor
1	+	ND	+	-
2	-	ND	+	-
3	+	ND	-	-
4	-	ND	+	-
5	+ (IE)	ND	+	-
6	+	ND	+	-
7	+ (IE)	ND	+	-
8	-	ND	+	-
9	+	ND	-	+
10	-	ND	+	-
11	-	ND	+	+
12	-	ND	+	+
13*	-	ND	-	-
14	+	+	+	+
15	+	+	+	+
16	+	+	+	+
17	+ (IE)	-	+	-
18	+ (IE)	-	+	-
19	-	-	+	-
20	+	+	+	-
21	+(IE)	+	+	-
22	+	-	+	-
23	+	+	-	-

Detection of mCMV glycoprotein B at the DNA level is depicted as “+” with no detection depicted as “-”. No detection in any of the tissues tested in the mouse is identified with *. ND=Not done. All salivary glands from the MMTV-PyVT mice were also tested for mCMV IE at the DNA level, (IE) = positive detection.

mice (Figure 5.12b). The detection of viral DNA was not observed in any control mice, including PBS, UV-inactivated or FCMV-treated mice, which suggests that the mice were uninfected prior to the start of the experiments (Figure 5.12b). The salivary glands from the MMTV-PyVT model were also analyzed for the expression of mCMV IE DNA. All samples that tested positive for the IE gene were also positive for gB, but not all of the gB positive samples were positive for IE (Figure 5.12b).

mCMV gB mRNA was also measured by qPCR to assess if there was an active infection. However, mRNA for gB was not detected in any tissues tested including salivary glands, spleens, lungs, metastatic nodules or breast tumors from the three latently infected mouse models, which all showed cycle numbers as undetermined (Figure 5.13a). Negative results were also obtained for mRNA detection of mCMV IE-1/3 (Figure 5.13b). In addition, tumors were stained for β -galactosidase activity, but no detection was observed in any of the experimental models (Figure 5.13c).

5.8 Cytokine expression was altered in breast tumors and plasma from mice with latent mCMV infections

The plasma collected from MMTV-PyVT mice was analyzed for the activity of ATX, which is a pro-inflammatory mediator, but no significant difference was observed between the mCMV-infected and uninfected mice (Figure 5.14).

The plasma and breast tumors collected from MMTV-PyVT mice were analyzed for expression of 32 cytokines/chemokines using a Discovery 32-plex Array and the significant changes found are described here. Breast tumors from MMTV-PyVT mice latently infected with mCMV had a decreased expression of IL-1 α (Figure 5.15a). mCMV-infected mice had increased plasma concentrations of IL-6 and IL-13 compared to FCMV-

treated mice (Figure 5.15b,c). There was a positive correlation between these concentrations of IL-6 and IL-13 for the mCMV-infected mice (Figure 5.15d; $p=0.0012$) but not for the FCMV-treated mice (Figure 5.15e; $p=0.34$).

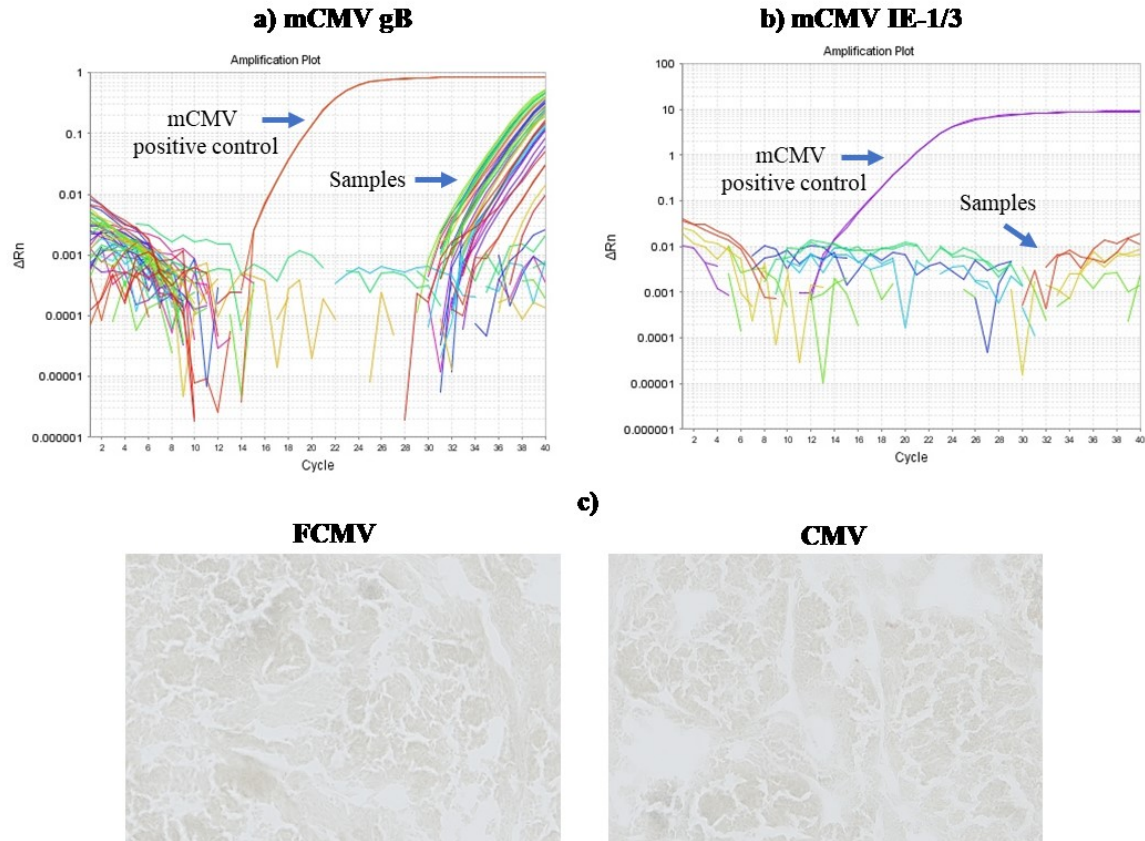


Figure 5.13. Negative detection for actively transcribing or replicating mCMV in the latently infected mouse models. mRNA for mCMV glycoprotein B (gB) (a) and immediate early-1/3 (IE-1/3) (b) genes were not detected in salivary glands, spleens, lungs, metastatic nodules and breast tumors. The positive control was generated from salivary gland harvested from mice infected with mCMV for 4 days. Tumors ($n=8$) from the latently infected MMTV-PyVT mice were stained for β -galactosidase activity (b). Images taken with a 20X magnification lens. Scale=100 μ m. Similar results were obtained in the BALB/c and C57BL/6 models.

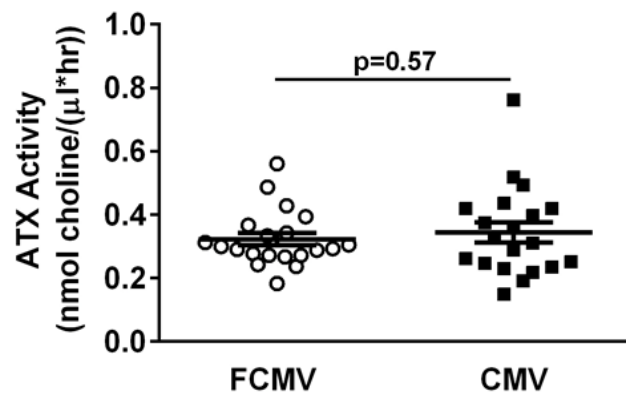


Figure 5.14. Autotaxin (ATX) activity in the plasma from MMTV-PyVT mice was not altered by mCMV latent infection. The enzyme activity of ATX from plasma of 25 mice treated with a filtered control solution (FCMV) and 23 mCMV-infected mice were determined by choline release assay. P-value was calculated by Student's t-test. P-value >0.05 is determined as not significant.

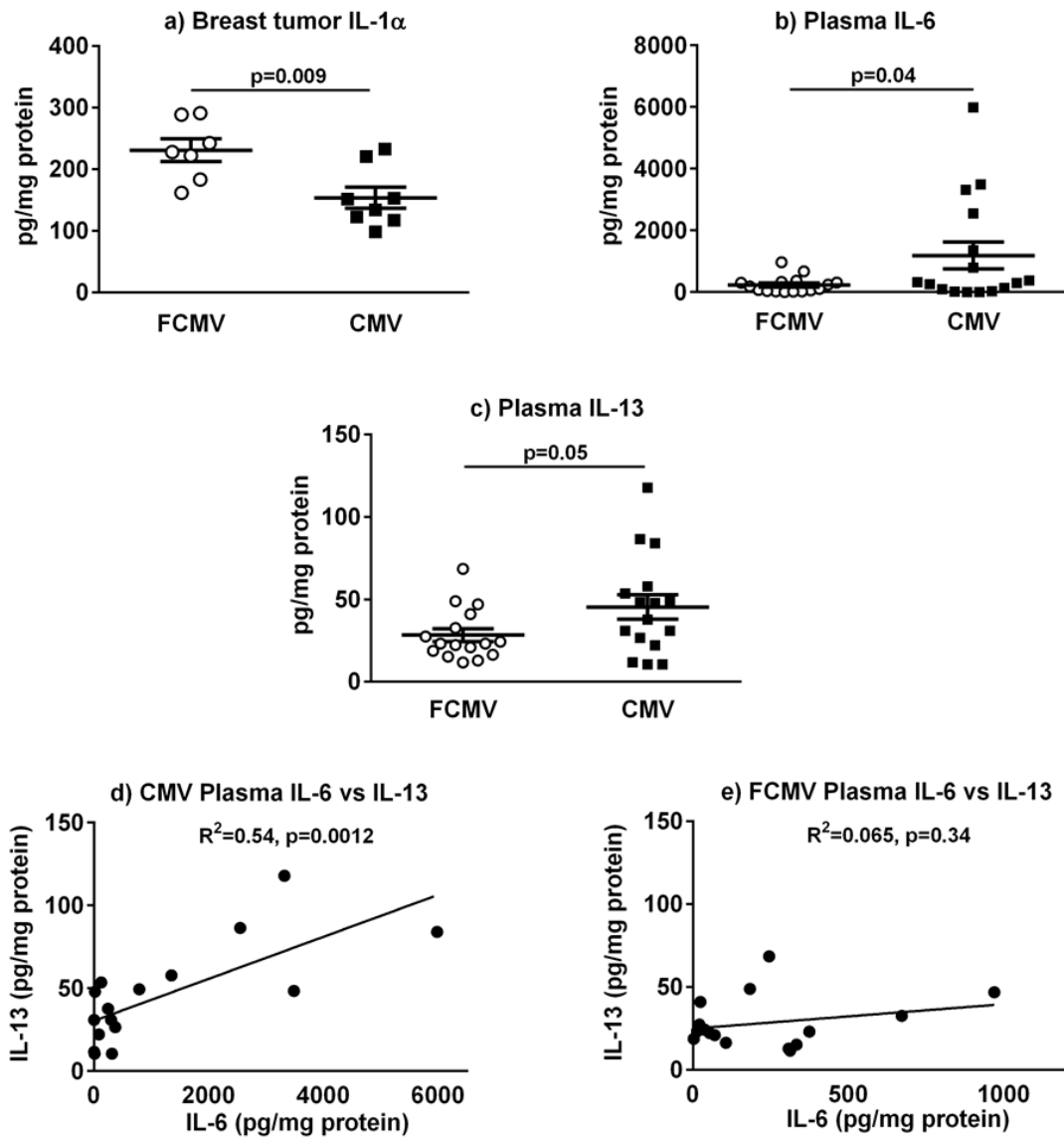


Figure 5.15. Differences in cytokine concentrations in breast tumors and plasma from MMTV-PyVT mice latently infected with mCMV. Breast tumor levels of IL-1 α , n=8 (a). Plasma concentrations of IL-6 (b) and IL-13 (c), n=16. Regression analysis of plasma concentrations IL-6 versus IL-13 in mCMV-infected (d) and mice treated with a filtered control solution (FCMV) (e). P-values were calculated by Student's t-test.

5.9 Discussion

Reports from the literature show an association exists between HCMV and breast cancer [271]. However, it is unclear how CMV infection would modify tumor progression.

We studied three mouse models of breast cancer that were infected with mCMV to investigate the effects of infection on breast cancer progression.

The BALB/c and C57BL/6 mice were orthotopically injected in the mammary fat pads with syngeneic 4T1 or E0771 breast cancer cells, respectively, and tumor development was measured. C57BL/6 mice are less affected by infection with mCMV because of an effective NK cell response [272]. By contrast, BALB/c mice are more negatively affected by infection with mCMV because they lack the NK cell Ly49H activating receptor that recognizes an MHC class I-like glycoprotein produced during an mCMV infection [205]. This leads initially to inefficient clearance of mCMV that impacts viral load and helps explain why we detected mCMV DNA more frequently in BALB/c than C57BL/6 mice. Despite this greater sensitivity of BALB/c mice to mCMV infection, we only found an effect on metastasis in latently infected mice. The absence of increased metastases in the mice acutely infected prior to tumor growth could have resulted from a more robust immune response to the virus when the syngeneic cancer cells were injected. If so, this only affected metastasis and not tumor growth.

We also examined the effect of a latent mCMV infection in a mouse model with spontaneous growth of multiple breast tumors. MMTV-PyVT mice express the polyomavirus middle T (PyVT) oncogene under the direction of the mouse mammary tumor virus (MMTV) promoter/enhancer [251]. These mice provided a highly relevant model for human breast cancer since they could be infected early in life and the effects of the mCMV infection on the development of spontaneous breast tumors and metastasis could be determined.

Mice that were treated with negative control solutions including PBS, FCMV, and UV-inactivated virus showed no evidence of infection as expected. The FCMV control would have included cytokines and growth factors produced by the mCMV-infected fibroblasts during mCMV propagation. This control could also have contained small mCMV viral fragments and small particles such as exosomes that were not removed by filtration. More importantly, the UV-inactivated control contained intact viral particles that were no longer infective. Both controls have the potential to stimulate a host immune response, which could have altered the breast cancer progression. However, the lack of effect on tumor growth and metastasis was similar regardless of whether PBS, FCMV, or UV-inactivated controls were used. This suggests that not just the presence of HCMV but the establishment of HCMV infection is required to stimulate an immune response that contributes to the alteration of cancer progression.

We evaluated the effects of active, intermediate and latent infections with mCMV on breast tumor growth and metastasis in BALB/c and C57BL/6 models. The results in the BALB/c model were consistent in that there was mostly no significant effect of the mCMV infection regardless of the length of infection prior to injection of cancer cells on breast tumor volume or mass when compared to the control treatments. The significantly higher tumor mass in latently infected BALB/c mice compared to control mice treated with PBS is probably not important since there was no significant difference between the infected mice and those treated with a UV-inactivated virus (Figure 5.4a). Treatment with a UV-inactivated virus involved the injection of intact virus particles, which cannot replicate but can be recognized by the host immune system, providing a highly relevant control. In the C57BL/6 model, while there was no effect of intermediate or latent infection on tumor

volume or mass, mCMV infection reduced tumor volume but not mass during an active infection. This is likely because the tumors in this model were less solid, reducing the accuracy of measurement with calipers.

The BALB/c model was established with an injection of 4T1 breast cancer cells, mimicking stage IV human breast cancer that forms macro-metastases in the lungs [273]. The C57BL/6 model with an injection of E0771 breast cancer cells [274] and the MMTV-PyVT mice [252] develop much smaller metastases in the lungs and liver at a late stage of breast tumor development. As expected, our study in the C57BL/6 model showed no metastases in the lungs and liver because of the ethical requirements to terminate our experiments at an earlier endpoint because of tumor size. The BALB/c and the MMTV-PyVT mice showed metastases in the lungs, which were increased significantly both in number and size when the mice were latently infected with mCMV prior to tumor development. The increased metastases observed with a latent mCMV infection were not observed in the active or intermediate mCMV infection models. This work provides evidence from a mouse model that supports the contribution of HCMV infection to breast cancer metastasis and high rate of detection of HCMV DNA and proteins in the metastatic sentinel lymph nodules and brain tissue of breast cancer patients [231, 245]. In contrast to our hypothesis, mCMV infection showed limited effect on breast tumor mass. However, the infection did alter breast tumor phenotypes. This led to revision of our initial hypothesis with a greater emphasis on metastasis, where mCMV infection will lead to tumor phenotypes that promote breast cancer metastasis.

The mechanisms for increased metastasis in mCMV-infected mice are probably complex, involving changes in the capacity of breast cancer cells to migrate from the

primary tumor and to increase their ability to travel, establish and divide in distant sites. The results from the MMTV-PyVT mice confirmed that a latent mCMV infection had no significant effects on breast tumor growth and final tumor mass, but it did lead to worse phenotypes with the potential to promote metastasis. Multiple breast tumors developed in each of the MMTV-PyVT mice, and we used the largest tumor for the endpoint measurements since these had almost identical sizes. Taking into account all breast tumors developed in each mouse, there was a greater incidence of small fused breast tumors that were bloodier in the mCMV-infected mice, which could be indicative of a more severe phenotype. When comparing the largest breast tumors developed, those from mCMV-infected mice showed increased numbers of blood vessels as indicated by staining for the endothelial marker, CD31. Together, these results showed that a latent mCMV infection of MMTV-PyVT mice increased angiogenesis in the breast tumors. Angiogenesis is important for metastasis to occur, where it provides easier access of the cancer cells to enter the circulation and spread throughout the body [275]. It is known that CMV infection is associated with angiogenesis in the normal wound healing process, by inducing genes such as angiopoietin, VEGF, TGF- β , and IL-6 [276, 277]. The increased angiogenesis observed in the breast tumors from latently infected mice could be due to similar mechanisms caused by CMV infection. In our analysis, the level of IL-6 and VEGF in the breast tumors of MMTV-PyVT mice showed no significant difference between mCMV-infected and control mice. However, analysis was only performed on the largest breast tumor developed in each mouse, where the level of cytokines and growth factors could have reached a level of saturation. On the systemic level, we did observe an increase of IL-6 in the plasma of mCMV-latently infected MMTV-PyVT mice, possibly promoting angiogenesis and

metastasis [278]. In contrast, breast tumors from the actively or latently infected mCMV BALB/c model did not show these phenotype changes. This is possibly due to the differences between the type of breast tumor developed by using 4T1 cells, which results in a relatively solid tumor with a low blood content.

Breast tumors from mCMV-infected MMTV-PyVT mice showed lower collagen content, which is compatible with increased cancer cell egress that leads to metastasis [279]. IL-1 α stimulates collagen synthesis [280, 281]. Our observation of a lower IL-1 α concentration in the breast tumors of mCMV-infected mice is compatible with the decreased collagen content. We also checked for evidence of an increased collagen breakdown, but there were no significant differences in the concentrations of the collagenase, MMP-8, in the tumors or for other MMPs (MMP-2 MMP-3, pro-MMP9 and MMP-12) that could favor metastasis. Despite this, other proteinases such as the urokinase form of the plasminogen activator system are involved in remodeling and degradation of the ECM for cancer cell escape from the primary tumor and should be investigated [282].

Along with changes in the tumor morphology that could promote metastasis, mCMV-induced changes could also modify the host immune response so that cancer cells escape from immune destruction and aggravate tumor-promoting inflammation that favors tumor metastasis [30]. The ATX activity in the plasma was not significantly different between the mCMV-infected and uninfected mice. Further investigation should also focus on the breast tumor local site, especially in the tumor-associated breast tissues, which are major sites of ATX production [250]. Plasma concentrations of the pro-inflammatory cytokine, IL-6, were increased in mCMV-infected mice. This is a common feature associated with CMV infection [283] and it is reported to have a role for carcinogenesis in

salivary gland cancer [222]. An increase was also observed for IL-13, which promotes cell migration and invasion in colorectal cancer [284]. We observed a significant positive correlation between IL-6 and IL-13 in mCMV-infected mice. These results provide important insights into potential mechanisms for CMV infection and metastasis in breast cancer.

Cell proliferation, as measured by Ki67, was not significantly different in the breast tumors between the mCMV-infected and control-treated MMTV-PyVT or BALB/c mice. This result is compatible with our finding that the average size of the tumors was not significantly different. This was despite the greater vascularization of the breast tumors from MMTV-PyVT mice that presumably increased O₂ and nutrient supply. By contrast, there was a greater cell proliferation in the lung micro-metastatic nodules of the infected MMTV-PyVT mice, which corresponds to the larger size of the nodules. The increased cell proliferation of lung nodules was only observed in the latently but not in the actively infected BALB/c model. These results were compatible with the increased numbers of macro-metastatic nodules that were seen only in the latently infected mice. The explanation for the specific effects of latent CMV infection prior to tumor growth in increasing metastasis could be in the specific expression of latency expressed viral genes and proteins, and this will be the subject of future investigations.

The latent CMV infection of the mouse models resembles the viral latency status commonly found in immunocompetent people. We determined if the presence of a breast tumor or metastasis initiated mCMV reactivation. We detected viral DNA in the latently infected mice in at least one of the following: metastatic nodules, breast tumors or various tissues including salivary gland, spleen or lungs. However, mRNA for mCMV gB and IE-

1/3 genes and β -galactosidase activity were not detected in tissues, nodules or tumors that were examined. These results are consistent with the analysis in human breast tumors, where viral DNA but not viral transcripts were detected, as described in Chapter 3 of this thesis. This is surprising since we had predicted that tumor-induced inflammation could cause viral reactivation [180]. Our results suggest that the full active replication of the virus was not required for the observed increase in lung metastasis. Furthermore, mice actively infected with mCMV prior to tumor development also showed no positive detection of β -galactosidase activity in the tumors, and this indicates that breast cancer cell inoculation and tumor growth did not maintain mCMV infection in an active status. However, the immune response to the active infection at the time the tumor is developing could establish a microenvironment that reduces the metastatic phenotype, conferring some protection similar to heterologous immunity where infection with one pathogen can protect against another [178, 179].

One limitation is that the mRNA and β -galactosidase analyses were only performed at the experimental endpoint and in a limited number of tissues. It is possible that viral reactivation could have occurred one or multiple times prior to the endpoint and/or in other tissues where reactivation would have been quickly controlled by an intact memory immune response. Short phases of viral reactivation would have an impact on the immune responses that could play a role in metastasis, especially since viral DNA has been detected in the lung metastatic nodules from our mouse model and in the metastatic sentinel lymph nodules of breast cancer patients [231]. Alternatively, proteins produced at a low level from latency associated transcripts, which include IE-1 in the absence of the transactivator IE-3 [285], or a splice variant of cmvIL-10 [196] could also play a role in metastasis by

controlling the immune response. It is also possible that the level of transcription for mCMV was below the limit of detection with our current technique.

The mouse models established in our study provide preclinical results that can have clinical relevance. The MMTV-PyVT model that spontaneously develops breast tumors and was latently infected with mCMV is a physiological representation of the human situation. However, CMV is a species-specific virus where the genomes of mCMV and HCMV are different. One of the examples is that cmvIL-10 is encoded by HCMV but not mCMV [134]. This is especially important when studying metastasis since exposure of breast cancer cells to cmvIL-10 has shown enhanced invasive and migratory properties [5, 135, 136]. However, it is possible that mCMV produces other viral encoded cytokines that lead to a similar immunosuppressive effect like cmvIL-10 and contribute to promote metastasis, but this requires further investigation.

In conclusion, this study provides the first direct evidence from three mouse models of breast cancer that preexisting mCMV infection does not affect the growth of primary tumors but modifies the tumor phenotypes leading to increased metastasis. This is compatible with the hypothesis that CMV is a tumor modulatory virus. It is also evident from the mouse models that a latent but not active mCMV infection prior to tumor development increases metastasis. This is especially important since HCMV infection is mostly latent in the infected population, but negative effects of infection have been underestimated due to no noticeable symptoms. However, our results indicate that latent CMV infection could play a crucial role in increasing metastasis and thus mortality in breast cancer patients.

Chapter 6: General discussion and future directions

6.1 Introduction

In this chapter, I will discuss the role of CMV infection in breast cancer based on the current literature and findings in this study. I will discuss the detection of HCMV DNA and proteins in human specimens of breast tumors and normal breast tissues. The presence of viral genome or proteins in cancerous tissues is one of the factors used to determine whether a virus is oncogenic. However, controversies exist for whether HCMV is present in several tumor types, especially for breast tumors. Our study contributes to a better understanding of this issue by carefully evaluating the sensitivity of commonly used PCR detection methods and then applying the best method to analyze the breast tumor samples from a demographic population that had not been studied previously (section 6.2). New insights from our study with respect to the effect of HCMV challenge on breast cancer cells will be discussed, including viral transcription, replication, and stimulation of inflammatory genes in the viral challenged breast cancer cells (section 6.3). Finally, our new findings on the effect of CMV infection on breast tumor progression and metastasis in mouse breast cancer models are discussed (section 6.4). This chapter will conclude with future research directions that can further investigate the role of CMV infection in breast cancer (section 6.5).

6.2 Evaluation of HCMV detection in human specimens

One of the criteria to determine a virus as oncogenic is the finding of integrated or episomal viral genomes and gene products of the virus in cancer cells [103]. This is evident for the well-accepted oncoviruses like EBV and HPV, with their detection in cancer cells of Burkitt's lymphoma and cervical cancer, respectively [104, 109]. This feature has also been suggested for HCMV, with reports showing detection of the viral genome and/or

proteins in several types of cancerous tissues, including glioblastoma, colorectal cancer, prostate cancer and breast cancer [114-116, 118].

The broad cell tropism of HCMV allows wide distribution of the virus throughout different parts of the body, since most cell types can be infected by HCMV [118, 170-172]. Therefore, it is not surprising that the HCMV genome and/or proteins can be detected at the breast site, especially for women who have undergone the process of lactation since HCMV can be transmitted through breast milk [145]. This indicates that we will not be able to assess the association between HCMV and breast tumors based solely on whether the virus is present or not. Therefore, a control group must be included for examining this issue, which is normal breast tissues from women free of cancer. This allows for a comparison of HCMV detection incidence between the two groups, where a significantly higher rate of detection in breast tumors could provide evidence for HCMV to fulfill one of the criteria to be an oncovirus [103]. In our study, normal breast tissues were obtained from patients who underwent breast-reduction surgery. However, the sample size was limited due to tissue availability. This could be resolved by further accumulation of samples or obtaining previously frozen breast tissues from other sources. An interesting comparison could also be made if matching breast tissues and breast tumors obtained from the same patient are available, which was not possible in our study. However, this has been done in other laboratories, with results showing a significantly higher detection of HCMV IE protein in the breast tumors [118].

It would be ideal if matching plasma samples are available for the patient specimens collected. Plasma can be used for determination of whether the individual has ever been infected with HCMV, through detection of IgG antibodies against HCMV [214]. If the rate

of positive detection for HCMV viral presence is different between the analyzed breast tumors and normal breast tissues from women free of cancer, it is important to know whether this is due to a difference in seropositivity or the presence of the virus at the breast site. In addition, if the viral infection is latent, which is likely in most of the cases, only a few copies of the virus are retained in the host and these may not be evenly distributed in every part of the body [260]. This leads to difficulty of detection where it is possible that the viral particles are not present or are simply not being detected in the piece of tissue analyzed. If the seropositivity information is available, it will at least provide us information on whether the negative detection is due to an absence of infection. Unfortunately, we did not have plasma samples or HCMV seropositivity information available for the samples analyzed, which is one of the limitations for this study. Therefore, we can only compare back to the general HCMV seroprevalence, which is 40-70% for the adult population in developed countries [149]. Our results as described in Chapter 3, showed HCMV DNA positivity as 30% and 40% in normal breast tissues and breast tumors, respectively. These results are on the low end of the expected range, but this is not surprising due to the difficulty of detecting the viral genome during latency [260].

Demographical differences contribute greatly to HCMV seroprevalence [151]. The presence of HCMV mRNA, DNA and/or proteins in breast tumors have been examined by laboratories across the world, including China, USA, Mexico, Australia, Sweden, New Zealand, Norway, Iran, Iraq, and Egypt (Table 1.1 and 1.2). Our study expands this list by providing an analysis of a Canadian population, where the HCMV seroprevalence is lower compared to most of the previously studied populations [151]. Nevertheless, 40-70% is still a major portion of the population, which could potentially be negatively affected by

the infection. It is unlikely that we will detect the HCMV genome in the majority of the breast tumors like some of the studies have reported [4, 118, 230-232]. This is expected since the population of our study should have an overall lower HCMV seroprevalence compared to populations from other parts of the world and our current results suggested a similar detection rate of HCMV DNA in the breast tumors and normal breast tissues from women free of cancer. Based on our results and the previous literature, detection of HCMV in breast tumors is more likely to be dependent on seroprevalence rather than whether it is cancerous tissue. Although there is still the possibility that the HCMV genome is retained in breast tumors at a higher rate compared to normal breast tissues from women free of cancer when the sample size increases, there is a lack of evidence for predicting that a causal relationship exists between HCMV infection and breast tumor development.

The methods for detecting HCMV genome and proteins must be carefully chosen in order to obtain reliable results. Sensitivity is key for maximizing the chance of detection, especially since HCMV can establish latency where very few copies of the virus are maintained in the host and difficult to detect in tissues [260]. The detection must also be specific to avoid any false-positive results. Inclusion of appropriate negative controls is required in all assessments as an indication of non-specificity and contamination. As mentioned earlier, a large sample size is needed for a better representation of the HCMV-breast cancer association, therefore the method chosen should be both convenient and economically friendly to process the large amount of tissues. In Chapter 3, I evaluated the specificity and sensitivity of the PCR methods that are commonly used for the detection of HCMV DNA, using LC-PCR and nested PCR. LC-PCR allows for real-time quantitative analysis of the viral load and gives high specificity by using hybridization probes, but it is

not the most sensitive technique for picking up the presence of DNA. On the other hand, nested PCR involves two rounds of reactions; therefore, it doubled the amplification cycles compared to standard PCR, leading to high sensitivity of detection. I used two different sets of primers with one nested in the other, which were used one after the other in two rounds of PCR reactions to ensure the specificity of amplification. Additional confirmation of the reaction specificity was verified by sequencing the PCR products. This is crucial since we found that the HCMV gB primers used produced highly specific products, but this was not the case for HCMV IE. This should be taken into consideration for future investigations and interpretation of the current literature showing detection of HCMV IE DNA [237, 244]. We have used the same HCMV IE primers and PCR conditions as described by El-Shinawi M *et al.*, but I showed that the PCR products were non-specific after being sequenced, suggesting that the observed products were false-positive. In our mouse models infected with mCMV, we found that samples tested for both mCMV IE and gB genes using nested PCR resulted in higher positivity when gB primers were used. However, the HCMV and mCMV genomes are different and this would affect the design of primers. As a suggestion, it would be beneficial to target different viral genes and test different primer sequences that are designed on the same set of samples to ensure specificity and sensitivity of detection.

The detection of HCMV antigens by IHC is another commonly used method in the literature [4, 118, 230, 233, 242]. The advantage of using IHC as a detection method is the visualization of viral antigens in the context of the tissue structure and within what cell types. For optimal results, the tissues should be formalin-fixed and paraffin-embedded or frozen in OCT to preserve the tissue structure. These were not done for the human

specimens that were analyzed in our study but can certainly be included as part of the study for future specimens obtained. A problem with IHC is the possibility of having non-specific staining and it is difficult to confirm that the stained product is the specific target antigen. Therefore, different antibodies against HCMV antigens should be compared and assessed carefully. More detailed analysis can also be performed using flow cytometry, as suggested in Chapter 3 if fresh samples are available.

We did not find presence of HCMV DNA to be statistically significantly associated with any of the patient characteristics analyzed. However, this could be due to the uneven distribution of the samples in each category of cellular receptor positivity and should be further examined after accumulating more samples in categories like triple-negative breast tumors. We also did not find evidence for active or reactivated CMV infection in the human specimens or in tissues from mouse breast cancer models as evidenced by the lack of CMV IE mRNA expression. However, there is a possibility that the expression was below the level of detection and different primers should also be tested.

In conclusion, we found that the use of nested PCR in the detection of HCMV gB DNA in human specimens is an optimal method in terms of both the detection limit and specificity. Ten normal breast tissues from women free of cancer and 147 breast tumors from a Canadian patient population were analyzed using this method for the presence of HCMV DNA. The proportion of tissues in which HCMV DNA was detected in these two groups was not statistically different, but there is a possibility for existence of associations between HCMV and characteristics of breast tumors such as those observed in our mCMV-infected mouse models [286]. Further study could contribute to our better understanding

of the association between HCMV and breast cancer, especially on how the infection is related with worse tumor outcomes.

6.3 CMV viral transcripts as stimuli for inflammation

It has been proposed that HCMV infection could have an oncomodulatory effect on breast cancer progression and metastasis, which is through the regulation of intracellular signaling pathways important in cancer [128]. This is supported by the fact that HCMV infection fulfills most of the criteria for hallmarks of cancer, such as being involved in tumor-promoting inflammation and avoiding immune destruction [30]. On the other hand, the viral encoded cmvIL-10 acts similarly to the cellular IL-10, which can serve as an immunosuppressive factor [134]. Exposure of breast cancer cells to cmvIL-10 promotes the invasiveness and migratory potential of these cells [5, 135, 136]. CMV infection leads to inflammation in the host cells through stimulating the production of cytokines and inflammatory mediators, which could be through binding of the viral particles to cell surface receptors or expression of viral transcripts and/or antigens [217, 220]. Our study showed that the expression of viral transcripts such as HCMV IE and cmvIL-10 are important for stimulating expression of inflammatory genes including IL-6, IL-1 β , and PTGS-2 in human breast cancer cells, as described in Chapter 4. Whether both HCMV IE and cmvIL-10 are required in this process will be further investigated.

The inflammation could also be enhanced at the tumor site through CMV infection in the tumor-associated breast adipose tissues. Our group has previously shown that a feedforward inflammatory cycle driven by ATX is observed at the breast tumor site, with crosstalk that exists between the breast tumor and tumor-associated breast adipose tissue [31]. Our ongoing study shows a promising trend that the transcription of ATX could be

regulated by CMV infection in the cultured breast tissues, although more detailed analysis is required. In Chapter 5, where we described our established mouse breast cancer models infected with mCMV, we did not observe a significant change for the expression of ATX in the plasma. However, even though a change in ATX was not observed at the systematic level, there could be a difference in expression at the breast local site. Our current models studied late stage development of breast tumors so metastasis could be analyzed, but this made it difficult to obtain the tumor-associated breast adipose tissues because the tumor occupied most of the breast fat pad. Future study could focus more on the early tumor development stage, when tumor-associated breast adipose tissues are still available and analysis on inflammation could be examined. This is particularly important since HCMV DNA can be detected in the breast tissues; it is therefore interesting to know if the infection will enhance inflammation in the associated breast tissues leading to the promotion of worse tumor phenotypes and metastasis. We only detected changes in expression of very few cytokines in the breast tumors and plasma, which could be due to extensive inflammation in all mice because of the large tumor size. In this case, the mCMV-induced differences might not be evident. The mCMV IE1/3 mRNA expression was not detected in the breast tumors at the experimental endpoint, but there is a possibility that viral transcripts were expressed at the early stage of tumor development to stimulate inflammatory signaling responses. Therefore, terminating the experiment at an early tumor stage might provide more information on the mechanisms of CMV-induced inflammation and how it leads to the observed worse outcomes in mouse breast cancer models.

Although we found that HCMV-challenged breast cancer cells do not produce new infectious viral particles, there were viral transcripts and antigens expressed which are

important in stimulating inflammatory genes. When put into the context of a breast tumor, the HCMV-induced expression of inflammatory genes in the breast cancer cells could lead to secretion of cytokines and inflammatory mediators that trigger further signalling responses in the surrounding cells, therefore leading to a long term effect that promotes tumor progression and metastasis [30, 62, 63]. There are multiple cell types in a breast tumor which are susceptible to CMV infection, including fibroblasts and macrophages [159-162]. These cells could retain the viral genome and generate new infectious viral particles during viral reactivation, therefore, further stimulating the breast cancer cells. This is especially interesting since CMV establishes latency in monocytes and can be reactivated when monocytes differentiate into macrophages that are found in the tumor microenvironment [185, 188]. It is evident that cells in the tumor microenvironment that are susceptible to HCMV infection is important to generate viral-induced responses in the breast tumor, since our study showed that only <1% of the HCMV-challenged breast cancer cells expressed IE antigen and with limited or no productive infection.

Our findings and proposed mechanisms for the effect of CMV infection on breast cancer cells within a tumor microenvironment are summarized in Figure 6.1. and the interaction with surrounding tissues are summarized in Figure 6.2. In conclusion, it is evident that CMV stimulates expression of inflammatory genes in the breast cancer cells and the breast tissues present at the tumor site, with viral transcription playing a crucial role. This CMV-induced inflammation could promote tumor progression and metastasis. However, the receptors and signaling pathways involved remains unclear.

CMV infection in tumor microenvironment

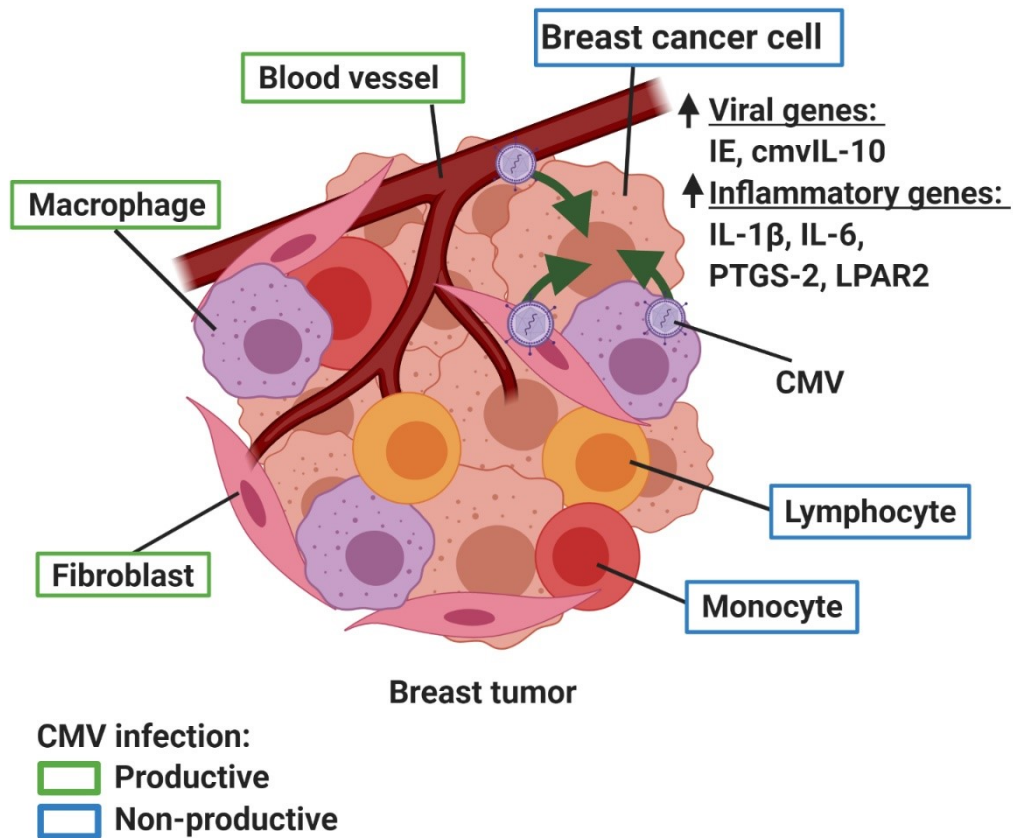


Figure 6.1. CMV infection in the tumor microenvironment and effects on breast cancer cells. Breast cancer cells are not productively infected by CMV, but other cell types in the tumor microenvironment can be infected. These surrounding cells can produce CMV and induce the breast cancer cells to express viral genes leading to an upregulation of inflammatory genes. IE: immediate early; cmv: cytomegalovirus; IL: interleukin; PTGS: prostaglandin-endoperoxide synthase; LPAR: lysophosphatidic acid receptor. Created with BioRender.com.

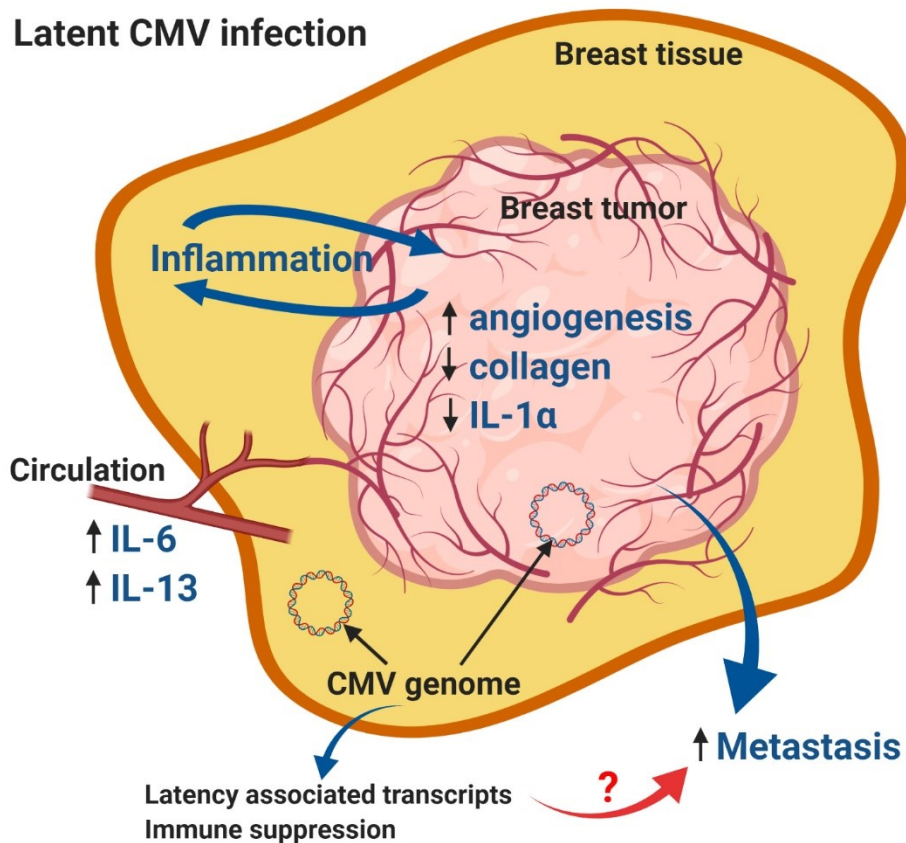


Figure 6.2. Latent CMV infection promotes breast cancer metastasis. Latent CMV infection promotes inflammation at the breast tumor site and the systemic level, leading to worse breast tumor phenotypes and enhanced metastasis. Production of latency associated transcripts and immune suppression during latent CMV infection are potentially involved in the mechanism leading to enhanced metastasis. cmv: cytomegalovirus; IL: interleukin. Created with BioRender.com.

6.4 Latent CMV infection as a factor promoting worse breast tumor phenotypes and metastasis

It has been suggested that HCMV infection could promote breast cancer metastasis. For example, breast cancer cells that are exposed to cmvIL-10 show enhanced invasion and migration [5, 135, 136]. Abundant HCMV DNA and proteins are detected in metastatic

sentinel lymph nodes and brain tissue of breast cancer patients [231, 245]. Our study directly linked CMV infection to breast cancer metastasis, where mice latently infected with mCMV developed a greater number and size of metastatic nodules in the lungs compared to the uninfected mice (Chapter 5) [286]. Our model also showed that the breast tumors developed in mCMV-infected mice had phenotypes that contribute to metastasis, including enhanced microvasculature for angiogenesis and decreased collagen content for cell egression. Our established models involved mice from different strain backgrounds and a spontaneous breast tumor model that more accurately mimics breast tumor growth in human beings. Further investigation of these models for other features important in metastasis, such as expression of genes involved in EMT, could lead to a better understanding of the mechanisms involved in causing the observed effect of CMV infection on breast cancer metastasis.

It is uncertain why only the latently infected mice showed enhanced lung metastasis. The immune responses are likely involved in causing this difference. When CMV infection is still at an active stage, there would be a robust innate immune response against the virus, which could contribute to control the breast tumor metastasis [203]. During the latency stage, CMV produces viral transcripts such as latency-associated-cmvIL10, beta 2.7, Inc4.9, and miR-UL112-3p, that protect the virus from being detected and cleared by the host immunity through immune suppression [196-198]. This could contribute to less control of the breast cancer cells and lead to enhanced metastasis. Evidence has shown that the recruitment of regulatory T cells to repress the cytotoxic CD8⁺ T cells during latent CMV infection resembles the immune-evasion mechanisms observed in breast cancer that showed abrogated cytotoxic CD8⁺ T cell effects [287, 288]. The specific role of CMV

latency should be investigated further for our in-depth understanding of the CMV-breast cancer association, focusing on latency-associated transcripts and proteins that regulate immune responses.

The effects of latent CMV infection on breast cancer and metastasis are summarized in Figure 6.2. In conclusion, this work provides the first direct evidence for a link between CMV and breast cancer metastasis. Treating or preventing HCMV infection could make a major contribution in decreasing metastasis for breast cancer patients. This is important since metastasis is what causes mortality in cancer, therefore targeting against HCMV infection should lead to decreased mortality in breast cancer patients.

6.5 Future directions

In our study, a low number of breast cancer cells showed expression of HCMV IE antigen when challenged with HCMV and there is a lack of productive infection. However, there is evidence for HCMV antigens detected by IHC in patient breast tumors that are associated with cancer cells [231]. One suggestion could be that infection of the breast cancer cells requires assistance from other cells in the tumor-microenvironment that are susceptible to HCMV. This should be examined by having breast cancer cells co-cultured with fibroblasts or breast tissues to determine whether infection in the breast cancer cells can be increased during HCMV challenge. To best represent the interaction between cells, three-dimensional cell culture should be performed so cells can grow in all directions [289]. This co-culture study will also allow an investigation of the HCMV infection effect on production of inflammatory mediators when crosstalk occurs between these cells. The effect of HCMV challenge on invasion and migration of breast cancer cells in the co-culture

should also be investigated, especially because we have observed an effect of enhanced metastasis in mice infected with mCMV.

Our current work showed phenotypical changes including enhanced angiogenesis and decreased collagen content in the breast tumors of mCMV-infected mice as evidence supporting the promotion of metastasis. However, the mechanistic changes driving the metastatic properties of breast tumors in these latently infected mice are unknown. Further investigation could focus on whether latent CMV infection alters the regulation of genes important for an EMT process in breast tumors. We have preserved all breast tumors from the established mouse models in both frozen and formalin-fixed and paraffin-embedded forms. Therefore, qPCR analysis for gene transcription and IHC analysis for protein expression are both feasible. Possible targets to be analyzed include E-cadherin 1, E-cadherin 2, vimentin, zinc finger E-box binding homeobox 1/2, Twist 1/2, Snail, and Slug, which are all known to be important in the EMT/MET processes [290, 291]. This would provide insight into our understanding of the mechanisms linking CMV infection to metastasis.

We have made an attempt in our study to investigate the contribution of CMV induced inflammation in breast cancer progression and metastasis. Our focus was on inflammatory mediators, cytokines and chemokines. It is well known that immune cells play a crucial role in inflammation, where they can be attracted by cytokines/chemokines but also produce these small signaling molecules. However, currently, we do not know how the immune cells contribute to our observed results in the mouse models. Immune cells that infiltrate into the tumor site form a major component of the tumor microenvironment, where they regulate tumor progression and metastasis [43, 45]. The

type of immune cell can be determined and quantified through IHC, which could be performed on the formalin-fixed and paraffin-embedded breast tumors collected from our established mouse models, with target cells including CD4⁺/CD8⁺ T cells and macrophages. The macrophages are particularly interesting since there is evidence that CMV can infect macrophages and influence its polarization into M1 or M2 phenotypes, although contradicting results exist [139-141]. The study of immune cells could also allow us to have a better understanding of their contribution to different CMV infection stages, especially during viral latency. Therefore, characterizing the different types of immune cells that infiltrated into the breast tumors could provide insight into the inflammatory signaling mechanisms induced by CMV infection.

Another important future research direction is examining the effectiveness of using antiviral drugs or vaccine candidates against CMV for reducing the risk of metastasis. This is important since metastasis is what really leads to the mortality of breast cancer patients. Currently, antiviral drugs are available for the treatment of HCMV infections, including ganciclovir, valganciclovir, foscarnet, and cidofovir, and fomivirsen [234]. Most of these drugs work by inhibition of CMV replication by binding to the cellular or viral DNA polymerases [234]. Fomivirsen, however, binds to mRNA to prevent the expression of the encoded gene, which is the CMV major IE transactivator gene. The use of fomivirsen could potentially have a beneficial effect on breast cancer progression by inhibiting the production of viral transcripts that are important for stimulating production of inflammatory mediators and cytokines by the infected cells [292]. The effects of administering drug or vaccine treatments against CMV for whether there is a change in tumor phenotype and metastasis can be studied using our latently infected mouse breast

cancer models. The significance of our work and the future investigations provide a novel target, HCMV infection, for decreasing metastasis in breast cancer patients and thus decreasing the mortality due to metastatic disease.

Bibliography

1. Bray, F., Ferlay, J., Soerjomataram, I., Siegel, R.L., Torre, L.A., and Jemal, A., *Global cancer statistics 2018: GLOBOCAN estimates of incidence and mortality worldwide for 36 cancers in 185 countries*. CA Cancer J Clin, 2018. **68**(6): p. 394-424.
2. American Cancer Society. Breast Cancer Facts & Figures 2017-2018. Atlanta: American Cancer Society, I.
3. Plummer, M., de Martel, C., Vignat, J., Ferlay, J., Bray, F., and Franceschi, S., *Global burden of cancers attributable to infections in 2012: a synthetic analysis*. Lancet Glob Health, 2016. **4**(9): p. e609-16.
4. Taher, C., de Boniface, J., Mohammad, A.A., Religa, P., Hartman, J., Yaiw, K.C., Frisell, J., Rahbar, A., and Soderberg-Naucler, C., *High prevalence of human cytomegalovirus proteins and nucleic acids in primary breast cancer and metastatic sentinel lymph nodes*. PLoS One, 2013. **8**(2): p. e56795.
5. Valle Oseguera, C.A. and Spencer, J.V., *Human cytomegalovirus interleukin-10 enhances matrigel invasion of MDA-MB-231 breast cancer cells*. Cancer Cell Int, 2017. **17**: p. 24.
6. Kumar, A., Tripathy, M.K., Pasquereau, S., Al Moussawi, F., Abbas, W., Coquard, L., Khan, K.A., Russo, L., Algros, M.P., Valmary-Degano, S., Adotevi, O., Morot-Bizot, S., and Herbein, G., *The Human Cytomegalovirus Strain DB Activates Oncogenic Pathways in Mammary Epithelial Cells*. EBioMedicine, 2018. **30**: p. 167-183.
7. Canadian Cancer Statistics Advisory Committee. Canadian Cancer Statistics 2019. Toronto, O.C.C.S.
8. Akram, M., Iqbal, M., Daniyal, M., and Khan, A.U., *Awareness and current knowledge of breast cancer*. Biol Res, 2017. **50**(1): p. 33.
9. Brewer, H.R., Jones, M.E., Schoemaker, M.J., Ashworth, A., and Swerdlow, A.J., *Family history and risk of breast cancer: an analysis accounting for family structure*. Breast Cancer Res Treat, 2017. **165**(1): p. 193-200.
10. Endogenous, H., Breast Cancer Collaborative, G., Key, T.J., Appleby, P.N., Reeves, G.K., Travis, R.C., Alberg, A.J., Barricarte, A., Berrino, F., Krogh, V., Sieri, S., Brinton, L.A., Dorgan, J.F., Dossus, L., Dowsett, M., Eliassen, A.H., Fortner, R.T., Hankinson, S.E., Helzlsouer, K.J., Hoffman-Bolton, J., Comstock, G.W., Kaaks, R., Kahle, L.L., Muti, P., Overvad, K., Peeters, P.H., Riboli, E., Rinaldi, S., Rollison, D.E., Stanczyk, F.Z., Trichopoulos, D., Tworoger, S.S., and Vineis, P., *Sex hormones and risk of breast cancer in premenopausal women: a collaborative reanalysis of individual participant data from seven prospective studies*. Lancet Oncol, 2013. **14**(10): p. 1009-19.
11. Makarem, N., Chandran, U., Bandera, E.V., and Parekh, N., *Dietary fat in breast cancer survival*. Annu Rev Nutr, 2013. **33**: p. 319-48.
12. Jung, S., Wang, M., Anderson, K., Baglietto, L., Bergkvist, L., Bernstein, L., van den Brandt, P.A., Brinton, L., Buring, J.E., Eliassen, A.H., Falk, R., Gapstur, S.M., Giles, G.G., Goodman, G., Hoffman-Bolton, J., Horn-Ross, P.L., Inoue, M., Kolonel, L.N., Krogh, V., Lof, M., Maas, P., Miller, A.B., Neuhauser, M.L., Park, Y., Robien, K., Rohan, T.E., Scarmo, S., Schouten, L.J., Sieri, S., Stevens, V.L., Tsugane, S., Visvanathan, K., Wilkens, L.R., Wolk, A., Weiderpass, E., Willett,

- W.C., Zeleniuch-Jacquotte, A., Zhang, S.M., Zhang, X., Ziegler, R.G., and Smith-Warner, S.A., *Alcohol consumption and breast cancer risk by estrogen receptor status: in a pooled analysis of 20 studies*. *Int J Epidemiol*, 2016. **45**(3): p. 916-28.
13. Veronesi, U., Boyle, P., Goldhirsch, A., Orecchia, R., and Viale, G., *Breast cancer*. *Lancet*, 2005. **365**(9472): p. 1727-41.
 14. Tanis, P.J., Nieweg, O.E., Valdes Olmos, R.A., and Kroon, B.B., *Anatomy and physiology of lymphatic drainage of the breast from the perspective of sentinel node biopsy*. *J Am Coll Surg*, 2001. **192**(3): p. 399-409.
 15. Stingl, J., Raouf, A., Eirew, P., and Eaves, C.J., *Deciphering the mammary epithelial cell hierarchy*. *Cell Cycle*, 2006. **5**(14): p. 1519-22.
 16. Feng, Y., Spezia, M., Huang, S., Yuan, C., Zeng, Z., Zhang, L., Ji, X., Liu, W., Huang, B., Luo, W., Liu, B., Lei, Y., Du, S., Vuppalapati, A., Luu, H.H., Haydon, R.C., He, T.C., and Ren, G., *Breast cancer development and progression: Risk factors, cancer stem cells, signaling pathways, genomics, and molecular pathogenesis*. *Genes Dis*, 2018. **5**(2): p. 77-106.
 17. Heim, E., Valach, L., and Schaffner, L., *Coping and psychosocial adaptation: longitudinal effects over time and stages in breast cancer*. *Psychosom Med*, 1997. **59**(4): p. 408-18.
 18. Houssami, N., Turner, R.M., and Morrow, M., *Meta-analysis of pre-operative magnetic resonance imaging (MRI) and surgical treatment for breast cancer*. *Breast Cancer Res Treat*, 2017. **165**(2): p. 273-283.
 19. Fisher, B., Anderson, S., Redmond, C.K., Wolmark, N., Wickerham, D.L., and Cronin, W.M., *Reanalysis and results after 12 years of follow-up in a randomized clinical trial comparing total mastectomy with lumpectomy with or without irradiation in the treatment of breast cancer*. *N Engl J Med*, 1995. **333**(22): p. 1456-61.
 20. Shah, R., Rosso, K., and Nathanson, S.D., *Pathogenesis, prevention, diagnosis and treatment of breast cancer*. *World J Clin Oncol*, 2014. **5**(3): p. 283-98.
 21. Independent, U.K.P.o.B.C.S., *The benefits and harms of breast cancer screening: an independent review*. *Lancet*, 2012. **380**(9855): p. 1778-86.
 22. Morrow, M., Waters, J., and Morris, E., *MRI for breast cancer screening, diagnosis, and treatment*. *Lancet*, 2011. **378**(9805): p. 1804-11.
 23. Diego, E.J., McAuliffe, P.F., Soran, A., McGuire, K.P., Johnson, R.R., Bonaventura, M., and Ahrendt, G.M., *Axillary Staging After Neoadjuvant Chemotherapy for Breast Cancer: A Pilot Study Combining Sentinel Lymph Node Biopsy with Radioactive Seed Localization of Pre-treatment Positive Axillary Lymph Nodes*. *Ann Surg Oncol*, 2016. **23**(5): p. 1549-53.
 24. Ibrahim, M.M., *Subcutaneous and visceral adipose tissue: structural and functional differences*. *Obes Rev*, 2010. **11**(1): p. 11-8.
 25. Macias, H. and Hinck, L., *Mammary gland development*. *Wiley Interdiscip Rev Dev Biol*, 2012. **1**(4): p. 533-57.
 26. Sever, R. and Brugge, J.S., *Signal transduction in cancer*. *Cold Spring Harb Perspect Med*, 2015. **5**(4).
 27. Elizalde, P.V., Cordo Russo, R.I., Chervo, M.F., and Schillaci, R., *ErbB-2 nuclear function in breast cancer growth, metastasis and resistance to therapy*. *Endocr Relat Cancer*, 2016. **23**(12): p. T243-T257.

28. Deng, C.X., *BRCA1: cell cycle checkpoint, genetic instability, DNA damage response and cancer evolution*. Nucleic Acids Res, 2006. **34**(5): p. 1416-26.
29. Bane, A.L., Beck, J.C., Bleiweiss, I., Buys, S.S., Catalano, E., Daly, M.B., Giles, G., Godwin, A.K., Hibshoosh, H., Hopper, J.L., John, E.M., Layfield, L., Longacre, T., Miron, A., Senie, R., Southey, M.C., West, D.W., Whittemore, A.S., Wu, H., Andrulis, I.L., and O'Malley, F.P., *BRCA2 mutation-associated breast cancers exhibit a distinguishing phenotype based on morphology and molecular profiles from tissue microarrays*. Am J Surg Pathol, 2007. **31**(1): p. 121-8.
30. Hanahan, D. and Weinberg, R.A., *Hallmarks of cancer: the next generation*. Cell, 2011. **144**(5): p. 646-74.
31. Benesch, M.G., Tang, X., Dewald, J., Dong, W.F., Mackey, J.R., Hemmings, D.G., McMullen, T.P., and Brindley, D.N., *Tumor-induced inflammation in mammary adipose tissue stimulates a vicious cycle of autotaxin expression and breast cancer progression*. FASEB J, 2015. **29**(9): p. 3990-4000.
32. Qian, B.Z. and Pollard, J.W., *Macrophage diversity enhances tumor progression and metastasis*. Cell, 2010. **141**(1): p. 39-51.
33. Fraser, H.M. and Lunn, S.F., *Angiogenesis and its control in the female reproductive system*. Br Med Bull, 2000. **56**(3): p. 787-97.
34. Bergers, G. and Benjamin, L.E., *Tumorigenesis and the angiogenic switch*. Nat Rev Cancer, 2003. **3**(6): p. 401-10.
35. Folkman, J., *Angiogenesis*. Annu Rev Med, 2006. **57**: p. 1-18.
36. Liu, Y., Wada, R., Yamashita, T., Mi, Y., Deng, C.X., Hobson, J.P., Rosenfeldt, H.M., Nava, V.E., Chae, S.S., Lee, M.J., Liu, C.H., Hla, T., Spiegel, S., and Proia, R.L., *Edg-1, the G protein-coupled receptor for sphingosine-1-phosphate, is essential for vascular maturation*. J Clin Invest, 2000. **106**(8): p. 951-61.
37. Tauseef, M., Kini, V., Knezevic, N., Brannan, M., Ramchandaran, R., Fyrst, H., Saba, J., Vogel, S.M., Malik, A.B., and Mehta, D., *Activation of sphingosine kinase-1 reverses the increase in lung vascular permeability through sphingosine-1-phosphate receptor signaling in endothelial cells*. Circ Res, 2008. **103**(10): p. 1164-72.
38. Rasanen, K. and Vaheri, A., *Activation of fibroblasts in cancer stroma*. Exp Cell Res, 2010. **316**(17): p. 2713-22.
39. Erez, N., Glanz, S., Raz, Y., Avivi, C., and Barshack, I., *Cancer associated fibroblasts express pro-inflammatory factors in human breast and ovarian tumors*. Biochem Biophys Res Commun, 2013. **437**(3): p. 397-402.
40. Kalluri, R. and Zeisberg, M., *Fibroblasts in cancer*. Nat Rev Cancer, 2006. **6**(5): p. 392-401.
41. Wu, T. and Dai, Y., *Tumor microenvironment and therapeutic response*. Cancer Lett, 2017. **387**: p. 61-68.
42. Duluc, D., Corvaisier, M., Blanchard, S., Catala, L., Descamps, P., Gamelin, E., Ponsoda, S., Delneste, Y., Hebbard, M., and Jeannin, P., *Interferon-gamma reverses the immunosuppressive and protumoral properties and prevents the generation of human tumor-associated macrophages*. Int J Cancer, 2009. **125**(2): p. 367-73.

43. Sica, A., Larghi, P., Mancino, A., Rubino, L., Porta, C., Totaro, M.G., Rimoldi, M., Biswas, S.K., Allavena, P., and Mantovani, A., *Macrophage polarization in tumour progression*. *Semin Cancer Biol*, 2008. **18**(5): p. 349-55.
44. Pollard, J.W., *Trophic macrophages in development and disease*. *Nat Rev Immunol*, 2009. **9**(4): p. 259-70.
45. DeNardo, D.G., Barreto, J.B., Andreu, P., Vasquez, L., Tawfik, D., Kolhatkar, N., and Coussens, L.M., *CD4(+) T cells regulate pulmonary metastasis of mammary carcinomas by enhancing protumor properties of macrophages*. *Cancer Cell*, 2009. **16**(2): p. 91-102.
46. Medzhitov, R., *Origin and physiological roles of inflammation*. *Nature*, 2008. **454**(7203): p. 428-35.
47. Krishnamoorthy, S. and Honn, K.V., *Inflammation and disease progression*. *Cancer Metastasis Rev*, 2006. **25**(3): p. 481-91.
48. Turner, M.D., Nedjai, B., Hurst, T., and Pennington, D.J., *Cytokines and chemokines: At the crossroads of cell signalling and inflammatory disease*. *Biochim Biophys Acta*, 2014. **1843**(11): p. 2563-2582.
49. Ono, S.J., Nakamura, T., Miyazaki, D., Ohbayashi, M., Dawson, M., and Toda, M., *Chemokines: roles in leukocyte development, trafficking, and effector function*. *J Allergy Clin Immunol*, 2003. **111**(6): p. 1185-99; quiz 1200.
50. Serhan, C.N., Chiang, N., and Van Dyke, T.E., *Resolving inflammation: dual anti-inflammatory and pro-resolution lipid mediators*. *Nat Rev Immunol*, 2008. **8**(5): p. 349-61.
51. Lawrence, T. and Gilroy, D.W., *Chronic inflammation: a failure of resolution?* *Int J Exp Pathol*, 2007. **88**(2): p. 85-94.
52. Umezu-Goto, M., Kishi, Y., Taira, A., Hama, K., Dohmae, N., Takio, K., Yamori, T., Mills, G.B., Inoue, K., Aoki, J., and Arai, H., *Autotaxin has lysophospholipase D activity leading to tumor cell growth and motility by lysophosphatidic acid production*. *J Cell Biol*, 2002. **158**(2): p. 227-33.
53. Brindley, D.N., *Lipid phosphate phosphatases and related proteins: signaling functions in development, cell division, and cancer*. *J Cell Biochem*, 2004. **92**(5): p. 900-12.
54. Bourgoin, S.G. and Zhao, C., *Autotaxin and lysophospholipids in rheumatoid arthritis*. *Curr Opin Investig Drugs*, 2010. **11**(5): p. 515-26.
55. Okudaira, S., Yukiura, H., and Aoki, J., *Biological roles of lysophosphatidic acid signaling through its production by autotaxin*. *Biochimie*, 2010. **92**(6): p. 698-706.
56. So, J., Wang, F.Q., Navari, J., Schreher, J., and Fishman, D.A., *LPA-induced epithelial ovarian cancer (EOC) in vitro invasion and migration are mediated by VEGF receptor-2 (VEGF-R2)*. *Gynecol Oncol*, 2005. **97**(3): p. 870-8.
57. Murph, M.M., Hurst-Kennedy, J., Newton, V., Brindley, D.N., and Radhakrishna, H., *Lysophosphatidic acid decreases the nuclear localization and cellular abundance of the p53 tumor suppressor in A549 lung carcinoma cells*. *Mol Cancer Res*, 2007. **5**(11): p. 1201-11.
58. Liu, S., Umezu-Goto, M., Murph, M., Lu, Y., Liu, W., Zhang, F., Yu, S., Stephens, L.C., Cui, X., Murrow, G., Coombes, K., Muller, W., Hung, M.C., Perou, C.M., Lee, A.V., Fang, X., and Mills, G.B., *Expression of autotaxin and*

- lysophosphatidic acid receptors increases mammary tumorigenesis, invasion, and metastases.* *Cancer Cell*, 2009. **15**(6): p. 539-50.
59. Liu, S., Murph, M., Panupinthu, N., and Mills, G.B., *ATX-LPA receptor axis in inflammation and cancer.* *Cell Cycle*, 2009. **8**(22): p. 3695-701.
 60. Benesch, M.G., Ko, Y.M., Tang, X., Dewald, J., Lopez-Campistrous, A., Zhao, Y.Y., Lai, R., Curtis, J.M., Brindley, D.N., and McMullen, T.P., *Autotaxin is an inflammatory mediator and therapeutic target in thyroid cancer.* *Endocr Relat Cancer*, 2015. **22**(4): p. 593-607.
 61. Dvorak, H.F., *Tumors: wounds that do not heal. Similarities between tumor stroma generation and wound healing.* *N Engl J Med*, 1986. **315**(26): p. 1650-9.
 62. Grivennikov, S.I., Greten, F.R., and Karin, M., *Immunity, inflammation, and cancer.* *Cell*, 2010. **140**(6): p. 883-99.
 63. Karnoub, A.E. and Weinberg, R.A., *Chemokine networks and breast cancer metastasis.* *Breast Dis*, 2006. **26**: p. 75-85.
 64. Steeg, P.S., *Tumor metastasis: mechanistic insights and clinical challenges.* *Nat Med*, 2006. **12**(8): p. 895-904.
 65. Spano, D., Heck, C., De Antonellis, P., Christofori, G., and Zollo, M., *Molecular networks that regulate cancer metastasis.* *Semin Cancer Biol*, 2012. **22**(3): p. 234-49.
 66. Brooks, S.A., Lomax-Browne, H.J., Carter, T.M., Kinch, C.E., and Hall, D.M., *Molecular interactions in cancer cell metastasis.* *Acta Histochem*, 2010. **112**(1): p. 3-25.
 67. Blood, C.H. and Zetter, B.R., *Tumor interactions with the vasculature: angiogenesis and tumor metastasis.* *Biochim Biophys Acta*, 1990. **1032**(1): p. 89-118.
 68. Cavallaro, U. and Christofori, G., *Cell adhesion and signalling by cadherins and Ig-CAMs in cancer.* *Nat Rev Cancer*, 2004. **4**(2): p. 118-32.
 69. Friedl, P. and Wolf, K., *Tumour-cell invasion and migration: diversity and escape mechanisms.* *Nat Rev Cancer*, 2003. **3**(5): p. 362-74.
 70. Tse, J.C. and Kalluri, R., *Mechanisms of metastasis: epithelial-to-mesenchymal transition and contribution of tumor microenvironment.* *J Cell Biochem*, 2007. **101**(4): p. 816-29.
 71. Price, J.T., Bonovich, M.T., and Kohn, E.C., *The biochemistry of cancer dissemination.* *Crit Rev Biochem Mol Biol*, 1997. **32**(3): p. 175-253.
 72. Deryugina, E.I. and Quigley, J.P., *Matrix metalloproteinases and tumor metastasis.* *Cancer Metastasis Rev*, 2006. **25**(1): p. 9-34.
 73. Paget, S., *The distribution of secondary growths in cancer of the breast. 1889.* *Cancer Metastasis Rev*, 1989. **8**(2): p. 98-101.
 74. Ewing, J., *Neoplastic Diseases. A Treatise on Tumors.* W. B. Saunders Co., Philadelphia & London, 1928 p. 77-89.
 75. Fidler, I.J., *The pathogenesis of cancer metastasis: the 'seed and soil' hypothesis revisited.* *Nat Rev Cancer*, 2003. **3**(6): p. 453-8.
 76. Kumar, P. and Aggarwal, R., *An overview of triple-negative breast cancer.* *Arch Gynecol Obstet*, 2016. **293**(2): p. 247-69.
 77. Goldhirsch, A., Wood, W.C., Coates, A.S., Gelber, R.D., Thurlimann, B., Senn, H.J., and Panel, m., *Strategies for subtypes--dealing with the diversity of breast*

- cancer: highlights of the St. Gallen International Expert Consensus on the Primary Therapy of Early Breast Cancer 2011*. *Ann Oncol*, 2011. **22**(8): p. 1736-47.
78. Hammond, M.E., Hayes, D.F., Wolff, A.C., Mangu, P.B., and Temin, S., *American society of clinical oncology/college of american pathologists guideline recommendations for immunohistochemical testing of estrogen and progesterone receptors in breast cancer*. *J Oncol Pract*, 2010. **6**(4): p. 195-7.
 79. Wolff, A.C., Hammond, M.E., Schwartz, J.N., Hagerty, K.L., Allred, D.C., Cote, R.J., Dowsett, M., Fitzgibbons, P.L., Hanna, W.M., Langer, A., McShane, L.M., Paik, S., Pegram, M.D., Perez, E.A., Press, M.F., Rhodes, A., Sturgeon, C., Taube, S.E., Tubbs, R., Vance, G.H., van de Vijver, M., Wheeler, T.M., Hayes, D.F., American Society of Clinical, O., and College of American, P., *American Society of Clinical Oncology/College of American Pathologists guideline recommendations for human epidermal growth factor receptor 2 testing in breast cancer*. *J Clin Oncol*, 2007. **25**(1): p. 118-45.
 80. Horwitz, K.B. and McGuire, W.L., *Predicting response to endocrine therapy in human breast cancer: a hypothesis*. *Science*, 1975. **189**(4204): p. 726-7.
 81. Early Breast Cancer Trialists' Collaborative, G., Davies, C., Godwin, J., Gray, R., Clarke, M., Cutter, D., Darby, S., McGale, P., Pan, H.C., Taylor, C., Wang, Y.C., Dowsett, M., Ingle, J., and Peto, R., *Relevance of breast cancer hormone receptors and other factors to the efficacy of adjuvant tamoxifen: patient-level meta-analysis of randomised trials*. *Lancet*, 2011. **378**(9793): p. 771-84.
 82. Robinson, E., Kimmick, G.G., and Muss, H.B., *Tamoxifen in postmenopausal women a safety perspective*. *Drugs Aging*, 1996. **8**(5): p. 329-37.
 83. Ricketts, D., Turnbull, L., Ryall, G., Bakhshi, R., Rawson, N.S., Gazet, J.C., Nolan, C., and Coombes, R.C., *Estrogen and progesterone receptors in the normal female breast*. *Cancer Res*, 1991. **51**(7): p. 1817-22.
 84. Kininis, M. and Kraus, W.L., *A global view of transcriptional regulation by nuclear receptors: gene expression, factor localization, and DNA sequence analysis*. *Nucl Recept Signal*, 2008. **6**: p. e005.
 85. Russo, J. and Russo, I.H., *Development of the human breast*. *Maturitas*, 2004. **49**(1): p. 2-15.
 86. Hewitt, S.C., Harrell, J.C., and Korach, K.S., *Lessons in estrogen biology from knockout and transgenic animals*. *Annu Rev Physiol*, 2005. **67**: p. 285-308.
 87. Conneely, O.M., Mulac-Jericevic, B., Lydon, J.P., and De Mayo, F.J., *Reproductive functions of the progesterone receptor isoforms: lessons from knock-out mice*. *Mol Cell Endocrinol*, 2001. **179**(1-2): p. 97-103.
 88. Tyson, J.J., Baumann, W.T., Chen, C., Verdugo, A., Tavassoly, I., Wang, Y., Weiner, L.M., and Clarke, R., *Dynamic modelling of oestrogen signalling and cell fate in breast cancer cells*. *Nat Rev Cancer*, 2011. **11**(7): p. 523-32.
 89. McGowan, E.M., Saad, S., Bendall, L.J., Bradstock, K.F., and Clarke, C.L., *Effect of progesterone receptor a predominance on breast cancer cell migration into bone marrow fibroblasts*. *Breast Cancer Res Treat*, 2004. **83**(3): p. 211-20.
 90. Ross, J.S., Slodkowska, E.A., Symmans, W.F., Pusztai, L., Ravdin, P.M., and Hortobagyi, G.N., *The HER-2 receptor and breast cancer: ten years of targeted*

- anti-HER-2 therapy and personalized medicine. Oncologist, 2009. 14(4): p. 320-68.*
91. Schechter, A.L., Stern, D.F., Vaidyanathan, L., Decker, S.J., Drebin, J.A., Greene, M.I., and Weinberg, R.A., *The neu oncogene: an erb-B-related gene encoding a 185,000-Mr tumour antigen. Nature, 1984. 312(5994): p. 513-6.*
 92. Hudis, C.A., *Trastuzumab--mechanism of action and use in clinical practice. N Engl J Med, 2007. 357(1): p. 39-51.*
 93. Moasser, M.M., *The oncogene HER2: its signaling and transforming functions and its role in human cancer pathogenesis. Oncogene, 2007. 26(45): p. 6469-87.*
 94. Slamon, D.J., Clark, G.M., Wong, S.G., Levin, W.J., Ullrich, A., and McGuire, W.L., *Human breast cancer: correlation of relapse and survival with amplification of the HER-2/neu oncogene. Science, 1987. 235(4785): p. 177-82.*
 95. Bendell, J.C., Domchek, S.M., Burstein, H.J., Harris, L., Younger, J., Kuter, I., Bunnell, C., Rue, M., Gelman, R., and Winer, E., *Central nervous system metastases in women who receive trastuzumab-based therapy for metastatic breast carcinoma. Cancer, 2003. 97(12): p. 2972-7.*
 96. Ryan, Q., Ibrahim, A., Cohen, M.H., Johnson, J., Ko, C.W., Sridhara, R., Justice, R., and Pazdur, R., *FDA drug approval summary: lapatinib in combination with capecitabine for previously treated metastatic breast cancer that overexpresses HER-2. Oncologist, 2008. 13(10): p. 1114-9.*
 97. Slamon, D.J., Leyland-Jones, B., Shak, S., Fuchs, H., Paton, V., Bajamonde, A., Fleming, T., Eiermann, W., Wolter, J., Pegram, M., Baselga, J., and Norton, L., *Use of chemotherapy plus a monoclonal antibody against HER2 for metastatic breast cancer that overexpresses HER2. N Engl J Med, 2001. 344(11): p. 783-92.*
 98. Rakha, E.A. and Ellis, I.O., *Triple-negative/basal-like breast cancer: review. Pathology, 2009. 41(1): p. 40-7.*
 99. Perou, C.M., Sorlie, T., Eisen, M.B., van de Rijn, M., Jeffrey, S.S., Rees, C.A., Pollack, J.R., Ross, D.T., Johnsen, H., Akslen, L.A., Fluge, O., Pergamenschikov, A., Williams, C., Zhu, S.X., Lonning, P.E., Borresen-Dale, A.L., Brown, P.O., and Botstein, D., *Molecular portraits of human breast tumours. Nature, 2000. 406(6797): p. 747-52.*
 100. Engebraaten, O., Vollan, H.K.M., and Borresen-Dale, A.L., *Triple-negative breast cancer and the need for new therapeutic targets. Am J Pathol, 2013. 183(4): p. 1064-1074.*
 101. Nabholz, J.M., Reese, D.M., Lindsay, M.A., and Riva, A., *Docetaxel in the treatment of breast cancer: an update on recent studies. Semin Oncol, 2002. 29(3 Suppl 12): p. 28-34.*
 102. Cao, J. and Li, D., *Searching for human oncoviruses: Histories, challenges, and opportunities. J Cell Biochem, 2018. 119(6): p. 4897-4906.*
 103. Pagano, J.S., Blaser, M., Buendia, M.A., Damania, B., Khalili, K., Raab-Traub, N., and Roizman, B., *Infectious agents and cancer: criteria for a causal relation. Semin Cancer Biol, 2004. 14(6): p. 453-71.*
 104. Epstein, M.A., Achong, B.G., and Barr, Y.M., *Virus Particles in Cultured Lymphoblasts from Burkitt's Lymphoma. Lancet, 1964. 1(7335): p. 702-3.*
 105. Cohen, J.I., *Epstein-Barr virus infection. N Engl J Med, 2000. 343(7): p. 481-92.*

106. de-The, G., Geser, A., Day, N.E., Tukei, P.M., Williams, E.H., Beri, D.P., Smith, P.G., Dean, A.G., Bronkamm, G.W., Feorino, P., and Henle, W., *Epidemiological evidence for causal relationship between Epstein-Barr virus and Burkitt's lymphoma from Ugandan prospective study*. *Nature*, 1978. **274**(5673): p. 756-61.
107. Pope, J.H., Horne, M.K., and Scott, W., *Transformation of foetal human keukocytes in vitro by filtrates of a human leukaemic cell line containing herpes-like virus*. *Int J Cancer*, 1968. **3**(6): p. 857-66.
108. zur Hausen, H., *Human papillomaviruses and their possible role in squamous cell carcinomas*. *Curr Top Microbiol Immunol*, 1977. **78**: p. 1-30.
109. Durst, M., Gissmann, L., Ikenberg, H., and zur Hausen, H., *A papillomavirus DNA from a cervical carcinoma and its prevalence in cancer biopsy samples from different geographic regions*. *Proc Natl Acad Sci U S A*, 1983. **80**(12): p. 3812-5.
110. Munger, K., Phelps, W.C., Bubb, V., Howley, P.M., and Schlegel, R., *The E6 and E7 genes of the human papillomavirus type 16 together are necessary and sufficient for transformation of primary human keratinocytes*. *J Virol*, 1989. **63**(10): p. 4417-21.
111. Nicol, A.F., de Andrade, C.V., Russomano, F.B., Rodrigues, L.S., Oliveira, N.S., Provance, D.W., Jr., and Nuovo, G.J., *HPV vaccines: their pathology-based discovery, benefits, and adverse effects*. *Ann Diagn Pathol*, 2015. **19**(6): p. 418-22.
112. Brotherton, J.M.L., *Impact of HPV vaccination: Achievements and future challenges*. *Papillomavirus Res*, 2019. **7**: p. 138-140.
113. Price, R.L., Song, J., Bingmer, K., Kim, T.H., Yi, J.Y., Nowicki, M.O., Mo, X., Hollon, T., Murnan, E., Alvarez-Breckenridge, C., Fernandez, S., Kaur, B., Rivera, A., Oglesbee, M., Cook, C., Chiocca, E.A., and Kwon, C.H., *Cytomegalovirus contributes to glioblastoma in the context of tumor suppressor mutations*. *Cancer Res*, 2013. **73**(11): p. 3441-50.
114. Dziurzynski, K., Chang, S.M., Heimberger, A.B., Kalejta, R.F., McGregor Dallas, S.R., Smit, M., Soroceanu, L., Cobbs, C.S., Hcmv, and Gliomas, S., *Consensus on the role of human cytomegalovirus in glioblastoma*. *Neuro Oncol*, 2012. **14**(3): p. 246-55.
115. Bai, B., Wang, X., Chen, E., and Zhu, H., *Human cytomegalovirus infection and colorectal cancer risk: a meta-analysis*. *Oncotarget*, 2016. **7**(47): p. 76735-76742.
116. Samanta, M., Harkins, L., Klemm, K., Britt, W.J., and Cobbs, C.S., *High prevalence of human cytomegalovirus in prostatic intraepithelial neoplasia and prostatic carcinoma*. *J Urol*, 2003. **170**(3): p. 998-1002.
117. Radestad, A.F., Estekizadeh, A., Cui, H.L., Kostopoulou, O.N., Davoudi, B., Hirschberg, A.L., Carlson, J., Rahbar, A., and Soderberg-Naucler, C., *Impact of Human Cytomegalovirus Infection and its Immune Response on Survival of Patients with Ovarian Cancer*. *Transl Oncol*, 2018. **11**(6): p. 1292-1300.
118. Harkins, L.E., Matlaf, L.A., Soroceanu, L., Klemm, K., Britt, W.J., Wang, W., Bland, K.I., and Cobbs, C.S., *Detection of human cytomegalovirus in normal and neoplastic breast epithelium*. *Herpesviridae*, 2010. **1**(1): p. 8.
119. Lau, S.K., Chen, Y.Y., Chen, W.G., Diamond, D.J., Mamelak, A.N., Zaia, J.A., and Weiss, L.M., *Lack of association of cytomegalovirus with human brain tumors*. *Mod Pathol*, 2005. **18**(6): p. 838-43.

120. Hart, H., Neill, W.A., and Norval, M., *Lack of association of cytomegalovirus with adenocarcinoma of the colon*. Gut, 1982. **23**(1): p. 21-30.
121. Bakhtiyarizadeh, S., Hosseini, S.Y., Yaghoobi, R., Safaei, A., and Sarvari, J., *Almost Complete Lack of Human Cytomegalovirus and Human papillomaviruses Genome in Benign and Malignant Breast Lesions in Shiraz, Southwest of Iran*. Asian Pac J Cancer Prev, 2017. **18**(12): p. 3319-3324.
122. Akhter, J., Ali Aziz, M.A., Al Ajlan, A., Tulbah, A., and Akhtar, M., *Breast cancer: is there a viral connection?* Adv Anat Pathol, 2014. **21**(5): p. 373-81.
123. Guyard, A., Boyez, A., Pujals, A., Robe, C., Tran Van Nhieu, J., Allory, Y., Moroch, J., Georges, O., Fournet, J.C., Zafrani, E.S., and Leroy, K., *DNA degrades during storage in formalin-fixed and paraffin-embedded tissue blocks*. Virchows Arch, 2017. **471**(4): p. 491-500.
124. Castillo, J.P., Yurochko, A.D., and Kowalik, T.F., *Role of human cytomegalovirus immediate-early proteins in cell growth control*. J Virol, 2000. **74**(17): p. 8028-37.
125. Hsu, C.H., Chang, M.D., Tai, K.Y., Yang, Y.T., Wang, P.S., Chen, C.J., Wang, Y.H., Lee, S.C., Wu, C.W., and Juan, L.J., *HCMV IE2-mediated inhibition of HAT activity downregulates p53 function*. EMBO J, 2004. **23**(11): p. 2269-80.
126. Cobbs, C.S., Soroceanu, L., Denham, S., Zhang, W., and Kraus, M.H., *Modulation of oncogenic phenotype in human glioma cells by cytomegalovirus IE1-mediated mitogenicity*. Cancer Res, 2008. **68**(3): p. 724-30.
127. Moussawi, F.A., Kumar, A., Pasquereau, S., Tripathy, M.K., Karam, W., Diab-Assaf, M., and Herbein, G., *The transcriptome of human mammary epithelial cells infected with the HCMV-DB strain displays oncogenic traits*. Sci Rep, 2018. **8**(1): p. 12574.
128. Cinatl, J., Jr., Cinatl, J., Vogel, J.U., Rabenau, H., Kornhuber, B., and Doerr, H.W., *Modulatory effects of human cytomegalovirus infection on malignant properties of cancer cells*. Intervirology, 1996. **39**(4): p. 259-69.
129. Michaelis, M., Doerr, H.W., and Cinatl, J., *The story of human cytomegalovirus and cancer: increasing evidence and open questions*. Neoplasia, 2009. **11**(1): p. 1-9.
130. Blaheta, R.A., Beecken, W.D., Engl, T., Jonas, D., Oppermann, E., Hundemer, M., Doerr, H.W., Scholz, M., and Cinatl, J., *Human cytomegalovirus infection of tumor cells downregulates NCAM (CD56): a novel mechanism for virus-induced tumor invasiveness*. Neoplasia, 2004. **6**(4): p. 323-31.
131. Teo, W.H., Chen, H.P., Huang, J.C., and Chan, Y.J., *Human cytomegalovirus infection enhances cell proliferation, migration and upregulation of EMT markers in colorectal cancer-derived stem cell-like cells*. Int J Oncol, 2017. **51**(5): p. 1415-1426.
132. Oberstein, A. and Shenk, T., *Cellular responses to human cytomegalovirus infection: Induction of a mesenchymal-to-epithelial transition (MET) phenotype*. Proc Natl Acad Sci U S A, 2017. **114**(39): p. E8244-E8253.
133. Kumar, A., Coquard, L., Pasquereau, S., Russo, L., Valmary-Degano, S., Borg, C., Pothier, P., and Herbein, G., *Tumor control by human cytomegalovirus in a murine model of hepatocellular carcinoma*. Mol Ther Oncolytics, 2016. **3**: p. 16012.

134. Jones, B.C., Logsdon, N.J., Josephson, K., Cook, J., Barry, P.A., and Walter, M.R., *Crystal structure of human cytomegalovirus IL-10 bound to soluble human IL-10R1*. Proc Natl Acad Sci U S A, 2002. **99**(14): p. 9404-9.
135. Valle Oseguera, C.A. and Spencer, J.V., *cmvIL-10 stimulates the invasive potential of MDA-MB-231 breast cancer cells*. PLoS One, 2014. **9**(2): p. e88708.
136. Bishop, R.K., Valle Oseguera, C.A., and Spencer, J.V., *Human Cytomegalovirus interleukin-10 promotes proliferation and migration of MCF-7 breast cancer cells*. Cancer Cell Microenviron, 2015. **2**(1).
137. Herbein, G., *The Human Cytomegalovirus, from Oncomodulation to Oncogenesis*. Viruses, 2018. **10**(8).
138. Mantovani, A., Marchesi, F., Malesci, A., Laghi, L., and Allavena, P., *Tumour-associated macrophages as treatment targets in oncology*. Nat Rev Clin Oncol, 2017. **14**(7): p. 399-416.
139. Dziurzynski, K., Wei, J., Qiao, W., Hatiboglu, M.A., Kong, L.Y., Wu, A., Wang, Y., Cahill, D., Levine, N., Prabhu, S., Rao, G., Sawaya, R., and Heimberger, A.B., *Glioma-associated cytomegalovirus mediates subversion of the monocyte lineage to a tumor propagating phenotype*. Clin Cancer Res, 2011. **17**(14): p. 4642-9.
140. Avdic, S., Cao, J.Z., McSharry, B.P., Clancy, L.E., Brown, R., Steain, M., Gottlieb, D.J., Abendroth, A., and Slobedman, B., *Human cytomegalovirus interleukin-10 polarizes monocytes toward a deactivated M2c phenotype to repress host immune responses*. J Virol, 2013. **87**(18): p. 10273-82.
141. Chan, G., Bivins-Smith, E.R., Smith, M.S., Smith, P.M., and Yurochko, A.D., *Transcriptome analysis reveals human cytomegalovirus reprograms monocyte differentiation toward an M1 macrophage*. J Immunol, 2008. **181**(1): p. 698-711.
142. Dunn, W., Chou, C., Li, H., Hai, R., Patterson, D., Stolc, V., Zhu, H., and Liu, F., *Functional profiling of a human cytomegalovirus genome*. Proc Natl Acad Sci U S A, 2003. **100**(24): p. 14223-8.
143. Davison, A.J., Eberle, R., Ehlers, B., Hayward, G.S., McGeoch, D.J., Minson, A.C., Pellett, P.E., Roizman, B., Studdert, M.J., and Thiry, E., *The order Herpesvirales*. Arch Virol, 2009. **154**(1): p. 171-7.
144. Asanuma, H., Numazaki, K., Nagata, N., Hotsubo, T., Horino, K., and Chiba, S., *Role of milk whey in the transmission of human cytomegalovirus infection by breast milk*. Microbiol Immunol, 1996. **40**(3): p. 201-4.
145. Hayes, K., Danks, D.M., Gibas, H., and Jack, I., *Cytomegalovirus in human milk*. N Engl J Med, 1972. **287**(4): p. 177-8.
146. Griffiths, P., Baraniak, I., and Reeves, M., *The pathogenesis of human cytomegalovirus*. J Pathol, 2015. **235**(2): p. 288-97.
147. Forbes, B.A., *Acquisition of cytomegalovirus infection: an update*. Clin Microbiol Rev, 1989. **2**(2): p. 204-16.
148. Goodrum, F., Caviness, K., and Zagallo, P., *Human cytomegalovirus persistence*. Cell Microbiol, 2012. **14**(5): p. 644-55.
149. Bate, S.L., Dollard, S.C., and Cannon, M.J., *Cytomegalovirus seroprevalence in the United States: the national health and nutrition examination surveys, 1988-2004*. Clin Infect Dis, 2010. **50**(11): p. 1439-47.

150. Pawelec, G., McElhaney, J.E., Aiello, A.E., and Derhovanessian, E., *The impact of CMV infection on survival in older humans*. *Curr Opin Immunol*, 2012. **24**(4): p. 507-11.
151. Adland, E., Klenerman, P., Goulder, P., and Matthews, P.C., *Ongoing burden of disease and mortality from HIV/CMV coinfection in Africa in the antiretroviral therapy era*. *Front Microbiol*, 2015. **6**: p. 1016.
152. Cannon, M.J., Schmid, D.S., and Hyde, T.B., *Review of cytomegalovirus seroprevalence and demographic characteristics associated with infection*. *Rev Med Virol*, 2010. **20**(4): p. 202-13.
153. Kocak, E.D., Sherwin, J.C., and Hall, A.J., *Cytomegalovirus disease in immunocompetent adults*. *Med J Aust*, 2015. **202**(8): p. 419.
154. Wreghitt, T.G., Teare, E.L., Sule, O., Devi, R., and Rice, P., *Cytomegalovirus infection in immunocompetent patients*. *Clin Infect Dis*, 2003. **37**(12): p. 1603-6.
155. Ishii, T., Sasaki, Y., Maeda, T., Komatsu, F., Suzuki, T., and Urita, Y., *Clinical differentiation of infectious mononucleosis that is caused by Epstein-Barr virus or cytomegalovirus: A single-center case-control study in Japan*. *J Infect Chemother*, 2019. **25**(6): p. 431-436.
156. Goderis, J., De Leenheer, E., Smets, K., Van Hoecke, H., Keymeulen, A., and Dhooze, I., *Hearing loss and congenital CMV infection: a systematic review*. *Pediatrics*, 2014. **134**(5): p. 972-82.
157. McDevitt, L.M., *Etiology and impact of cytomegalovirus disease on solid organ transplant recipients*. *Am J Health Syst Pharm*, 2006. **63**(19 Suppl 5): p. S3-9.
158. Savva, G.M., Pachnio, A., Kaul, B., Morgan, K., Huppert, F.A., Brayne, C., Moss, P.A., Medical Research Council Cognitive, F., and Ageing, S., *Cytomegalovirus infection is associated with increased mortality in the older population*. *Aging Cell*, 2013. **12**(3): p. 381-7.
159. Sinzger, C., Digel, M., and Jahn, G., *Cytomegalovirus cell tropism*. *Curr Top Microbiol Immunol*, 2008. **325**: p. 63-83.
160. Wang, D. and Shenk, T., *Human cytomegalovirus virion protein complex required for epithelial and endothelial cell tropism*. *Proc Natl Acad Sci U S A*, 2005. **102**(50): p. 18153-8.
161. Belzile, J.P., Stark, T.J., Yeo, G.W., and Spector, D.H., *Human cytomegalovirus infection of human embryonic stem cell-derived primitive neural stem cells is restricted at several steps but leads to the persistence of viral DNA*. *J Virol*, 2014. **88**(8): p. 4021-39.
162. Khan, K.A., Coquette, A., Davrinche, C., and Herbein, G., *Bcl-3-regulated transcription from major immediate-early promoter of human cytomegalovirus in monocyte-derived macrophages*. *J Immunol*, 2009. **182**(12): p. 7784-94.
163. Murphy, E., Yu, D., Grimwood, J., Schmutz, J., Dickson, M., Jarvis, M.A., Hahn, G., Nelson, J.A., Myers, R.M., and Shenk, T.E., *Coding potential of laboratory and clinical strains of human cytomegalovirus*. *Proc Natl Acad Sci U S A*, 2003. **100**(25): p. 14976-81.
164. Vanarsdall, A.L. and Johnson, D.C., *Human cytomegalovirus entry into cells*. *Curr Opin Virol*, 2012. **2**(1): p. 37-42.

165. Compton, T., Nowlin, D.M., and Cooper, N.R., *Initiation of human cytomegalovirus infection requires initial interaction with cell surface heparan sulfate*. *Virology*, 1993. **193**(2): p. 834-41.
166. Wang, X., Huong, S.M., Chiu, M.L., Raab-Traub, N., and Huang, E.S., *Epidermal growth factor receptor is a cellular receptor for human cytomegalovirus*. *Nature*, 2003. **424**(6947): p. 456-61.
167. Soroceanu, L., Akhavan, A., and Cobbs, C.S., *Platelet-derived growth factor- α receptor activation is required for human cytomegalovirus infection*. *Nature*, 2008. **455**(7211): p. 391-5.
168. Straschewski, S., Patrone, M., Walther, P., Gallina, A., Mertens, T., and Frascaroli, G., *Protein pUL128 of human cytomegalovirus is necessary for monocyte infection and blocking of migration*. *J Virol*, 2011. **85**(10): p. 5150-8.
169. Xu, S., Schafer, X., and Munger, J., *Expression of Oncogenic Alleles Induces Multiple Blocks to Human Cytomegalovirus Infection*. *J Virol*, 2016. **90**(9): p. 4346-4356.
170. Rice, G.P., Schrier, R.D., and Oldstone, M.B., *Cytomegalovirus infects human lymphocytes and monocytes: virus expression is restricted to immediate-early gene products*. *Proc Natl Acad Sci U S A*, 1984. **81**(19): p. 6134-8.
171. Landolfo, S., Gariglio, M., Gribaudo, G., and Lembo, D., *The human cytomegalovirus*. *Pharmacol Ther*, 2003. **98**(3): p. 269-97.
172. Balthesen, M., Messerle, M., and Reddehase, M.J., *Lungs are a major organ site of cytomegalovirus latency and recurrence*. *J Virol*, 1993. **67**(9): p. 5360-6.
173. Jean Beltran, P.M. and Cristea, I.M., *The life cycle and pathogenesis of human cytomegalovirus infection: lessons from proteomics*. *Expert Rev Proteomics*, 2014. **11**(6): p. 697-711.
174. Rana, R. and Biegelke, B.J., *Human cytomegalovirus UL34 early and late proteins are essential for viral replication*. *Viruses*, 2014. **6**(2): p. 476-88.
175. Cheng, S., Caviness, K., Buehler, J., Smithey, M., Nikolich-Zugich, J., and Goodrum, F., *Transcriptome-wide characterization of human cytomegalovirus in natural infection and experimental latency*. *Proc Natl Acad Sci U S A*, 2017. **114**(49): p. E10586-E10595.
176. Britt, W., *Manifestations of human cytomegalovirus infection: proposed mechanisms of acute and chronic disease*. *Curr Top Microbiol Immunol*, 2008. **325**: p. 417-70.
177. Sinclair, J., *Human cytomegalovirus: Latency and reactivation in the myeloid lineage*. *J Clin Virol*, 2008. **41**(3): p. 180-5.
178. Barton, E.S., White, D.W., Cathelyn, J.S., Brett-McClellan, K.A., Engle, M., Diamond, M.S., Miller, V.L., and Virgin, H.W.t., *Herpesvirus latency confers symbiotic protection from bacterial infection*. *Nature*, 2007. **447**(7142): p. 326-9.
179. Che, J.W., Daniels, K.A., Selin, L.K., and Welsh, R.M., *Heterologous Immunity and Persistent Murine Cytomegalovirus Infection*. *J Virol*, 2017. **91**(2).
180. Rahbar, A., Bostrom, L., Lagerstedt, U., Magnusson, I., Soderberg-Naucler, C., and Sundqvist, V.A., *Evidence of active cytomegalovirus infection and increased production of IL-6 in tissue specimens obtained from patients with inflammatory bowel diseases*. *Inflamm Bowel Dis*, 2003. **9**(3): p. 154-61.

181. Frantzeskaki, F.G., Karampi, E.S., Kottaridi, C., Alepaki, M., Routsis, C., Tzanela, M., Vassiliadi, D.A., Douka, E., Tsaousi, S., Gennimata, V., Ilias, I., Nikitas, N., Armaganidis, A., Karakitsos, P., Papaevangelou, V., and Dimopoulou, I., *Cytomegalovirus reactivation in a general, nonimmunosuppressed intensive care unit population: incidence, risk factors, associations with organ dysfunction, and inflammatory biomarkers*. J Crit Care, 2015. **30**(2): p. 276-81.
182. Tu, W. and Rao, S., *Mechanisms Underlying T Cell Immunosenescence: Aging and Cytomegalovirus Infection*. Front Microbiol, 2016. **7**: p. 2111.
183. Jain, M., Duggal, S., and Chugh, T.D., *Cytomegalovirus infection in non-immunosuppressed critically ill patients*. J Infect Dev Ctries, 2011. **5**(8): p. 571-9.
184. Schlick, K., Grundbichler, M., Auberger, J., Kern, J.M., Hell, M., Hohla, F., Hopfinger, G., and Greil, R., *Cytomegalovirus reactivation and its clinical impact in patients with solid tumors*. Infect Agent Cancer, 2015. **10**: p. 45.
185. von Laer, D., Meyer-Koenig, U., Serr, A., Finke, J., Kanz, L., Fauser, A.A., Neumann-Haefelin, D., Brugger, W., and Hufert, F.T., *Detection of cytomegalovirus DNA in CD34+ cells from blood and bone marrow*. Blood, 1995. **86**(11): p. 4086-90.
186. Mendelson, M., Monard, S., Sissons, P., and Sinclair, J., *Detection of endogenous human cytomegalovirus in CD34+ bone marrow progenitors*. J Gen Virol, 1996. **77 (Pt 12)**: p. 3099-102.
187. Hahn, G., Jores, R., and Mocarski, E.S., *Cytomegalovirus remains latent in a common precursor of dendritic and myeloid cells*. Proc Natl Acad Sci U S A, 1998. **95**(7): p. 3937-42.
188. Soderberg-Naucler, C., Streblow, D.N., Fish, K.N., Allan-Yorke, J., Smith, P.P., and Nelson, J.A., *Reactivation of latent human cytomegalovirus in CD14(+) monocytes is differentiation dependent*. J Virol, 2001. **75**(16): p. 7543-54.
189. Reeves, M.B., MacAry, P.A., Lehner, P.J., Sissons, J.G., and Sinclair, J.H., *Latency, chromatin remodeling, and reactivation of human cytomegalovirus in the dendritic cells of healthy carriers*. Proc Natl Acad Sci U S A, 2005. **102**(11): p. 4140-5.
190. Murphy, E., Rigoutsos, I., Shibuya, T., and Shenk, T.E., *Reevaluation of human cytomegalovirus coding potential*. Proc Natl Acad Sci U S A, 2003. **100**(23): p. 13585-90.
191. Cunningham, C., Gatherer, D., Hilfrich, B., Baluchova, K., Dargan, D.J., Thomson, M., Griffiths, P.D., Wilkinson, G.W., Schulz, T.F., and Davison, A.J., *Sequences of complete human cytomegalovirus genomes from infected cell cultures and clinical specimens*. J Gen Virol, 2010. **91**(Pt 3): p. 605-15.
192. Stenberg, R.M., Thomsen, D.R., and Stinski, M.F., *Structural analysis of the major immediate early gene of human cytomegalovirus*. J Virol, 1984. **49**(1): p. 190-9.
193. Perng, G.C., Jones, C., Ciacci-Zanella, J., Stone, M., Henderson, G., Yukht, A., Slanina, S.M., Hofman, F.M., Ghiasi, H., Nesburn, A.B., and Wechsler, S.L., *Virus-induced neuronal apoptosis blocked by the herpes simplex virus latency-associated transcript*. Science, 2000. **287**(5457): p. 1500-3.
194. Reeves, M.B. and Sinclair, J.H., *Analysis of latent viral gene expression in natural and experimental latency models of human cytomegalovirus and its*

- correlation with histone modifications at a latent promoter.* J Gen Virol, 2010. **91**(Pt 3): p. 599-604.
195. Goodrum, F., Reeves, M., Sinclair, J., High, K., and Shenk, T., *Human cytomegalovirus sequences expressed in latently infected individuals promote a latent infection in vitro.* Blood, 2007. **110**(3): p. 937-45.
 196. Jenkins, C., Abendroth, A., and Slobedman, B., *A novel viral transcript with homology to human interleukin-10 is expressed during latent human cytomegalovirus infection.* J Virol, 2004. **78**(3): p. 1440-7.
 197. Rossetto, C.C., Tarrant-Elorza, M., and Pari, G.S., *Cis and trans acting factors involved in human cytomegalovirus experimental and natural latent infection of CD14 (+) monocytes and CD34 (+) cells.* PLoS Pathog, 2013. **9**(5): p. e1003366.
 198. Landais, I., Pelton, C., Streblov, D., DeFilippis, V., McWeeney, S., and Nelson, J.A., *Human Cytomegalovirus miR-UL112-3p Targets TLR2 and Modulates the TLR2/IRAK1/NFkappaB Signaling Pathway.* PLoS Pathog, 2015. **11**(5): p. e1004881.
 199. Boehme, K.W., Guerrero, M., and Compton, T., *Human cytomegalovirus envelope glycoproteins B and H are necessary for TLR2 activation in permissive cells.* J Immunol, 2006. **177**(10): p. 7094-102.
 200. Szomolanyi-Tsuda, E., Liang, X., Welsh, R.M., Kurt-Jones, E.A., and Finberg, R.W., *Role for TLR2 in NK cell-mediated control of murine cytomegalovirus in vivo.* J Virol, 2006. **80**(9): p. 4286-91.
 201. Krug, A., French, A.R., Barchet, W., Fischer, J.A., Dzionek, A., Pingel, J.T., Orihuela, M.M., Akira, S., Yokoyama, W.M., and Colonna, M., *TLR9-dependent recognition of MCMV by IPC and DC generates coordinated cytokine responses that activate antiviral NK cell function.* Immunity, 2004. **21**(1): p. 107-19.
 202. DeFilippis, V.R., Robinson, B., Keck, T.M., Hansen, S.G., Nelson, J.A., and Fruh, K.J., *Interferon regulatory factor 3 is necessary for induction of antiviral genes during human cytomegalovirus infection.* J Virol, 2006. **80**(2): p. 1032-7.
 203. Vivier, E., Tomasello, E., Baratin, M., Walzer, T., and Ugolini, S., *Functions of natural killer cells.* Nat Immunol, 2008. **9**(5): p. 503-10.
 204. Kuijpers, T.W., Baars, P.A., Dantin, C., van den Burg, M., van Lier, R.A., and Roosnek, E., *Human NK cells can control CMV infection in the absence of T cells.* Blood, 2008. **112**(3): p. 914-5.
 205. Krmpotic, A., Busch, D.H., Bubic, I., Gebhardt, F., Hengel, H., Hasan, M., Scalzo, A.A., Koszinowski, U.H., and Jonjic, S., *MCMV glycoprotein gp40 confers virus resistance to CD8+ T cells and NK cells in vivo.* Nat Immunol, 2002. **3**(6): p. 529-35.
 206. Adam, S.G., Caraux, A., Fodil-Cornu, N., Loredó-Osti, J.C., Lesjean-Pottier, S., Jaubert, J., Bubic, I., Jonjic, S., Guenet, J.L., Vidal, S.M., and Colucci, F., *Cmv4, a new locus linked to the NK cell gene complex, controls innate resistance to cytomegalovirus in wild-derived mice.* J Immunol, 2006. **176**(9): p. 5478-85.
 207. Fielding, C.A., Aicheler, R., Stanton, R.J., Wang, E.C., Han, S., Seirafian, S., Davies, J., McSharry, B.P., Weekes, M.P., Antrobus, P.R., Prod'homme, V., Blanchet, F.P., Sugrue, D., Cuff, S., Roberts, D., Davison, A.J., Lehner, P.J., Wilkinson, G.W., and Tomasec, P., *Two novel human cytomegalovirus NK cell*

- evasion functions target MICA for lysosomal degradation.* PLoS Pathog, 2014. **10**(5): p. e1004058.
208. Chang, W.L. and Barry, P.A., *Attenuation of innate immunity by cytomegalovirus IL-10 establishes a long-term deficit of adaptive antiviral immunity.* Proc Natl Acad Sci U S A, 2010. **107**(52): p. 22647-52.
 209. van Leeuwen, E.M., Remmerswaal, E.B., Vossen, M.T., Rowshani, A.T., Wertheim-van Dillen, P.M., van Lier, R.A., and ten Berge, I.J., *Emergence of a CD4+CD28- granzyme B+, cytomegalovirus-specific T cell subset after recovery of primary cytomegalovirus infection.* J Immunol, 2004. **173**(3): p. 1834-41.
 210. Gibson, L., Dooley, S., Trzmielina, S., Somasundaran, M., Fisher, D., Revello, M.G., and Luzuriaga, K., *Cytomegalovirus (CMV) IE1- and pp65-specific CD8+ T cell responses broaden over time after primary CMV infection in infants.* J Infect Dis, 2007. **195**(12): p. 1789-98.
 211. Sylwester, A.W., Mitchell, B.L., Edgar, J.B., Taormina, C., Pelte, C., Ruchti, F., Sleath, P.R., Grabstein, K.H., Hosken, N.A., Kern, F., Nelson, J.A., and Picker, L.J., *Broadly targeted human cytomegalovirus-specific CD4+ and CD8+ T cells dominate the memory compartments of exposed subjects.* J Exp Med, 2005. **202**(5): p. 673-85.
 212. Sinclair, J. and Sissons, P., *Latency and reactivation of human cytomegalovirus.* J Gen Virol, 2006. **87**(Pt 7): p. 1763-79.
 213. BaAlawi, F., Robertson, P.W., Lahra, M., and Rawlinson, W.D., *Comparison of five CMV IgM immunoassays with CMV IgG avidity for diagnosis of primary CMV infection.* Pathology, 2012. **44**(4): p. 381-3.
 214. Bodeus, M., Feyder, S., and Goubau, P., *Avidity of IgG antibodies distinguishes primary from non-primary cytomegalovirus infection in pregnant women.* Clin Diagn Virol, 1998. **9**(1): p. 9-16.
 215. Bellone, G., Turletti, A., Artusio, E., Mareschi, K., Carbone, A., Tibaudi, D., Robecchi, A., Emanuelli, G., and Rodeck, U., *Tumor-associated transforming growth factor-beta and interleukin-10 contribute to a systemic Th2 immune phenotype in pancreatic carcinoma patients.* Am J Pathol, 1999. **155**(2): p. 537-47.
 216. Levi, M., *CMV endothelitis as a factor in the pathogenesis of atherosclerosis.* Cardiovasc Res, 2001. **50**(3): p. 432-3.
 217. Compton, T., Kurt-Jones, E.A., Boehme, K.W., Belko, J., Latz, E., Golenbock, D.T., and Finberg, R.W., *Human cytomegalovirus activates inflammatory cytokine responses via CD14 and Toll-like receptor 2.* J Virol, 2003. **77**(8): p. 4588-96.
 218. Browne, E.P., Wing, B., Coleman, D., and Shenk, T., *Altered cellular mRNA levels in human cytomegalovirus-infected fibroblasts: viral block to the accumulation of antiviral mRNAs.* J Virol, 2001. **75**(24): p. 12319-30.
 219. Zhu, H., Cong, J.P., Yu, D., Bresnahan, W.A., and Shenk, T.E., *Inhibition of cyclooxygenase 2 blocks human cytomegalovirus replication.* Proc Natl Acad Sci U S A, 2002. **99**(6): p. 3932-7.
 220. Iwamoto, G.K., Monick, M.M., Clark, B.D., Auron, P.E., Stinski, M.F., and Hunninghake, G.W., *Modulation of interleukin 1 beta gene expression by the*

- immediate early genes of human cytomegalovirus*. J Clin Invest, 1990. **85**(6): p. 1853-7.
221. Iwata, M., Vieira, J., Byrne, M., Horton, H., and Torok-Storb, B., *Interleukin-1 (IL-1) inhibits growth of cytomegalovirus in human marrow stromal cells: inhibition is reversed upon removal of IL-1*. Blood, 1999. **94**(2): p. 572-8.
 222. Radunovic, M., Tomanovic, N., Novakovic, I., Boricic, I., Milenkovic, S., Dimitrijevic, M., Radojevic-Skodric, S., Bogdanovic, L., and Basta-Jovanovic, G., *Cytomegalovirus induces Interleukin-6 mediated inflammatory response in salivary gland cancer*. J BUON, 2016. **21**(6): p. 1530-1536.
 223. Costa, H., Touma, J., Davoudi, B., Benard, M., Sauer, T., Geisler, J., Vetvik, K., Rahbar, A., and Soderberg-Naucler, C., *Human cytomegalovirus infection is correlated with enhanced cyclooxygenase-2 and 5-lipoxygenase protein expression in breast cancer*. J Cancer Res Clin Oncol, 2019. **145**(8): p. 2083-2095.
 224. Moore, D.H., Charney, J., Kramarsky, B., Lasfargues, E.Y., Sarkar, N.H., Brennan, M.J., Burrows, J.H., Sirsat, S.M., Paymaster, J.C., and Vaidya, A.B., *Search for a human breast cancer virus*. Nature, 1971. **229**(5287): p. 611-4.
 225. Ekblom, A., Hsieh, C.C., Trichopoulos, D., Yen, Y.Y., Petridou, E., and Adami, H.O., *Breast-feeding and breast cancer in the offspring*. Br J Cancer, 1993. **67**(4): p. 842-5.
 226. Richardson, A., *Is breast cancer caused by late exposure to a common virus?* Med Hypotheses, 1997. **48**(6): p. 491-7.
 227. Richardson, A.K., Cox, B., McCredie, M.R., Dite, G.S., Chang, J.H., Gertig, D.M., Southey, M.C., Giles, G.G., and Hopper, J.L., *Cytomegalovirus, Epstein-Barr virus and risk of breast cancer before age 40 years: a case-control study*. Br J Cancer, 2004. **90**(11): p. 2149-52.
 228. Cox, B., Richardson, A., Graham, P., Gislefoss, R.E., Jellum, E., and Rollag, H., *Breast cancer, cytomegalovirus and Epstein-Barr virus: a nested case-control study*. Br J Cancer, 2010. **102**(11): p. 1665-9.
 229. Surendran, A. and Chisthi, M.M., *Breast Cancer Association with Cytomegalovirus-A Tertiary Center Case-Control Study*. J Invest Surg, 2019. **32**(2): p. 172-177.
 230. Rahbar, A., Touma, J., Costa, H., Davoudi, B., Bukholm, I.R., Sauer, T., Vetvik, K., Geisler, J., and Soderberg-Naucler, C., *Low Expression of Estrogen Receptor-alpha and Progesterone Receptor in Human Breast Cancer Tissues Is Associated With High-Grade Human Cytomegalovirus Protein Expression*. Clin Breast Cancer, 2017. **17**(7): p. 526-535 e1.
 231. Cui, J., Wang, Q., Wang, H.B., Wang, B., and Li, L., *Protein and DNA evidences of HCMV infection in primary breast cancer tissues and metastatic sentinel lymph nodes*. Cancer Biomark, 2018. **21**(4): p. 769-780.
 232. Bareq N. Al-Nuaimi, R.H.A.-A.a.R.Z.N., *Association of human cytomegalovirus with HER2 proto-oncogene overexpression in Iraqi breast cancer patients*. Biochemical and Cellular Archives, 2019. **19**(1): p. 1691-1698.
 233. El Shazly, D.F., Bahnasse, A.A., Omar, O.S., Elsayed, E.T., Al-Hindawi, A., El-Desouky, E., Youssef, H., and Zekri, A.N., *Detection of Human Cytomegalovirus*

- in Malignant and Benign Breast Tumors in Egyptian Women.* Clin Breast Cancer, 2018. **18**(4): p. e629-e642.
234. Ahmed, A., *Antiviral treatment of cytomegalovirus infection.* Infect Disord Drug Targets, 2011. **11**(5): p. 475-503.
235. Tsai, J.H., Tsai, C.H., Cheng, M.H., Lin, S.J., Xu, F.L., and Yang, C.C., *Association of viral factors with non-familial breast cancer in Taiwan by comparison with non-cancerous, fibroadenoma, and thyroid tumor tissues.* J Med Virol, 2005. **75**(2): p. 276-81.
236. Sepahvand, P., Makvandi, M., Samarbafzadeh, A., Talaei-Zadeh, A., Ranjbari, N., Nisi, N., Azaran, A., Jalilian, S., Pirmoradi, R., Makvandi, K., and Ahmadi Angali, K., *Human Cytomegalovirus DNA among Women with Breast Cancer.* Asian Pac J Cancer Prev, 2019. **20**(8): p. 2275-2279.
237. El-Shinawi, M., Mohamed, H.T., Abdel-Fattah, H.H., Ibrahim, S.A., El-Halawany, M.S., Nouh, M.A., Schneider, R.J., and Mohamed, M.M., *Inflammatory and Non-inflammatory Breast Cancer: A Potential Role for Detection of Multiple Viral DNAs in Disease Progression.* Ann Surg Oncol, 2016. **23**(2): p. 494-502.
238. Mohammadizadeh, F. and Mahmudi, F., *Evaluation of human cytomegalovirus antigen expression in invasive breast carcinoma in a population of Iranian patients.* Infect Agent Cancer, 2017. **12**: p. 39.
239. Antonsson, A., Bialasiewicz, S., Rockett, R.J., Jacob, K., Bennett, I.C., and Sloots, T.P., *Exploring the prevalence of ten polyomaviruses and two herpes viruses in breast cancer.* PLoS One, 2012. **7**(8): p. e39842.
240. Richardson, A.K., Currie, M.J., Robinson, B.A., Morrin, H., Phung, Y., Pearson, J.F., Anderson, T.P., Potter, J.D., and Walker, L.C., *Cytomegalovirus and Epstein-Barr virus in breast cancer.* PLoS One, 2015. **10**(2): p. e0118989.
241. Utrera-Barillas, D., Valdez-Salazar, H.A., Gomez-Rangel, D., Alvarado-Cabrero, I., Aguilera, P., Gomez-Delgado, A., and Ruiz-Tachiquin, M.E., *Is human cytomegalovirus associated with breast cancer progression?* Infect Agent Cancer, 2013. **8**(1): p. 12.
242. Rehab Allah Ahmed, S.M.Y., *Immunohistochemical detection of human cytomegalovirus, Epstein-Barr virus and human papillomavirus in invasive breast carcinoma in Egyptian women: A tissue microarray study.* Journal of Solid Tumors, 2016. **6**(2).
243. Tsai, J.H., Hsu, C.S., Tsai, C.H., Su, J.M., Liu, Y.T., Cheng, M.H., Wei, J.C., Chen, F.L., and Yang, C.C., *Relationship between viral factors, axillary lymph node status and survival in breast cancer.* J Cancer Res Clin Oncol, 2007. **133**(1): p. 13-21.
244. El-Shinawi, M., Mohamed, H.T., El-Ghonaimy, E.A., Tantawy, M., Younis, A., Schneider, R.J., and Mohamed, M.M., *Human cytomegalovirus infection enhances NF-kappaB/p65 signaling in inflammatory breast cancer patients.* PLoS One, 2013. **8**(2): p. e55755.
245. Taher, C., Frisk, G., Fuentes, S., Religa, P., Costa, H., Assinger, A., Vetvik, K.K., Bukholm, I.R., Yaiw, K.C., Smedby, K.E., Backlund, M., Soderberg-Naucler, C., and Rahbar, A., *High prevalence of human cytomegalovirus in brain metastases*

- of patients with primary breast and colorectal cancers. *Transl Oncol*, 2014. **7**(6): p. 732-40.
246. Sijmons, S., Van Ranst, M., and Maes, P., *Genomic and functional characteristics of human cytomegalovirus revealed by next-generation sequencing*. *Viruses*, 2014. **6**(3): p. 1049-72.
247. Hemmings, D.G. and Guilbert, L.J., *Polarized release of human cytomegalovirus from placental trophoblasts*. *J Virol*, 2002. **76**(13): p. 6710-7.
248. Stoddart, C.A., Cardin, R.D., Boname, J.M., Manning, W.C., Abenes, G.B., and Mocarski, E.S., *Peripheral blood mononuclear phagocytes mediate dissemination of murine cytomegalovirus*. *J Virol*, 1994. **68**(10): p. 6243-53.
249. Meng, G., Tang, X., Yang, Z., Zhao, Y., Curtis, J.M., McMullen, T.P.W., and Brindley, D.N., *Dexamethasone decreases the autotaxin-lysophosphatidate-inflammatory axis in adipose tissue: implications for the metabolic syndrome and breast cancer*. *FASEB J*, 2019. **33**(2): p. 1899-1910.
250. Benesch, M.G., Tang, X., Maeda, T., Ohhata, A., Zhao, Y.Y., Kok, B.P., Dewald, J., Hitt, M., Curtis, J.M., McMullen, T.P., and Brindley, D.N., *Inhibition of autotaxin delays breast tumor growth and lung metastasis in mice*. *FASEB J*, 2014. **28**(6): p. 2655-66.
251. Guy, C.T., Cardiff, R.D., and Muller, W.J., *Induction of mammary tumors by expression of polyomavirus middle T oncogene: a transgenic mouse model for metastatic disease*. *Mol Cell Biol*, 1992. **12**(3): p. 954-61.
252. Davie, S.A., Maglione, J.E., Manner, C.K., Young, D., Cardiff, R.D., MacLeod, C.L., and Ellies, L.G., *Effects of FVB/NJ and C57Bl/6J strain backgrounds on mammary tumor phenotype in inducible nitric oxide synthase deficient mice*. *Transgenic Res*, 2007. **16**(2): p. 193-201.
253. Tang, X., Benesch, M.G., Dewald, J., Zhao, Y.Y., Patwardhan, N., Santos, W.L., Curtis, J.M., McMullen, T.P., and Brindley, D.N., *Lipid phosphate phosphatase-1 expression in cancer cells attenuates tumor growth and metastasis in mice*. *J Lipid Res*, 2014. **55**(11): p. 2389-400.
254. Pang, X.L., Chui, L., Fenton, J., LeBlanc, B., and Preiksaitis, J.K., *Comparison of LightCycler-based PCR, COBAS amplicor CMV monitor, and pp65 antigenemia assays for quantitative measurement of cytomegalovirus viral load in peripheral blood specimens from patients after solid organ transplantation*. *J Clin Microbiol*, 2003. **41**(7): p. 3167-74.
255. Nicoll, S., Brass, A., and Cubie, H.A., *Detection of herpes viruses in clinical samples using real-time PCR*. *J Virol Methods*, 2001. **96**(1): p. 25-31.
256. Koffron, A.J., Hummel, M., Patterson, B.K., Yan, S., Kaufman, D.B., Fryer, J.P., Stuart, F.P., and Abecassis, M.I., *Cellular localization of latent murine cytomegalovirus*. *J Virol*, 1998. **72**(1): p. 95-103.
257. Cook, C.H., Trgovcich, J., Zimmerman, P.D., Zhang, Y., and Sedmak, D.D., *Lipopolysaccharide, tumor necrosis factor alpha, or interleukin-1beta triggers reactivation of latent cytomegalovirus in immunocompetent mice*. *J Virol*, 2006. **80**(18): p. 9151-8.
258. Junqueira, L.C., Bignolas, G., and Brentani, R.R., *Picrosirius staining plus polarization microscopy, a specific method for collagen detection in tissue sections*. *Histochem J*, 1979. **11**(4): p. 447-55.

259. IBM Corporation. IBM SPSS Statistics for Windows; Version 25.0.; IBM Corporation: Armonk, N., USA, 2017.
260. Gombos, R.B., Brown, J.C., Teefy, J., Gibeault, R.L., Conn, K.L., Schang, L.M., and Hemmings, D.G., *Vascular dysfunction in young, mid-aged and aged mice with latent cytomegalovirus infections*. *Am J Physiol Heart Circ Physiol*, 2013. **304**(2): p. H183-94.
261. Cinatl, J., Jr., Vogel, J.U., Kotchetkov, R., and Wilhelm Doerr, H., *Oncomodulatory signals by regulatory proteins encoded by human cytomegalovirus: a novel role for viral infection in tumor progression*. *FEMS Microbiol Rev*, 2004. **28**(1): p. 59-77.
262. Feire, A.L., Koss, H., and Compton, T., *Cellular integrins function as entry receptors for human cytomegalovirus via a highly conserved disintegrin-like domain*. *Proc Natl Acad Sci U S A*, 2004. **101**(43): p. 15470-5.
263. Halary, F., Amara, A., Lortat-Jacob, H., Messerle, M., Delaunay, T., Houles, C., Fieschi, F., Arenzana-Seisdedos, F., Moreau, J.F., and Dechanet-Merville, J., *Human cytomegalovirus binding to DC-SIGN is required for dendritic cell infection and target cell trans-infection*. *Immunity*, 2002. **17**(5): p. 653-64.
264. Scholz, M., Doerr, H.W., and Cinatl, J., *Inhibition of cytomegalovirus immediate early gene expression: a therapeutic option?* *Antiviral Res*, 2001. **49**(3): p. 129-45.
265. Crump, J.W., Geist, L.J., Auron, P.E., Webb, A.C., Stinski, M.F., and Hunninghake, G.W., *The immediate early genes of human cytomegalovirus require only proximal promoter elements to upregulate expression of interleukin-1 beta*. *Am J Respir Cell Mol Biol*, 1992. **6**(6): p. 674-7.
266. Carlquist, J.F., Edelman, L., Bennion, D.W., and Anderson, J.L., *Cytomegalovirus induction of interleukin-6 in lung fibroblasts occurs independently of active infection and involves a G protein and the transcription factor, NF-kappaB*. *J Infect Dis*, 1999. **179**(5): p. 1094-100.
267. Speir, E., Yu, Z.X., Ferrans, V.J., Huang, E.S., and Epstein, S.E., *Aspirin attenuates cytomegalovirus infectivity and gene expression mediated by cyclooxygenase-2 in coronary artery smooth muscle cells*. *Circ Res*, 1998. **83**(2): p. 210-6.
268. Vanarsdall, A.L., Wisner, T.W., Lei, H., Kazlauskas, A., and Johnson, D.C., *PDGF receptor-alpha does not promote HCMV entry into epithelial and endothelial cells but increased quantities stimulate entry by an abnormal pathway*. *PLoS Pathog*, 2012. **8**(9): p. e1002905.
269. Ekpe-Adewuyi, E., Lopez-Campistrous, A., Tang, X., Brindley, D.N., and McMullen, T.P., *Platelet derived growth factor receptor alpha mediates nodal metastases in papillary thyroid cancer by driving the epithelial-mesenchymal transition*. *Oncotarget*, 2016. **7**(50): p. 83684-83700.
270. Carvalho, I., Milanezi, F., Martins, A., Reis, R.M., and Schmitt, F., *Overexpression of platelet-derived growth factor receptor alpha in breast cancer is associated with tumour progression*. *Breast Cancer Res*, 2005. **7**(5): p. R788-95.

271. Richardson, A.K., Walker, L.C., Cox, B., Rollag, H., Robinson, B.A., Morrin, H., Pearson, J.F., Potter, J.D., Paterson, M., Surcel, H.M., Pukkala, E., and Currie, M.J., *Breast cancer and cytomegalovirus*. Clin Transl Oncol, 2019.
272. Robbins, S.H., Tessmer, M.S., Mikayama, T., and Brossay, L., *Expansion and contraction of the NK cell compartment in response to murine cytomegalovirus infection*. J Immunol, 2004. **173**(1): p. 259-66.
273. Aslakson, C.J. and Miller, F.R., *Selective events in the metastatic process defined by analysis of the sequential dissemination of subpopulations of a mouse mammary tumor*. Cancer Res, 1992. **52**(6): p. 1399-405.
274. Ewens, A., Mihich, E., and Ehrke, M.J., *Distant metastasis from subcutaneously grown E0771 medullary breast adenocarcinoma*. Anticancer Res, 2005. **25**(6B): p. 3905-15.
275. Liotta, L.A., Kleinerman, J., and Saidel, G.M., *Quantitative relationships of intravascular tumor cells, tumor vessels, and pulmonary metastases following tumor implantation*. Cancer Res, 1974. **34**(5): p. 997-1004.
276. MacManiman, J.D., Meuser, A., Botto, S., Smith, P.P., Liu, F., Jarvis, M.A., Nelson, J.A., and Caposio, P., *Human cytomegalovirus-encoded pUL7 is a novel CEACAM1-like molecule responsible for promotion of angiogenesis*. MBio, 2014. **5**(6): p. e02035.
277. Dumortier, J., Streblow, D.N., Moses, A.V., Jacobs, J.M., Kreklywich, C.N., Camp, D., Smith, R.D., Orloff, S.L., and Nelson, J.A., *Human cytomegalovirus secretome contains factors that induce angiogenesis and wound healing*. J Virol, 2008. **82**(13): p. 6524-35.
278. Taher, M.Y., Davies, D.M., and Maher, J., *The role of the interleukin (IL)-6/IL-6 receptor axis in cancer*. Biochem Soc Trans, 2018. **46**(6): p. 1449-1462.
279. Friedl, P. and Wolf, K., *Plasticity of cell migration: a multiscale tuning model*. J Cell Biol, 2010. **188**(1): p. 11-9.
280. Canalis, E., *Interleukin-1 has independent effects on deoxyribonucleic acid and collagen synthesis in cultures of rat calvariae*. Endocrinology, 1986. **118**(1): p. 74-81.
281. Goldring, M.B. and Krane, S.M., *Modulation by recombinant interleukin 1 of synthesis of types I and III collagens and associated procollagen mRNA levels in cultured human cells*. J Biol Chem, 1987. **262**(34): p. 16724-9.
282. Schmitt, M., Harbeck, N., Thomssen, C., Wilhelm, O., Magdolen, V., Reuning, U., Ulm, K., Hofler, H., Janicke, F., and Graeff, H., *Clinical impact of the plasminogen activation system in tumor invasion and metastasis: prognostic relevance and target for therapy*. Thromb Haemost, 1997. **78**(1): p. 285-96.
283. Iwamoto, G.K. and Konicek, S.A., *Cytomegalovirus immediate early genes upregulate interleukin-6 gene expression*. J Investig Med, 1997. **45**(4): p. 175-82.
284. Cao, H., Zhang, J., Liu, H., Wan, L., Zhang, H., Huang, Q., Xu, E., and Lai, M., *IL-13/STAT6 signaling plays a critical role in the epithelial-mesenchymal transition of colorectal cancer cells*. Oncotarget, 2016. **7**(38): p. 61183-61198.
285. Simon, C.O., Seckert, C.K., Dreis, D., Reddehase, M.J., and Grzimek, N.K., *Role for tumor necrosis factor alpha in murine cytomegalovirus transcriptional reactivation in latently infected lungs*. J Virol, 2005. **79**(1): p. 326-40.

286. Yang, Z., Tang, X., Meng, G., Benesch, M.G.K., Mackova, M., Belon, A.P., Serrano-Lomelin, J., Goping, I.S., Brindley, D.N., and Hemmings, D.G., *Latent Cytomegalovirus Infection in Female Mice Increases Breast Cancer Metastasis*. *Cancers (Basel)*, 2019. **11**(4).
287. Almanan, M., Raynor, J., Sholl, A., Wang, M., Chougnet, C., Cardin, R.D., and Hildeman, D.A., *Tissue-specific control of latent CMV reactivation by regulatory T cells*. *PLoS Pathog*, 2017. **13**(8): p. e1006507.
288. Geisler, J., Touma, J., Rahbar, A., Soderberg-Naucler, C., and Vetvik, K., *A Review of the Potential Role of Human Cytomegalovirus (HCMV) Infections in Breast Cancer Carcinogenesis and Abnormal Immunity*. *Cancers (Basel)*, 2019. **11**(12).
289. Alhaque, S., Themis, M., and Rashidi, H., *Three-dimensional cell culture: from evolution to revolution*. *Philos Trans R Soc Lond B Biol Sci*, 2018. **373**(1750).
290. Lamouille, S., Xu, J., and Derynck, R., *Molecular mechanisms of epithelial-mesenchymal transition*. *Nat Rev Mol Cell Biol*, 2014. **15**(3): p. 178-96.
291. Dongre, A. and Weinberg, R.A., *New insights into the mechanisms of epithelial-mesenchymal transition and implications for cancer*. *Nat Rev Mol Cell Biol*, 2019. **20**(2): p. 69-84.
292. Griffiths, P.D. and Boeckh, M., *Antiviral therapy for human cytomegalovirus*, in *Human Herpesviruses: Biology, Therapy, and Immunoprophylaxis*, A. Arvin, et al., Editors. 2007: Cambridge.